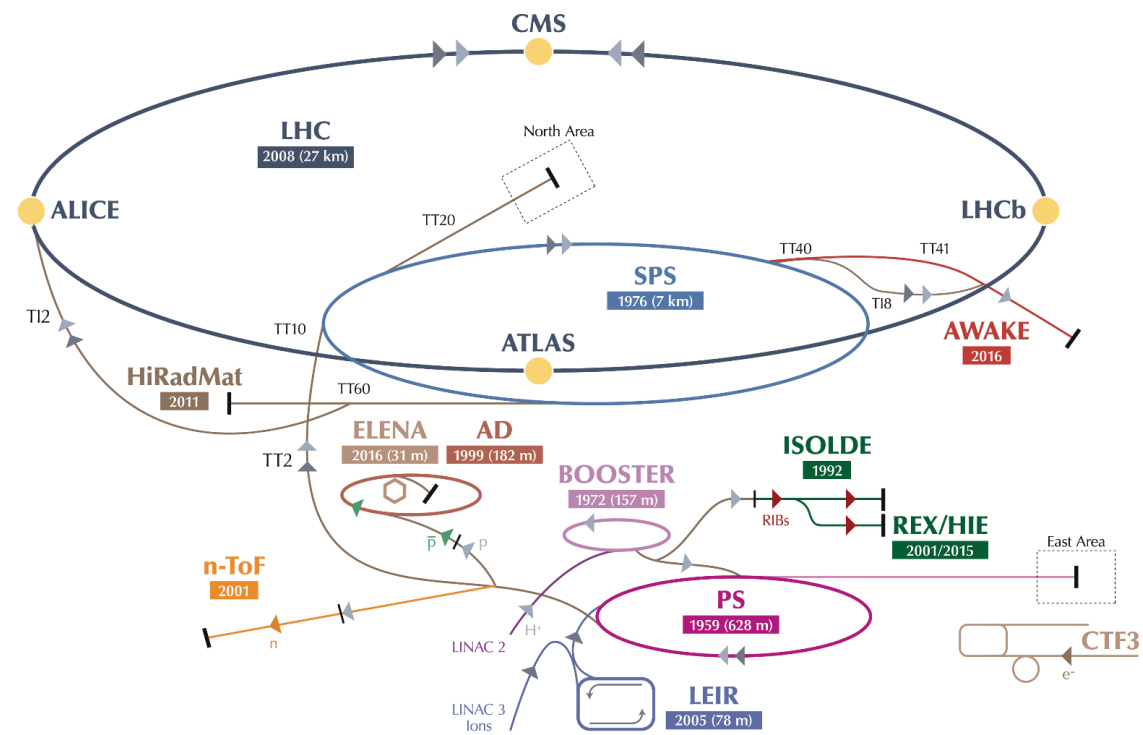


Two-Step Vacuum Design of Light Sources

R. Kersevan, CERN-TE-VSC-VSM – kersevan@cern.ch



Outline of tutorial:

- ~~1. Basics of gas dynamics: outgassing, conductance, pumping speed;~~
2. Basics of synchrotron radiation (SR), with examples relevant to vacuum design;
3. SR-induced desorption and materials for vacuum;
4. Computational methods for vacuum and SR: a review;
5. Practical examples of analysis, simulation, and design of key components of light sources;
6. Summary and conclusions.

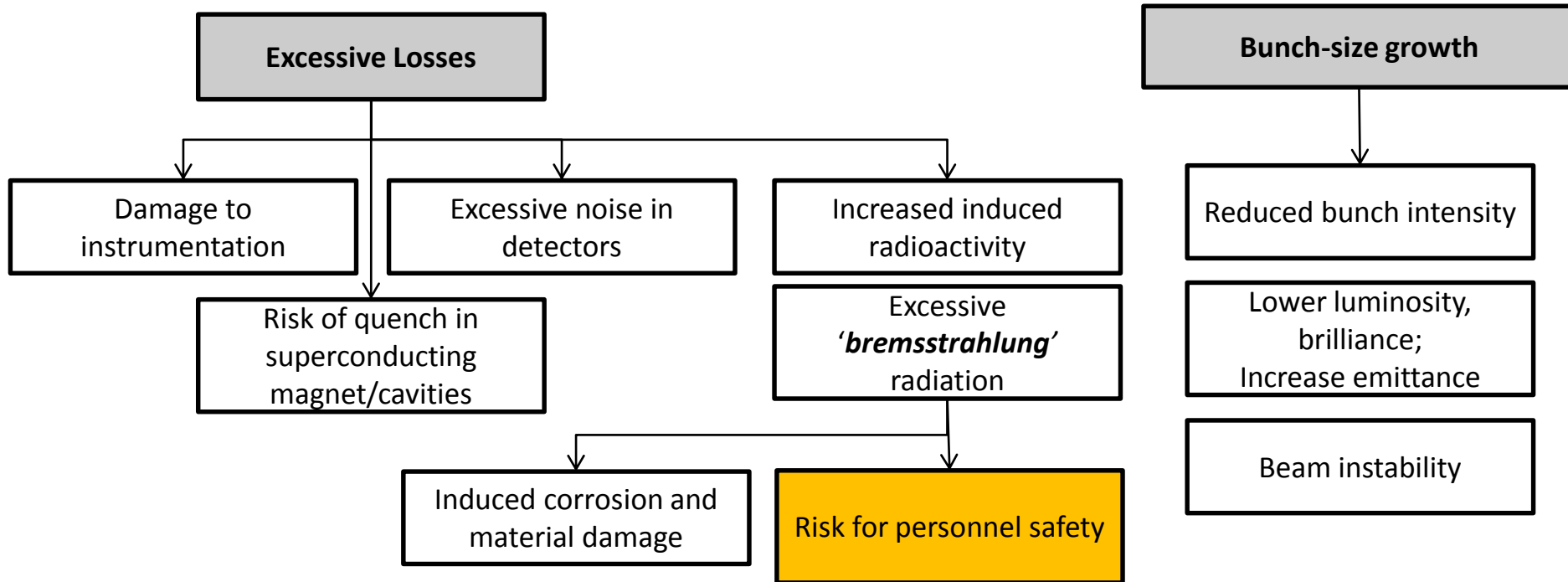
Overview:

- Modern particle accelerators, in particular synchrotron radiation light sources need rather **stringent conditions on their vacuum requirements**, namely:
 - Average pressures in the **low 1.0E-9 mbar range**;
 - Average **low-Z residual gas composition**: H_2 ($Z=1$) must be the main gas component during operation of the machine;
 - **Stable pressure profiles**, with, in particular, no pressure bumps along the straight sections where insertion devices (ID) are installed, in order to minimize the generation of high-energy bremsstrahlung (BS) photons;
- This translates into flows which are in the **molecular flow regime**, i.e. conditions for which the probability of the residual gas molecules to interact/collide with each other is much lower than the probability of hitting the walls of the vacuum system
- Apart from cases when the different molecular species can promptly react chemically with each other (e.g. chemical reactors, catalysed reactions), the flow regime of a gas can be described by the **mean free path** concept, i.e. the average distance travelled by a molecule between two collisions with another molecule at same density and temperature conditions in a 'infinite' volume;

Why do we need vacuum in accelerators?

Collisions between gas molecules and particles have to be minimized, otherwise:

Particle energy can be reduced and/or trajectories can be modified, so that:



A good vacuum is also necessary:

- To avoid electrical discharge in high-voltage devices (tens of MV/m in RF cavities);
- To reduce the heat transfer to cryogenic devices (e.g. SC wiggler with closed-loop compressors)

General case; arbitrary vacuum chamber shape:

- For tubes of arbitrary non-uniform cross-section and shape, there is no analytical solution to the **integro-differential equations** (seen during previous tutorial).
- **Unfortunately this is the case for most synchrotron light sources**, where e.g. the dipole/crotch chambers have a “Y” shape and are connected to straight parts going through the FODO sections (quadrupoles/sextupoles necessary for “beam optics”).
- In this case a number of approximate numerical methods have been developed during the years, and among them (*)
 - “Slicing” the system in short segments and applying the **Continuity Principle of Gas Flow (Finite-Elements codes**, either proprietary or custom-written);
 - Slicing/subdividing the system in short segments and applying the **Electric-Network Analogy (ENA)**, and then using codes like **LTSpice**;
 - **Angular coefficients method** (analogy to thermal radiation propagation);
 - Applying the **Test-Particle Monte Carlo method (TPMC)**. The components’ geometry is modelled in three dimensions, usually by means of a CAD program.

In a nutshell:

- The TPMC codes generate molecules at the entrance of the component pointing in ‘random’ directions according to the **Lambertian cosine distribution**. When the molecules impinge on the internal wall of the component, they are re-emitted again randomly, unless pumped.
- The program follows the molecular traces until they reach the exit of the component.

(*) For a review see for instance: “**Analytical and Numerical Tools for Vacuum Systems**”, R. Kersevan, CERN Accelerator School, 2017,... and references therein.

Transmission probability for the general case of arbitrary shapes:

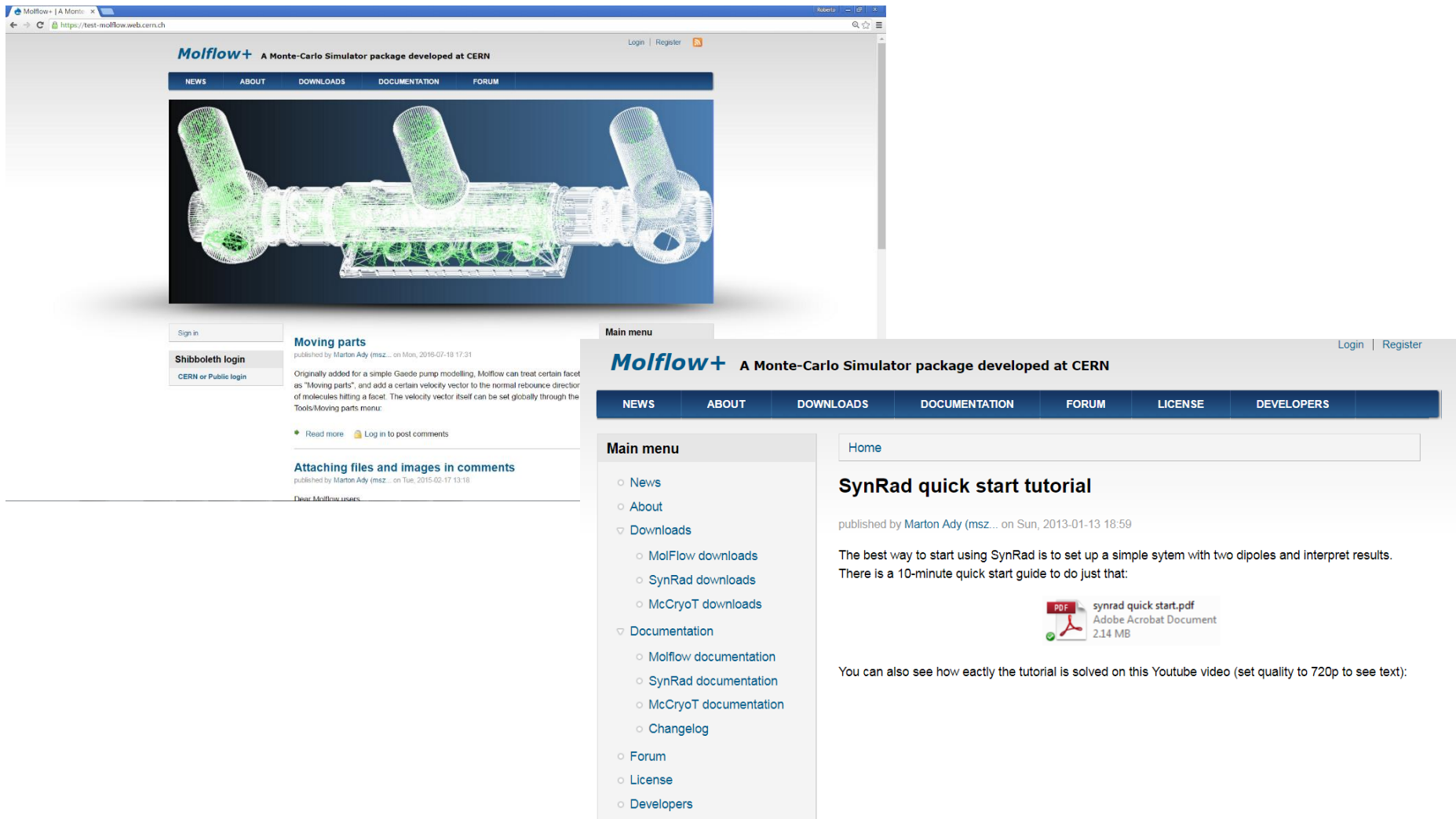
- The transmission probability is given by the ratio between the number of ‘escaped’ and ‘injected’ molecules. Many simulated molecules are needed to reduce the statistical scattering, sometimes billions! (e.g. **KATRIN** neutrino mass experiment case)
- The reference TPMC software at CERN is **MolFlow+**. This powerful tool for high-vacuum applications can import the 3-D drawing of the vacuum components and generate ‘random’ molecules on any surface of interest.
- The randomness of the generation follows the **physical laws of vacuum technology**: for **thermal desorption** it is assumed to be **spatially uniform** on surfaces and depending only on the wall material properties (temperature, surface finish, chemical cleaning procedure, bake-out,...) while for **synchrotron radiation (SR) induced gas desorption** it is derived from the distribution of photons hitting the walls of the system (e.g. see below, **SYNRAD+** code), which are then converted into molecular fluxes using **empirical/experimental data** (see further below).
- CERN develops, maintains, and uses on a daily basis the TPMC code Molflow+, which has become the *de-facto* standard in the field of particle accelerator design:

<https://test-molflow.web.cern.ch/>

For those participating to the “Practical Days at CERN” visits, a short tutorial on Molflow+ is foreseen, laptops will be provided on site

1. Basics of gas dynamics: outgassing, conductance, pumping speed

General case; arbitrary shapes: SYNRAD+ and Molflow+ codes run in sequence



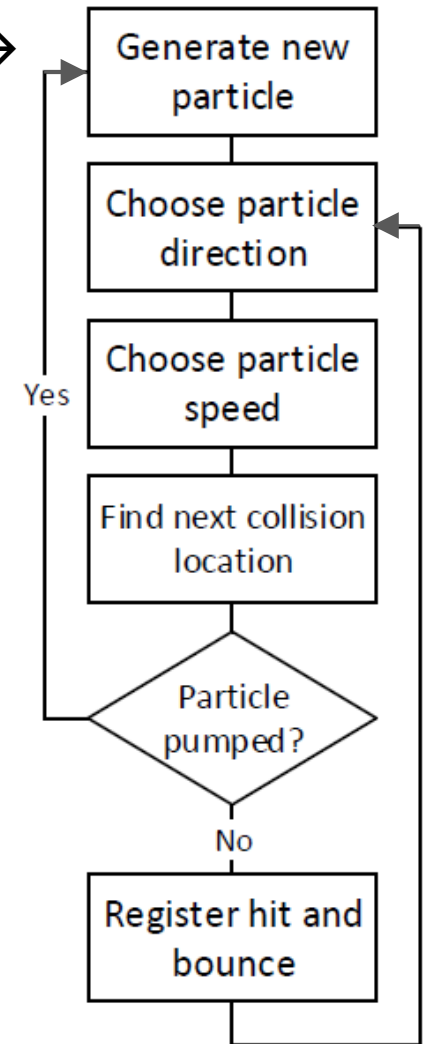
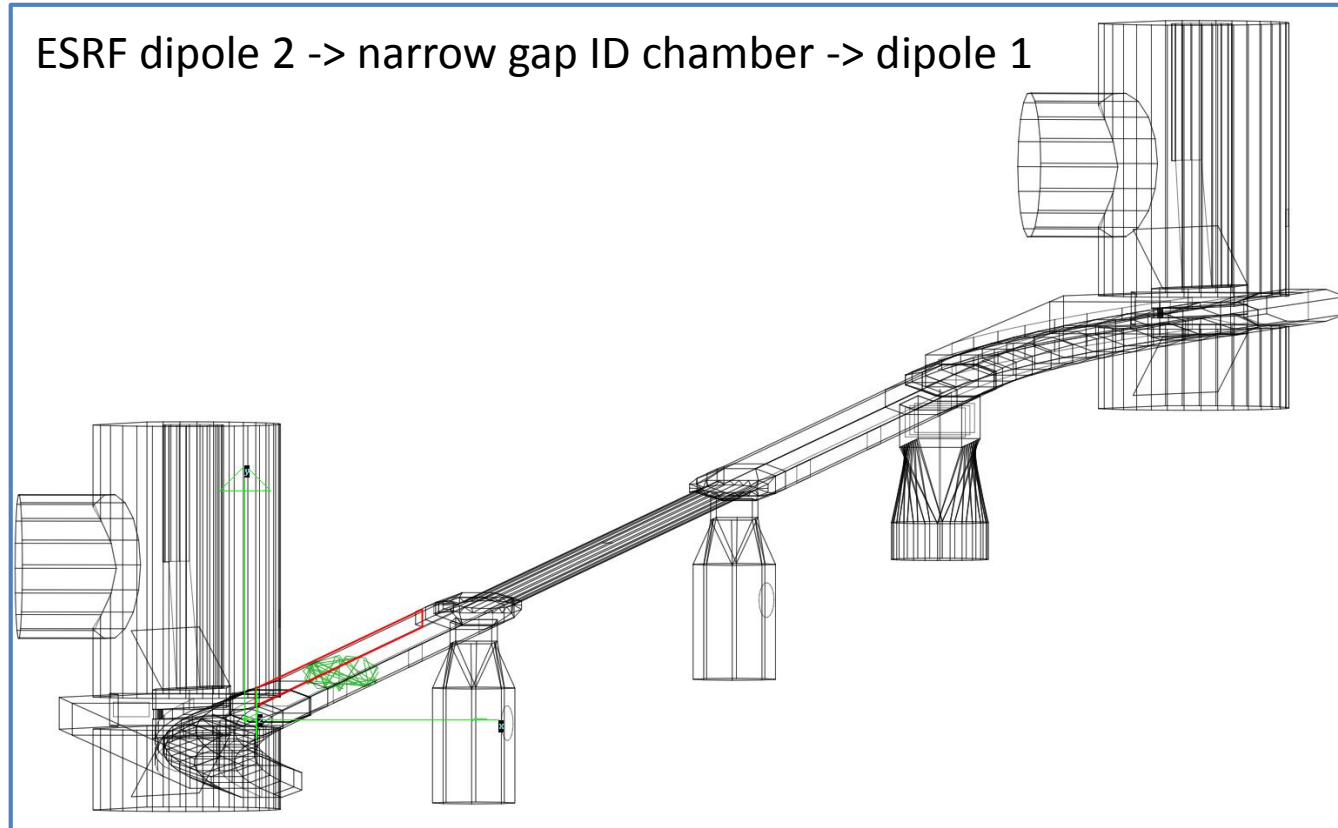
The image shows a screenshot of the Molflow+ website. The top navigation bar includes 'NEWS', 'ABOUT', 'DOWNLOADS', 'DOCUMENTATION', 'FORUM', 'LICENSE', and 'DEVELOPERS'. A main menu is visible on the left side of the page, listing 'News', 'About', 'Downloads' (with sub-items for MolFlow, SynRad, and McCryoT), 'Documentation' (with sub-items for Molflow, SynRad, and McCryoT), 'Changelog', 'Forum', 'License', and 'Developers'. The main content area features a 3D wireframe model of a complex vacuum chamber with several cylindrical ports. Below the model, there are two article teasers: 'Moving parts' and 'Attaching files and images in comments'. A search bar is located at the top right of the page, and a 'Home' button is visible below the navigation bar.

On **Molflow+** and the companion code **SYNRAD+**, please see the excellent reference “**Monte Carlo simulations of Ultra High Vacuum and Synchrotron Radiation for particle accelerators**”, M. Ady, CERN, doctoral dissertation at EPFL, Lausanne, CH, May 2016; Downloadable at <https://cds.cern.ch/record/2157666?ln=en>

Block diagram of the TPMC/ray-tracing algorithm:

Once a geometrical model of the vacuum system is defined, then... →

ESRF dipole 2 → narrow gap ID chamber → dipole 1



2. Basics of synchrotron radiation

Discovery of Synchrotron Radiation

1947, General Dynamics, Schenectady (NY), USA

70 MeV ring, tabletop size

The vacuum chamber was made of glass:

The discovery of synchrotron radiation is an interesting case history in the nature of scientific discovery: It was made possible by a trivial design change and by a conscious disregard for the rules of radiation safety. I was a particularly close witness to much of the history; in fact, had I only been more open-minded three years earlier, I might have been a co-discoverer of what would instead now be called "betatron radiation."

Visible light was observed by pure chance, after previous failures (opaque chamber, silver-coated glass, 1945):

Three years later, in the same laboratory, a 70-MeV synchrotron was completed under the direction of Herbert Pollock. At its initial location, it was not completely enclosed by a radiation shield; even more significantly, the doughnut coating was transparent, facilitating placement of electrodes for beam extraction.

Origin of synchrotron radiation

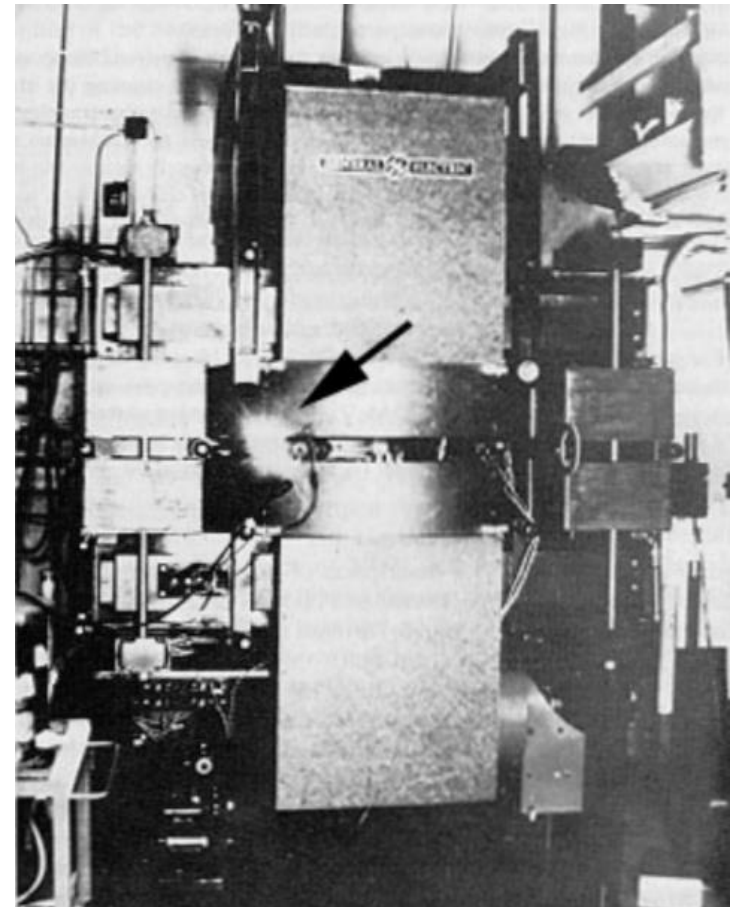
George C. Baldwin, and Donald W. Kerst

Citation: *Physics Today* 28, 1, 9 (1975); doi: 10.1063/1.3068762

View online: <https://doi.org/10.1063/1.3068762>

View Table of Contents: <https://physicstoday.scitation.org/toc/pto/28/1>

Published by the American Institute of Physics



2. Basics of synchrotron radiation

Sources: Schwinger; Sokolov-Ternov;

PHYSICAL REVIEW

VOLUME 75, NUMBER 12

JUNE 15, 1949

On the Classical Radiation of Accelerated Electrons

JULIAN SCHWINGER
Harvard University, Cambridge, Massachusetts
(Received March 8, 1949)

This paper is concerned with the properties of the radiation from a high energy accelerated electron, as recently observed in the General Electric synchrotron. An elementary derivation of the total rate of radiation is first presented, based on Larmor's formula for a slowly moving electron, and arguments of relativistic invariance. We then construct an expression for the instantaneous power radiated by an electron moving along an arbitrary, prescribed path. By casting this result into various forms, one obtains the angular distribution, the spectral distribution, or the combined angular and spectral distributions of the radiation. The method is based on an examination of the rate at which the electron irreversibly transfers energy to the electromagnetic field, as determined by half the difference of retarded and advanced electric field intensities. Formulas are obtained for an arbitrary charge-current distribution and then specialized to a point charge. The total radiated power and its angular distribution are obtained for an arbitrary trajectory. It is found that the direc-

tion of motion is a strongly preferred direction of emission at high energies. The spectral distribution of the radiation depends upon the detailed motion over a time interval large compared to the period of the radiation. However, the narrow cone of radiation generated by an energetic electron indicates that only a small part of the trajectory is effective in producing radiation observed in a given direction, which also implies that very high frequencies are emitted. Accordingly, we evaluate the spectral and angular distributions of the high frequency radiation by an energetic electron, in their dependence upon the parameters characterizing the instantaneous orbit. The average spectral distribution, as observed in the synchrotron measurements, is obtained by averaging the electron energy over an acceleration cycle. The entire spectrum emitted by an electron moving with constant speed in a circular path is also discussed. Finally, it is observed that quantum effects will modify the classical results here obtained only at extraordinarily large energies.

EARLY in 1945, much attention was focused on the design of accelerators for the production of very high energy electrons and other charged particles.¹ In connection with this activity, the author investigated in some detail the limitations to the attainment of high energy electrons imposed by the radiative energy loss² of the accelerated electrons. Although the results of this work were communicated to various interested persons,^{3,4} no serious attempt at publication⁵ was made. However, recent experiments on the radiation from the General Electric synchrotron⁶ have made it desirable to publish the portion of the investigation that is concerned with the properties of the radiation from individual electrons, apart from the considerations on the practical attainment of very high energies. Accordingly, we derive various properties of the radiation from a high energy accelerated electron; the comparison with experiment has been given in the paper by Elder, Langmuir, and Pollock.

I. GENERAL FORMULAS

Before launching into the general discussion, it is well to notice an elementary derivation of the total rate of radiation, based on Larmor's classical formula for a slowly moving electron, and arguments of relativistic invariance. The Larmor formula for the power radiated by an electron that

is instantaneously at rest is

$$P = \frac{2}{3} \frac{e^2}{c^3} \left(\frac{d\mathbf{v}}{dt} \right)^2 = \frac{2}{3} \frac{e^2}{m^2 c^3} \left(\frac{d\mathbf{p}}{dt} \right)^2. \quad (1.1)$$

Now, radiated energy and elapsed time transform in the same manner under Lorentz transformations, whence the radiated power must be an invariant. We shall have succeeded in deriving a formula for the power radiated by an electron of arbitrary velocity if we can exhibit an invariant that reduces to (1.1) in the rest system of the electron. To accomplish this, we first replace the time derivative by the derivative with respect to the invariant proper time. The differential of proper time is defined by

$$ds^2 = dt^2 - 1/c^2(dx^2 + dy^2 + dz^2),$$

or

$$ds = (1 - v^2/c^2)^{1/2} dt. \quad (1.2)$$

Secondly, we replace the square of the proper time derivative of the momentum by the invariant combination

$$\left(\frac{d\mathbf{p}}{ds} \right)^2 - 1/c^2 (dE/ds)^2.$$

Hence, as the desired invariant generalization of (1.1), we have

$$P = \frac{2}{3} \frac{e^2}{m^2 c^3} \left[\left(\frac{d\mathbf{p}}{ds} \right)^2 - \frac{1}{c^2} \left(\frac{dE}{ds} \right)^2 \right]$$

$$= \frac{2}{3} \frac{e^2}{m^2 c^3} \left(\frac{E}{mc^2} \right)^2 \left[\left(\frac{d\mathbf{p}}{dt} \right)^2 - \frac{1}{c^2} \left(\frac{dE}{dt} \right)^2 \right]. \quad (1.3)$$

The conventional form of this result is obtained on

¹ See L. I. Schiff, Rev. Sci. Inst. 17, 6 (1946).

² D. Iwanenko and I. Pomeranchuk, Phys. Rev. 65, 343 (1944).

³ Edwin M. McMillan, Phys. Rev. 68, 144 (1945).

⁴ John P. Blewett, Phys. Rev. 69, 87 (1946).

⁵ Julian Schwinger, Phys. Rev. 70, 798 (1946).

⁶ Elder, Langmuir, and Pollock, Phys. Rev. 74, 52 (1948).

1912

Fundamental paper by J Schwinger:

it gave for the first time quantitative and qualitative insights into the properties of radiation emitted by relativistic charged particles moving in a magnetic field.

Followed by second paper...

PHYSICAL REVIEW D

VOLUME 7, NUMBER 6

15 MARCH 1973

Classical Radiation of Accelerated Electrons. II. A Quantum Viewpoint*

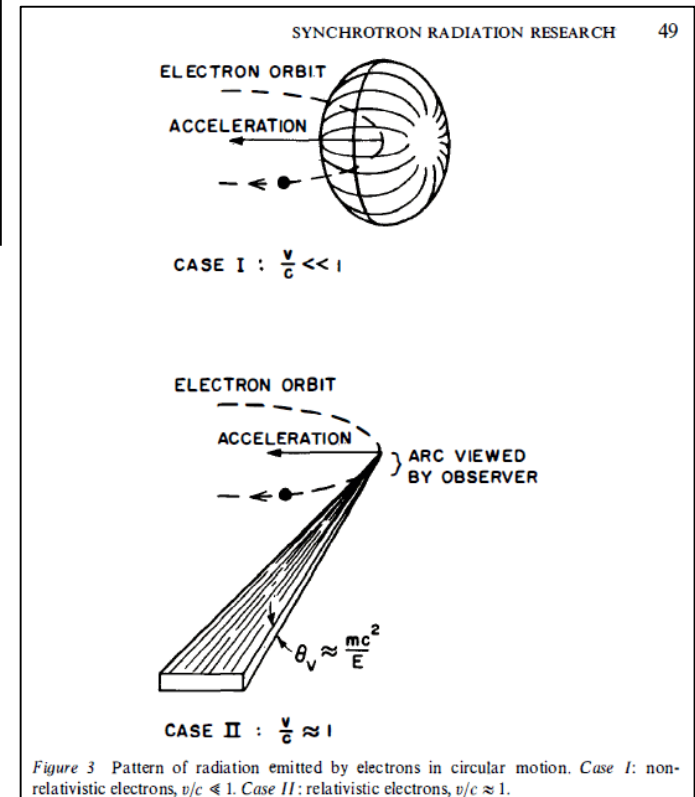
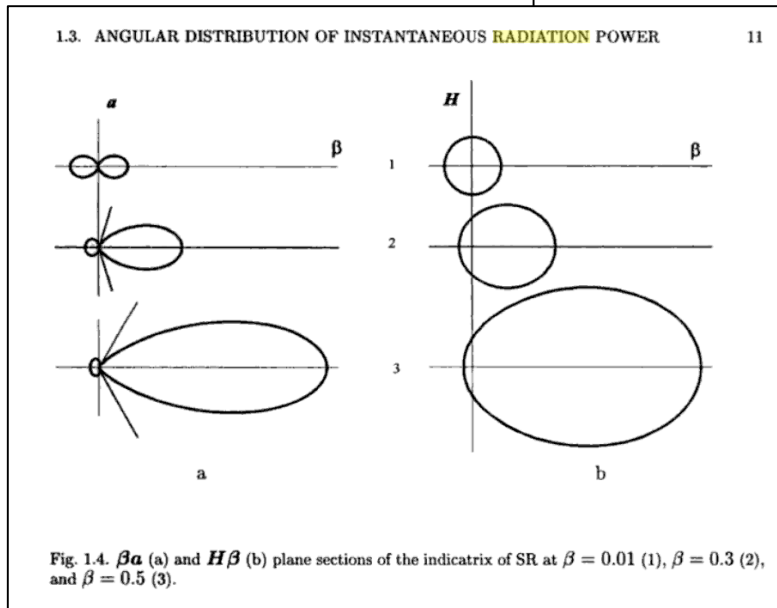
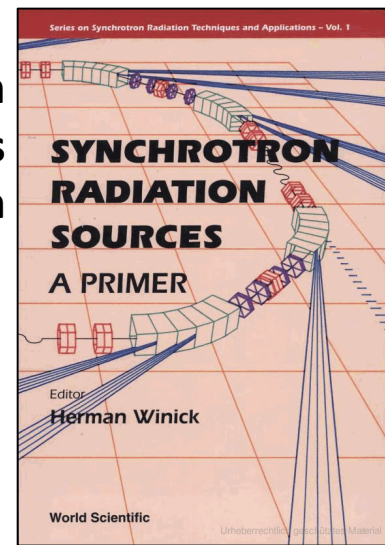
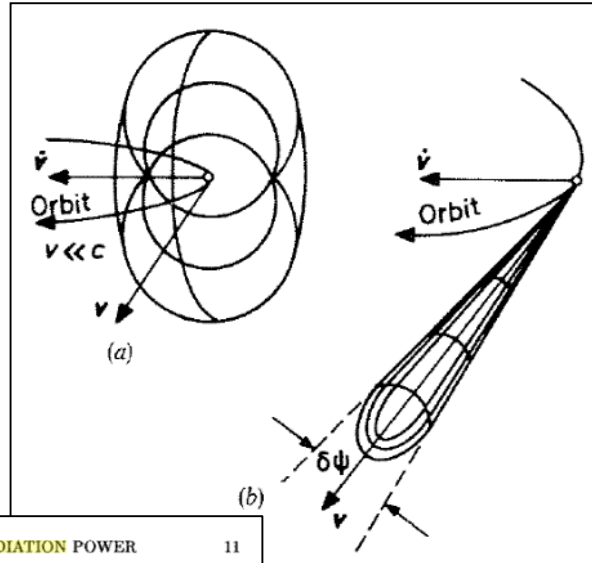
Julian Schwinger
University of California, Los Angeles, California 90024
(Received 27 November 1972)

The known classical radiation spectrum of a high-energy charged particle in a homogeneous magnetic field is rederived. The method applies, and illuminates, an exact (to order α) expression for the inverse propagation function of a spinless particle in a homogeneous field. An erratum list for paper I is appended.

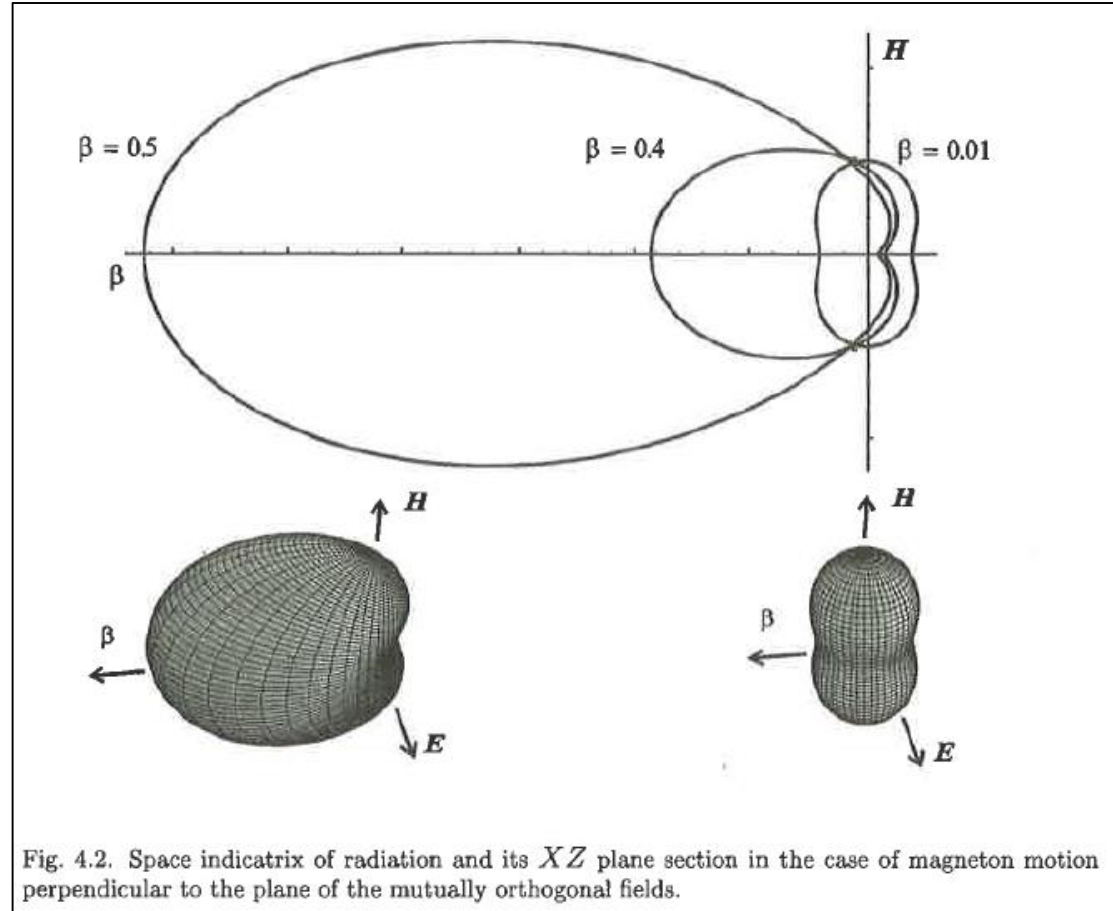
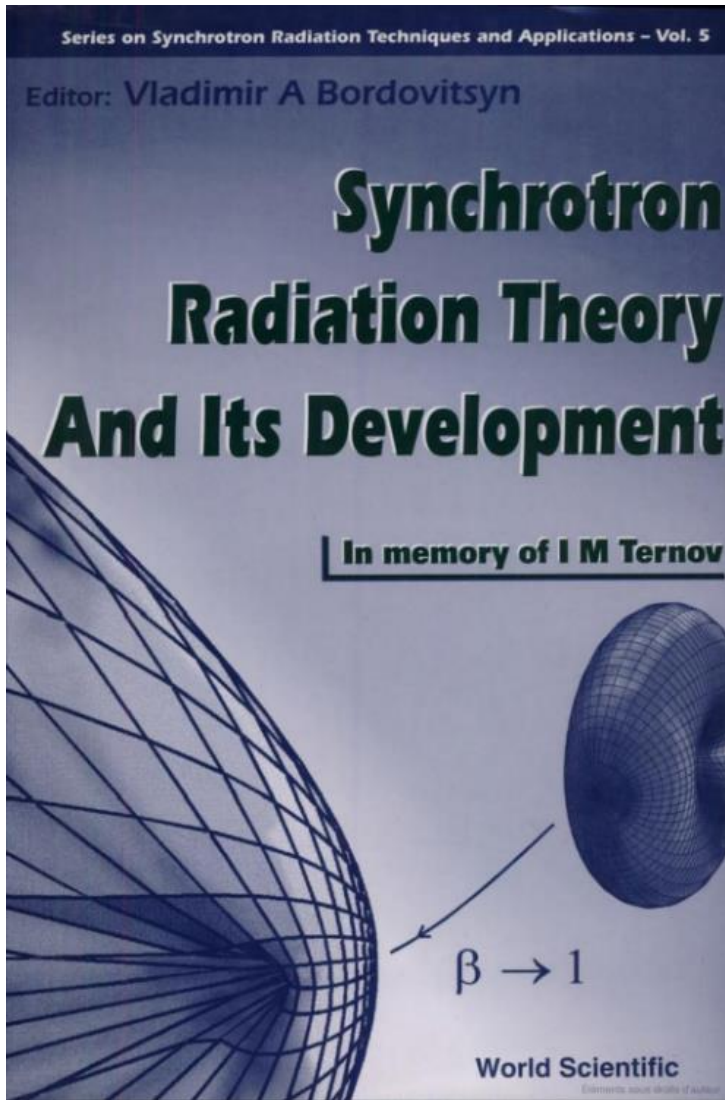
... while in the meantime Sokolov and Ternov in the USSR had come to similar results expanding the breadth of knowledge (radiative polarization of electrons and positrons in a magnetic field).

2. Basics of synchrotron radiation

As the velocity v increases, the emission of photons from an electron subjected to an acceleration perpendicular to its velocity vector changes and goes from being “isotropic” to being highly skewed and collimated in the forward direction



2. Basics of synchrotron radiation



Relativistic factor: $\gamma = \frac{1}{\sqrt{1 - \frac{v^2}{c^2}}}$

Practical Formulae, as a function of relativistic factor γ :

Integrated Photon Flux, F : $F = 4.1289 \cdot 10^{14} \cdot \gamma \cdot I(\text{mA}) \cdot k_F$ (ph/s/mA)

Integrated Photon Power, P : $P = 6.0344 \cdot 10^{-12} \cdot \frac{\gamma^4}{\rho(\text{m})} \cdot I(\text{mA}) \cdot k_P$ (W/mA)

Critical Energy, e_{crit} : $e_{\text{crit}} = 2.9596 \cdot 10^{-7} \cdot \frac{\gamma^3}{\rho(\text{m})}$ (eV)

As a function of beam energy (GeV), for e-/e+ machines:

$$F = 8.08 \cdot 10^{17} \cdot E(\text{GeV}) \cdot I(\text{mA}) \cdot k_F$$

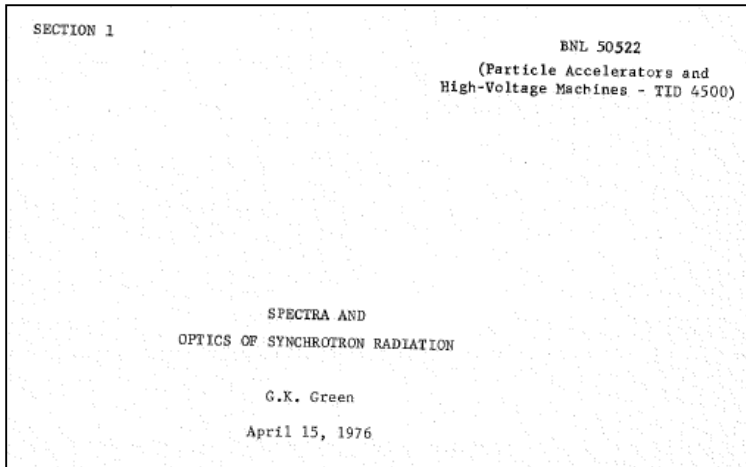
$$P = 88.46 \cdot \frac{E(\text{GeV})^4}{\rho(\text{m})} \cdot I(\text{mA}) \cdot k_P$$

$$e_{\text{crit}} = 2218 \cdot \frac{E(\text{GeV})^3}{\rho(\text{m})}$$

k_f, k_p = fraction of photon flux and power with energy above given energy threshold (see next slide);

2. Basics of synchrotron radiation

Photon distributions: power- and flux-wise



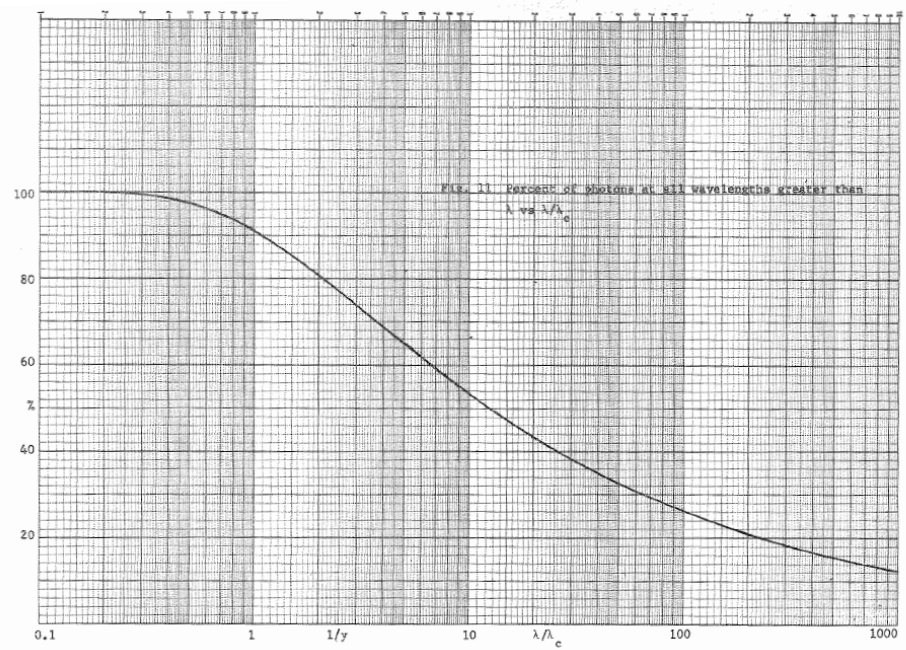
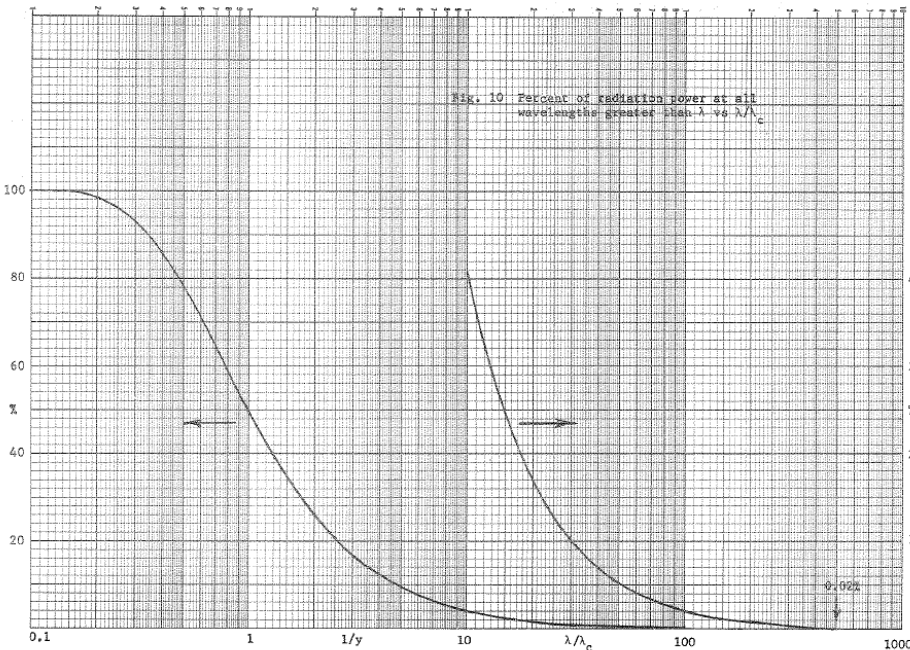
- **POWER:** the critical energy is the median of the SR power distribution: $\frac{1}{2}$ of the power at photon energies ABOVE e_c , $\frac{1}{2}$ BELOW
- **FLUX:** only 9% of the SR photons are generated above e_c .

→ Most photons have low energy! ←

Average photon energy: $0.30792 \cdot e_c$

Percent of FLUX at all wavelengths greater than λ vs λ/λ_c .

Percent of POWER at all wavelengths greater than λ vs λ/λ_c .



Photon distributions: Sources: X-Ray Data Booklet, LBNL; "Spectra and Optics of SR", BNL

LBNL/PUB-490 Rev. 3

Center for X-Ray Optics
and
Advanced Light Source

X-RAY DATA BOOKLET

Albert Thompson	Ingolf Lindau
David Attwood	Yanwei Liu
Eric Gullikson	Piero Pianetta
Malcolm Howells	Arthur Robinson
Kwang-Je Kim	James Scofield
Janos Kirz	James Underwood
Jeffrey Kortright	Gwyn Williams
Herman Winick	

October 2009

Lawrence Berkeley National Laboratory
University of California
Berkeley, CA 94720

This work was supported in part by the U.S. Department
of Energy under Contract No. DE-AC02-05CH11231

SECTION 1

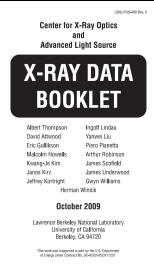
BNL 50522
(Particle Accelerators and
High-Voltage Machines - TID 4500)

SPECTRA AND
OPTICS OF SYNCHROTRON RADIATION

G.K. Green
April 15, 1976

ACCELERATOR DEPARTMENT
BROOKHAVEN NATIONAL LABORATORY
ASSOCIATED UNIVERSITIES, INC.
UPTON, NEW YORK 11973
under contract No. E(30-1)-16 with the
UNITED STATES ENERGY RESEARCH AND DEVELOPMENT ADMINISTRATION

Photon distributions: Sources: X-Ray Data Booklet, LBNL; “Spectra and Optics of SR”, BNL



SECTION 2
SYNCHROTRON RADIATION

2.1A CHARACTERISTICS OF SYNCHROTRON RADIATION

Kwang-Je Kim

Synchrotron radiation occurs when a charge moving at relativistic speeds follows a curved trajectory. In this section, formulas and supporting graphs are used to quantitatively describe characteristics of this radiation for the cases of circular motion (bending magnets) and sinusoidal motion (periodic magnetic structures).

We will first discuss the ideal case, where the effects due to the angular divergence and the finite size of the electron beam—the emittance effects—can be neglected.

A. BENDING MAGNETS

The angular distribution of radiation emitted by electrons moving through a bending magnet with a circular trajectory in the horizontal plane is given by

$$\frac{d^2\mathcal{G}_B(\omega)}{d\theta d\psi} = \frac{3\alpha}{4\pi^2} \gamma^2 \frac{\Delta\omega I}{\omega e} y^2 (1 + X^2)^2 \times \left[K_{2/3}^2(\xi) + \frac{X^2}{1 + X^2} K_{1/3}^2(\xi) \right] \quad (1)$$

2-2

where

- \mathcal{G}_B = photon flux (number of photons per second)
- θ = observation angle in the horizontal plane
- ψ = observation angle in the vertical plane
- α = fine-structure constant
- γ = electron energy/ $m_e c^2$ (m_e = electron mass, c = velocity of light)
- ω = angular frequency of photon ($\varepsilon = \hbar \omega$ = energy of photon)
- I = beam current
- e = electron charge = 1.602×10^{-19} coulomb
- y = $\omega/\omega_c = \varepsilon/\varepsilon_c$
- ω_c = critical frequency, defined as the frequency that divides the emitted power into equal halves, $= 3\gamma^3 c/2\rho$
- ρ = radius of instantaneous curvature of the electron trajectory (in practical units, $\rho[\text{m}] = 3.3 E[\text{GeV}]/B[\text{T}]$)
- E = electron beam energy
- B = magnetic field strength
- $\varepsilon_c = \hbar \omega_c$ (in practical units, $\varepsilon_c [\text{keV}] = 0.665 E^2 [\text{GeV}] B[\text{T}]$)
- $X = \gamma\psi$
- $\xi = y(1 + X^2)^{3/2}/2$

The subscripted K 's are modified Bessel functions of the second kind. In the horizontal direction ($\psi = 0$), Eq. (1) becomes

$$\left. \frac{d^2\mathcal{G}_B}{d\theta d\psi} \right|_{\psi=0} = \frac{3\alpha}{4\pi^2} \gamma^2 \frac{\Delta\omega I}{\omega e} H_2(y), \quad (2)$$

where

$$H_2(y) = y^2 K_{2/3}^2(y/2) \quad (3)$$

In practical units [photons \cdot s $^{-1}$ \cdot m r^{-2} \cdot (0.1% bandwidth) $^{-1}$],

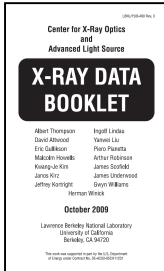
$$\left. \frac{d^2\mathcal{G}_B}{d\theta d\psi} \right|_{\psi=0} = 1.327 \times 10^{13} E^2 [\text{GeV}] I [\text{A}] H_2(y).$$

The function $H_2(y)$ is shown in Fig. 2-1.

From now on, θ is the horizontal observation angle, and ψ the vertical one, with respect to the plane of the orbit

2. Basics of synchrotron radiation

Sources: X-Ray Data Booklet, LBNL; "Spectra and Optics of SR", BNL



2-3

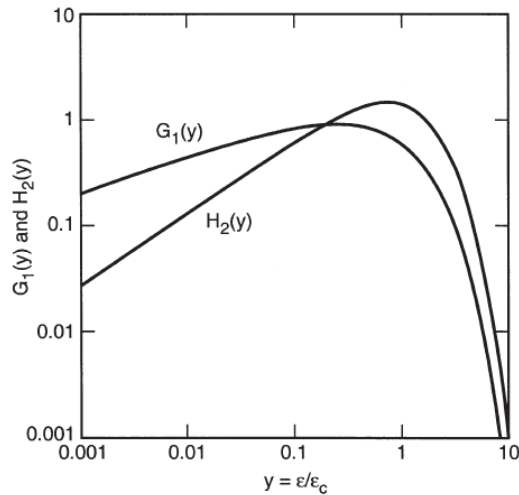


Fig. 2-1. The functions $G_1(y)$ and $H_2(y)$, where y is the ratio of photon energy to critical photon energy.

The distribution integrated over ψ is given by

$$\frac{d^3\mathcal{N}_B}{d\theta} = \frac{\sqrt{3}}{2\pi} \alpha\gamma \frac{\Delta\omega}{\omega} \frac{I}{e} G_1(y), \quad (4)$$

where

$$G_1(y) = y \int_y^\infty K_{5/3}(y') dy' \quad (5)$$

In practical units [photons \cdot s $^{-1}$ \cdot m $^{-1}$ \cdot (0.1% bandwidth) $^{-1}$],

$$\frac{d^3\mathcal{N}_B}{d\theta} = 2.457 \times 10^{13} E[\text{GeV}] I[\text{A}] G_1(y).$$

The function $G_1(y)$ is also plotted in Fig. 2-1.

Radiation from a bending magnet is linearly polarized when observed in the bending plane. Out of this plane, the polarization is elliptical and can be decomposed into its horizontal and vertical components. The first

2-4

and second terms in the last bracket of Eq. (1) correspond, respectively, to the intensity of the horizontally and vertically polarized radiation. Figure 2-2 gives the normalized intensities of these two components, as functions of emission angle, for different energies. The square root of the ratio of these intensities is the ratio of the major and minor axes of the polarization ellipse. The sense of the electric field rotation reverses as the vertical observation angle changes from positive to negative.

Synchrotron radiation occurs in a narrow cone of nominal angular width $\sim 1/\gamma$. To provide a more specific measure of this angular width, in terms of electron and photon energies, it is convenient to introduce the effective rms half-angle σ_ψ as follows:

$$\left. \frac{d^3\mathcal{N}_B}{d\theta} \frac{d^2\mathcal{N}_B}{d\theta d\psi} \right|_{\psi=0} = \sqrt{2\pi} \sigma_\psi, \quad (6)$$

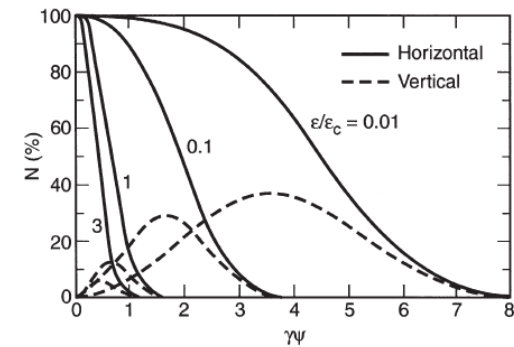


Fig. 2-2. Normalized intensities of horizontal and vertical polarization components, as functions of the vertical observation angle ψ , for different photon energies. (Adapted from Ref. 1.)

From now on, θ is the horizontal observation angle, and Ψ the vertical one, with respect to the plane of the orbit

2. Basics of synchrotron radiation

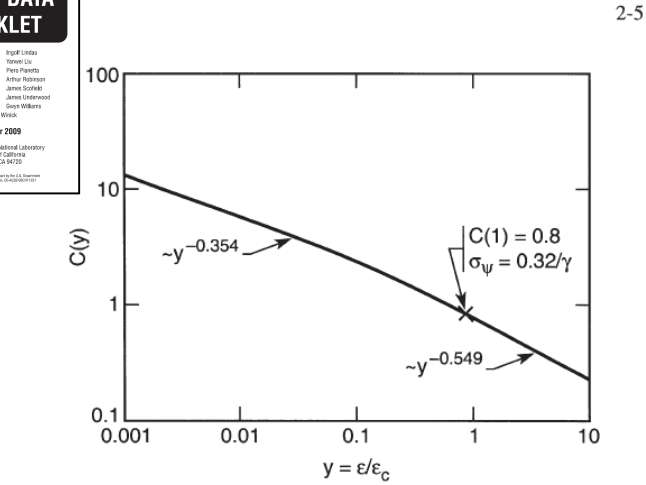


Fig. 2-3. The function $C(y)$. The limiting slopes, for $\epsilon/\epsilon_c \ll 1$ and $\epsilon/\epsilon_c \gg 1$, are indicated.

where σ_ψ is given by

$$\sigma_\psi = \frac{2}{\gamma\sqrt{2\pi}} C(y) = 0.408 \frac{C(y)[\text{mrad}]}{E[\text{GeV}]} \quad (7)$$

The function $C(y)$ is plotted in Fig. 2-3. In terms of σ_ψ , Eq. (2) may now be rewritten as

$$\left. \frac{d^2 \bar{r}_B}{d\theta d\psi} \right|_{\psi=0} = \frac{d \bar{r}_B}{d\theta} \frac{1}{\sigma_\psi \sqrt{2\pi}} \quad (2a)$$

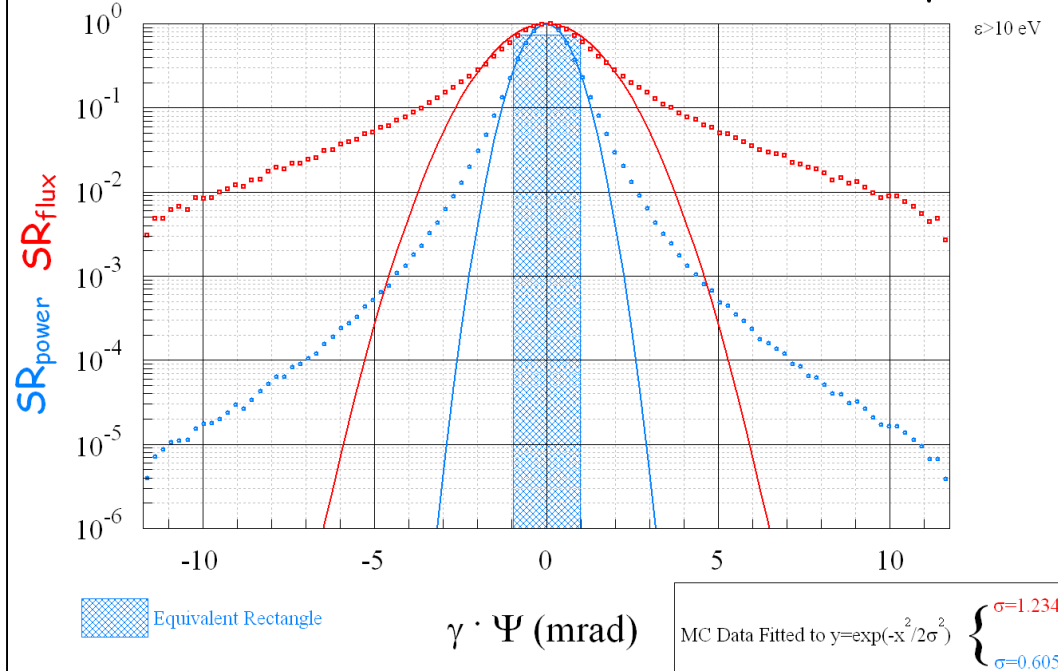
B. PERIODIC MAGNETIC STRUCTURES

In a wiggler or an undulator, electrons travel through a periodic magnetic structure. We consider the case where the magnetic field B varies sinusoidally and is in the vertical direction:

$$B(z) = B_0 \cos(2\pi z/\lambda_u) \quad (8)$$

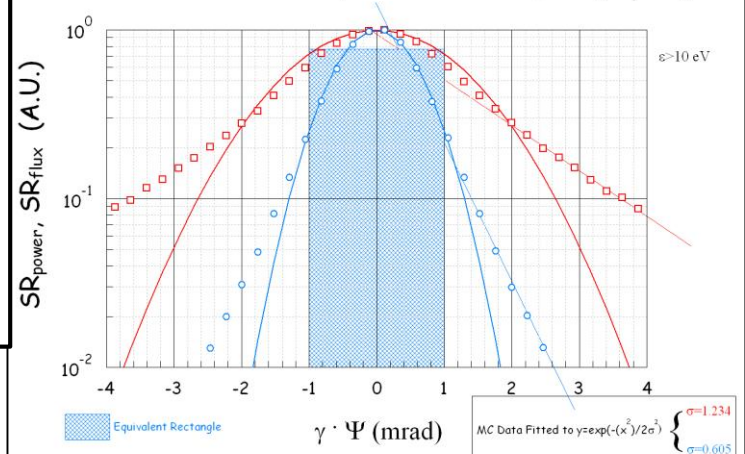
where z is the distance along the wiggler axis, B_0 the peak magnetic field, and λ_u the magnetic period. Electron motion is also sinusoidal and lies in

Vertical Distribution of SR Power and Flux (Dipole)



MC simulation, SYNRAD ->
author;

Vertical Distribution of SR Power and Flux (Dipole)



2. Basics of synchrotron radiation

Source: "Monte Carlo simulations of Ultra High Vacuum and Synchrotron Radiation for particle accelerators", M. Ady, CERN

At $\psi = 0$

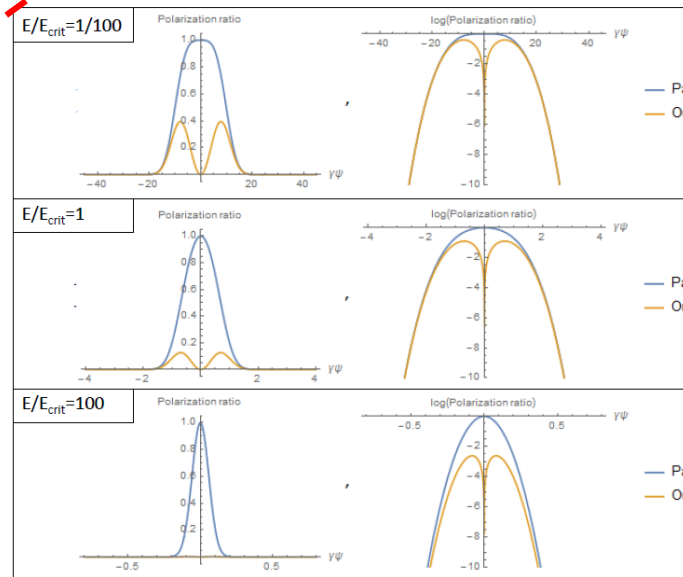
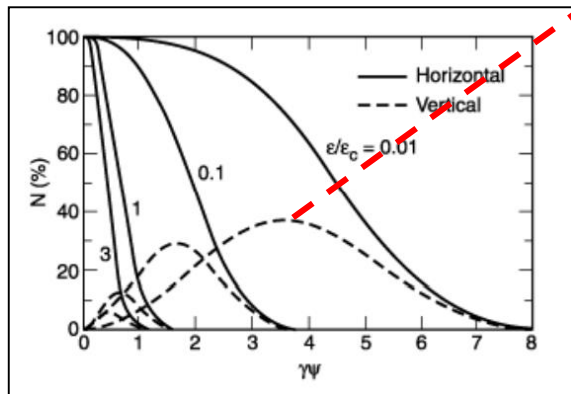
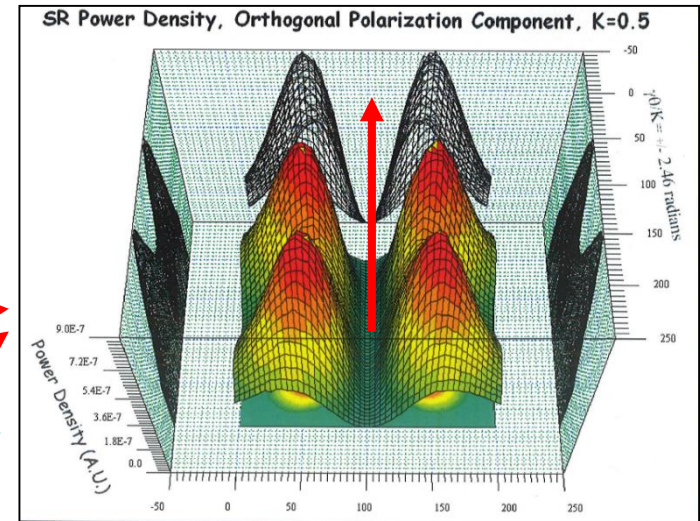
$$F\left(\frac{\lambda_c}{2\lambda}, 0\right) = F_{\parallel}(0) = K_{2/3}^2\left(\frac{\lambda_c}{2\lambda}\right)$$

And generally at angle ψ

$$F_{\parallel}(\psi) = (1 + \gamma^2 \psi^2) K_{2/3}^2\left[\frac{\lambda_c}{2\lambda}(1 + \gamma^2 \psi^2)^{3/2}\right]$$

$$F_{\perp}(\psi) = \gamma^2 \psi^2 (1 + \gamma^2 \psi^2) K_{1/3}^2\left[\frac{\lambda_c}{2\lambda}(1 + \gamma^2 \psi^2)^{3/2}\right]$$

where $K_{1/3}$ and $K_{2/3}$ are modified Bessel functions. We often use the expression *degree of polarization* which is defined as $P_{lin} = (F_{\parallel} - F_{\perp}) / (F_{\parallel} + F_{\perp})$. The solution of this analytic expression can be visualized (see Fig.2.6) on a relative scale where the vertical angle is expressed in units of γ , and with a different X axis range for each energy.



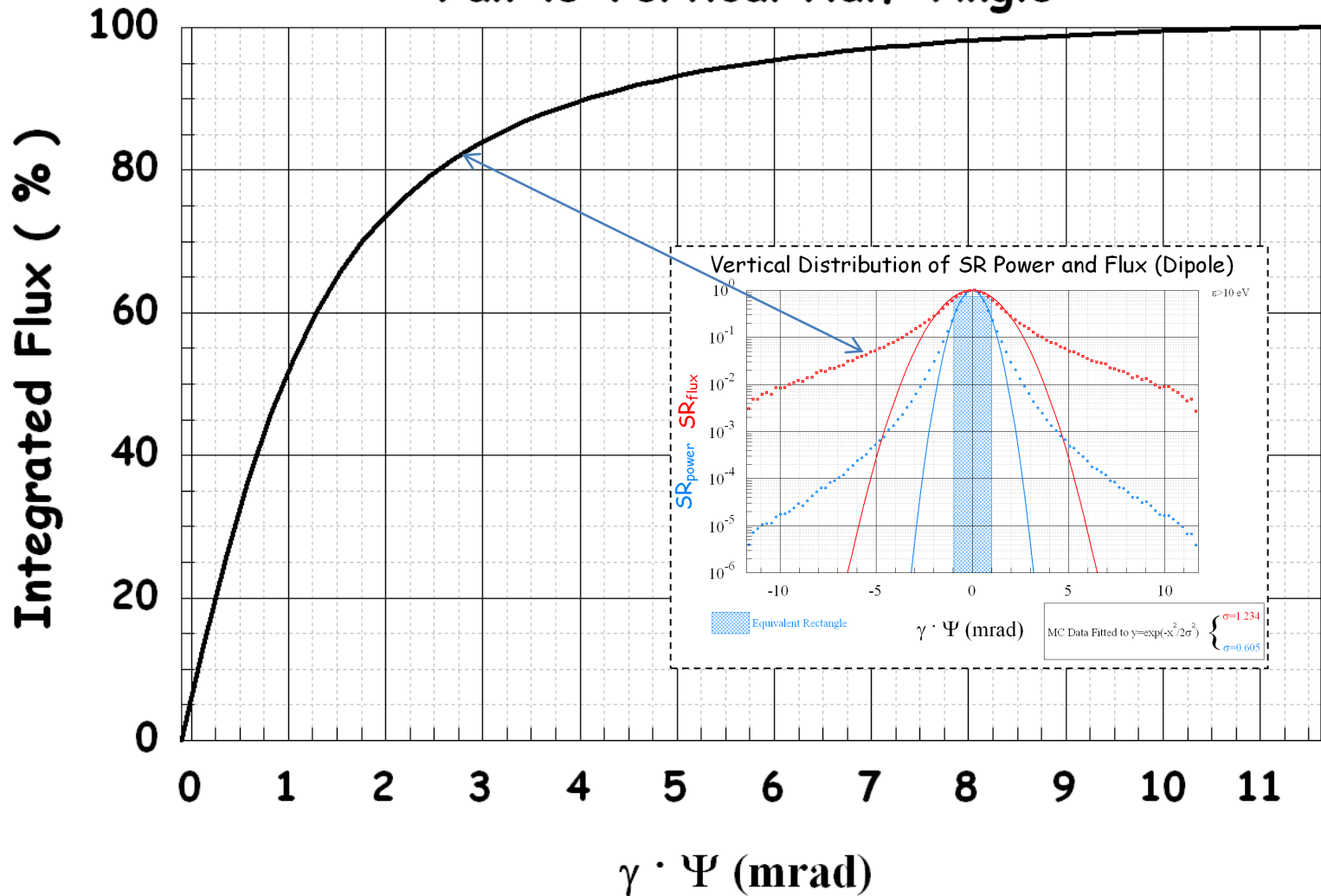
7/8 of the total power is generated as parallel polarization photons, 1/8 only in the perpendicular case;

Figure 2.6: Polarization components for different lambda ratios. Each plot has an X scale that depends on the relative photon energy:

$$\gamma\psi = [-4/(E/E_c)^{0.35} .. +4/(E/E_c)^{0.35}]$$

Left: linear scale, Right: logarithmic scale

Distribution of the Synchrotron Radiation Fan vs Vertical Half-Angle

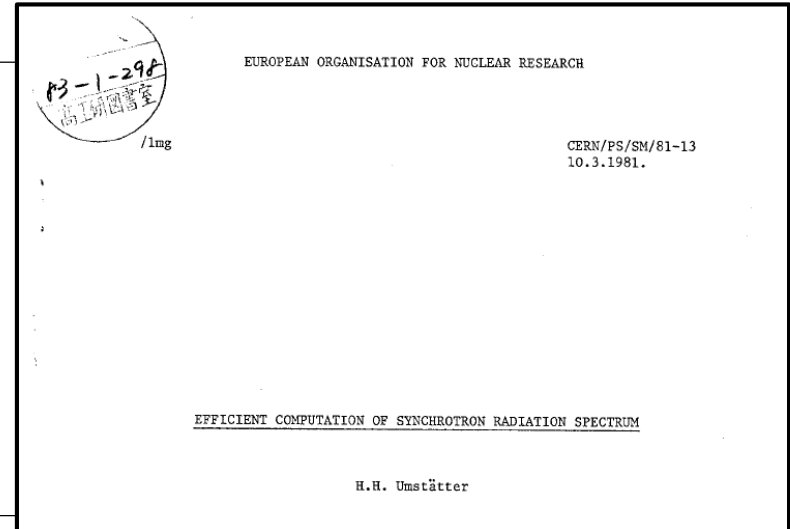


Source: "Efficient computation of synchrotron radiation spectrum", H.H. Umstätter, CERN/PS/SM/81-13, 1981

How can spectra and fluxes be calculated efficiently and fast?

- Several numerical algorithms have been developed during the years:
- This one, is particularly fast:

f) The highest speed is obtained if one computes directly $\int K_{5/3}$ by a Chebyshev series instead of separate computation of $K_{2/3}$ and $\int K_{1/3}$. Since it is not known whether Chebyshev expansion coefficients of $\int K_{5/3}$ exist in the literature they are given in the following listing of subroutine SYNRAD, rounded to 10 digits after the decimal point. Coefficients of 19 - 20 digit precision are given in the following table. They have been computed by linear combination of Luke's coefficients for $K_{2/3}$ and $\int K_{1/3}$. SYNRAD calls no external subroutine and uses no array in order to gain more speed. It is about 400 times faster than method a. On the IBM it evaluates $\int K_{5/3}$ in $7.6 \cdot 10^{-5}$ sec. on the CDC 7600 in $2.6 \cdot 10^{-5}$ sec. (i.e. 38600 values in 1 sec. computing time).



- Note: compared to the CDC 7600 supercomputer of the 70's, the same code running on just one core of a modern multi-core CPU looks like a rocket: 1.6M values/sec vs 38600 values/sec, an improvement of > 40x:

This means that today Montecarlo simulations of SR are affordable even on laptops and desktops.

3. SR-induced desorption

Since SR has been observed for the first time in an accelerator (1949), scientists have immediately realized that X-ray photons of energies higher than few eV were capable of causing desorption of molecules from the walls of the vacuum system, via a number of different phenomena, namely:

- Generation of photo-electrons;
- Direct desorption via X-ray excitation (e.g. Auger);
- Thermal desorption caused by power deposited by SR;
- In order to design the vacuum system of e-/e+ storage rings-- **in particular light sources where the e- beam needs to be stored sometimes for tens of hours without interruptions**--, the scientists developed an experimental program in order to measure carefully the **photon-induced desorption (PID)** yield, usually indicated in literature by the letter η .
- η gives the average number of molecules of a given gas species per incident photon, and allows the designer of the vacuum system to size and space properly the pumping system, a **major input to the budget of a light source**;

Some examples of PID yield measurements: design of 2.75 GeV SOLEIL light source



Photon stimulated desorption of an unbaked stainless steel chamber by 3.75 keV critical energy photons

C. Herbeaux, P. Marin, V. Baglin, and O. Gröbner

Citation: *Journal of Vacuum Science & Technology A* 17, 635 (1999); doi: 10.1116/1.581630

View online: <http://dx.doi.org/10.1116/1.581630>

View Table of Contents: <http://scitation.aip.org/content/avs/journal/jvsta/17/2?ver=pdfcov>

Published by the AVS: Science & Technology of Materials, Interfaces, and Processing

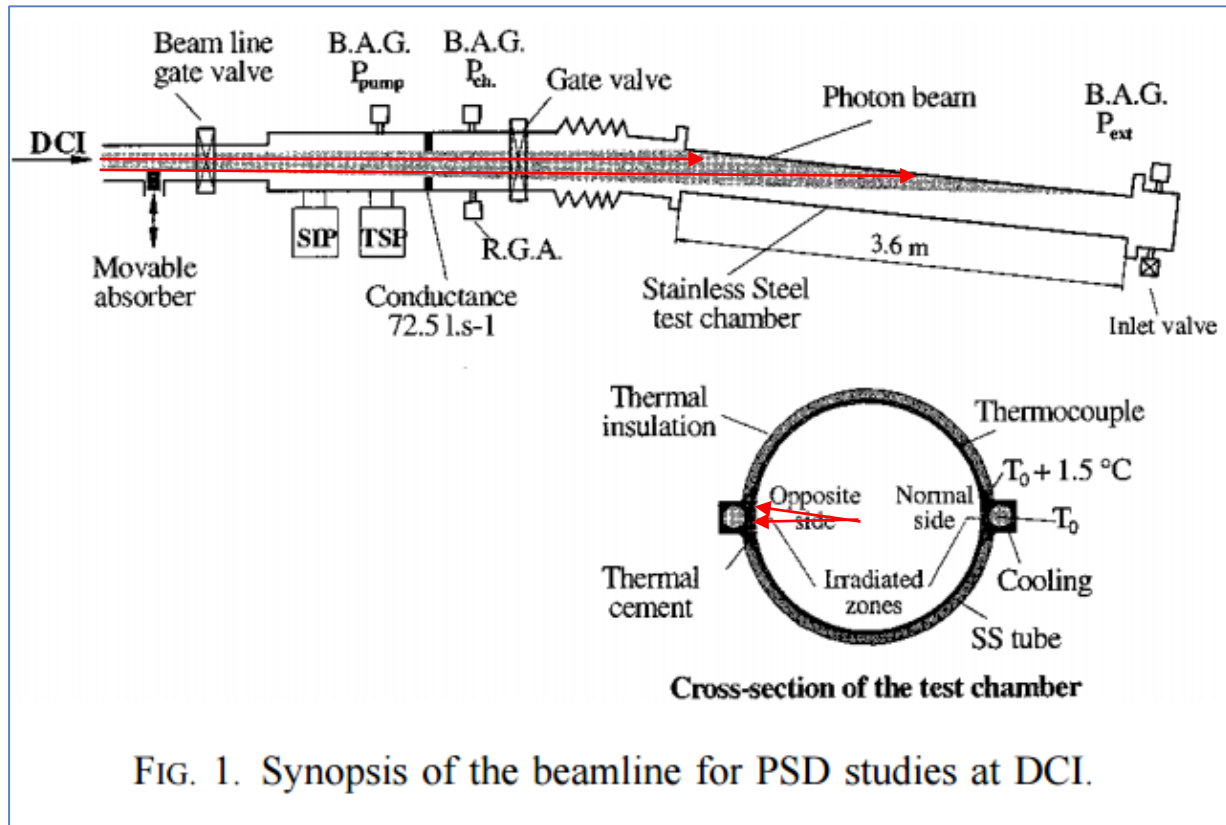


FIG. 1. Synopsis of the beamline for PSD studies at DCI.

3. SR-induced desorption

Some examples of PID yield measurements: design of 2.75 GeV SOLEIL light source

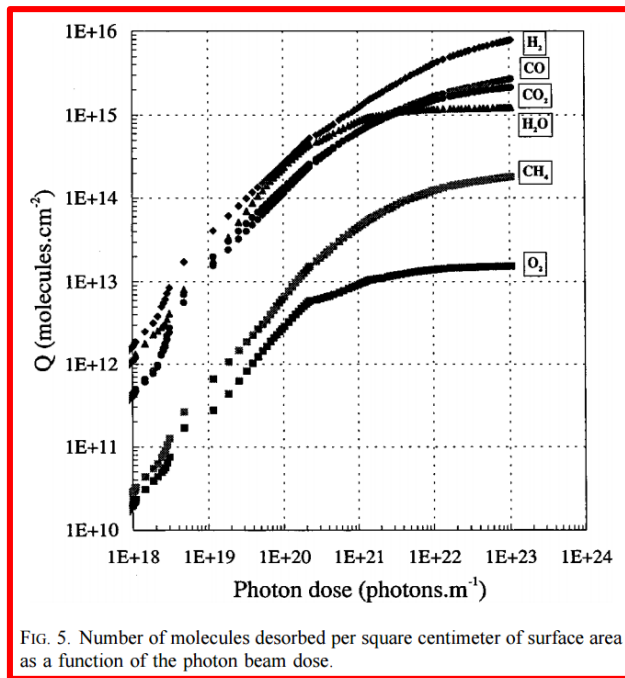
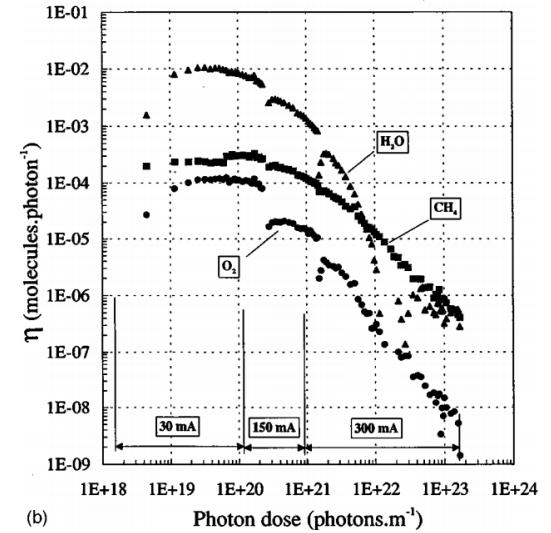
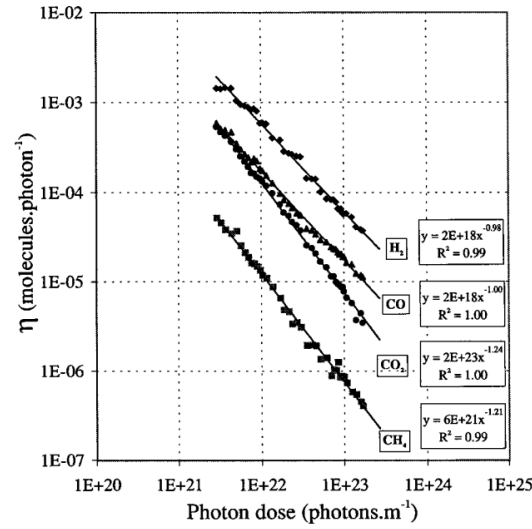
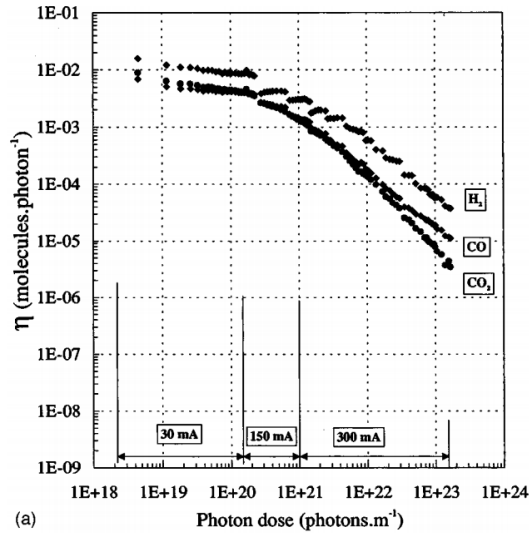


FIG. 5. Number of molecules desorbed per square centimeter of surface area as a function of the photon beam dose.

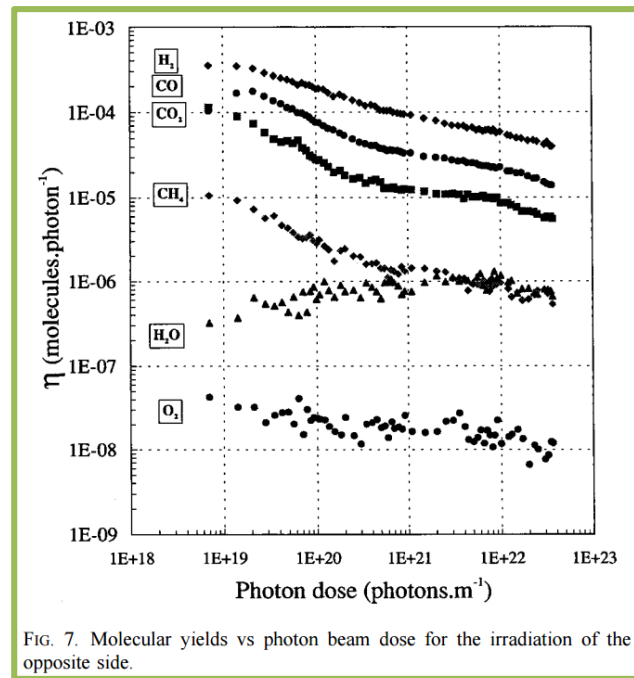


FIG. 7. Molecular yields vs photon beam dose for the irradiation of the opposite side.

Some examples of PID yield measurements: design of 6 GeV ESRF light source

(NEG-coating developments, 1999 onwards)

TUPS002

Proceedings of IPAC2011, San Sebastián, Spain

PHOTODESORPTION MEASUREMENTS AT ESRF D31

H.P. Marques*, G. Debut, M. Hahn, ESRF, Grenoble, France

Abstract

Since 1998 exists at ESRF a dedicated beamline for photodesorption measurement from vacuum chambers - D31. The original goal of this installation was to study the wall pumping effect. When exposed to synchrotron radiation surfaces exhibit strong outgassing of the adsorbed gas layer despite UHV conditions. Long term outgassing leads to the depletion of the adsorbed layer and produces a very clean surface which turns the walls of the vacuum chamber into an active pumping surface.

At D31 have been tested chambers of stainless steel, aluminium and copper, with or without coatings (e.g. NEG, copper), designed by ESRF and other institutes like ALBA, CERN, ELETTRA and Soleil. Here we review some of the results obtained and outline the future plans of D31.

leading to the requirement of additional shielding and thus reducing the availability of the beamline to the users.

PHOTODESORPTION

The first successful models to describe electron stimulated desorption (ESD) or photon stimulated desorption (PSD) where the MGR model, independently proposed by Menzer and Gomer [6] and Redhead[7], and later the Knotek-Feibelman [8] (KF) model. Briefly, in the MGR model an atom is excited to an anti-bonding state and it may gain sufficient kinetic energy so that it overcomes the lower potential barrier of one of the bonding states in the de-excitation pathway. The KF model is based in an interatomic Auger decay. The original excitation leaves a hole in the core level to be filled by an electron from a neighbour atom and, due to Auger decay, further electrons are ejected from the

Draft
group
at LLU

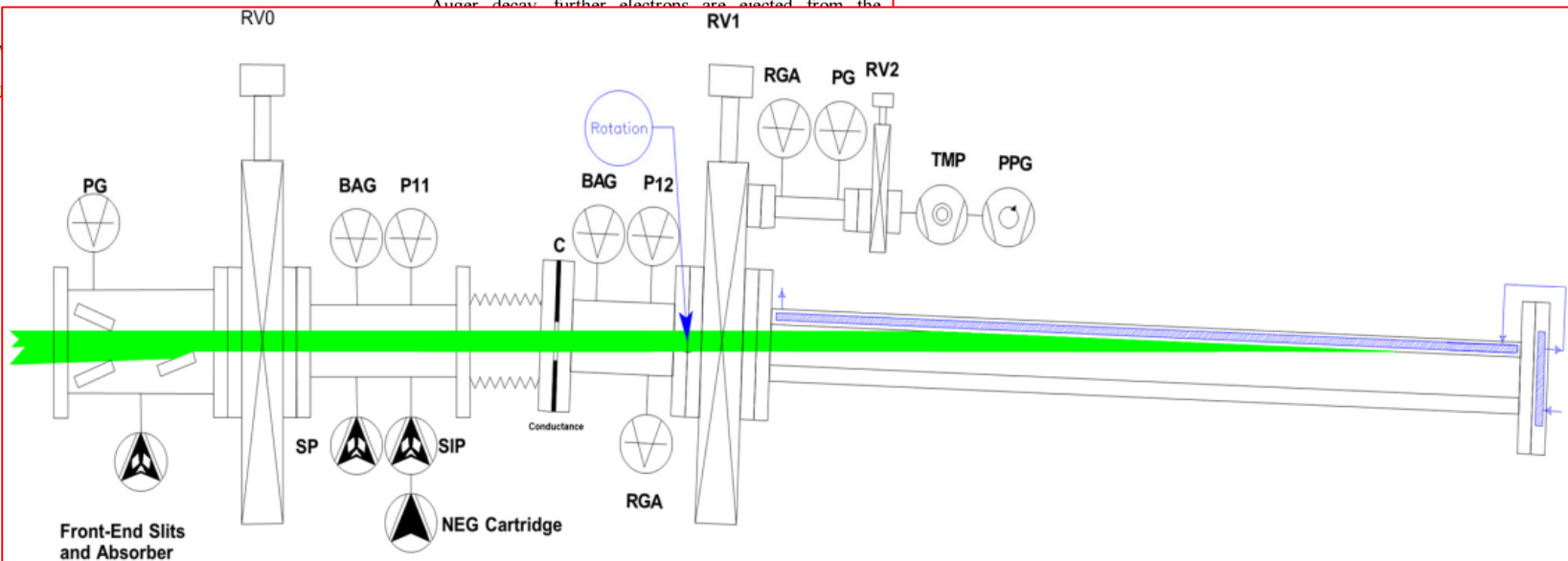
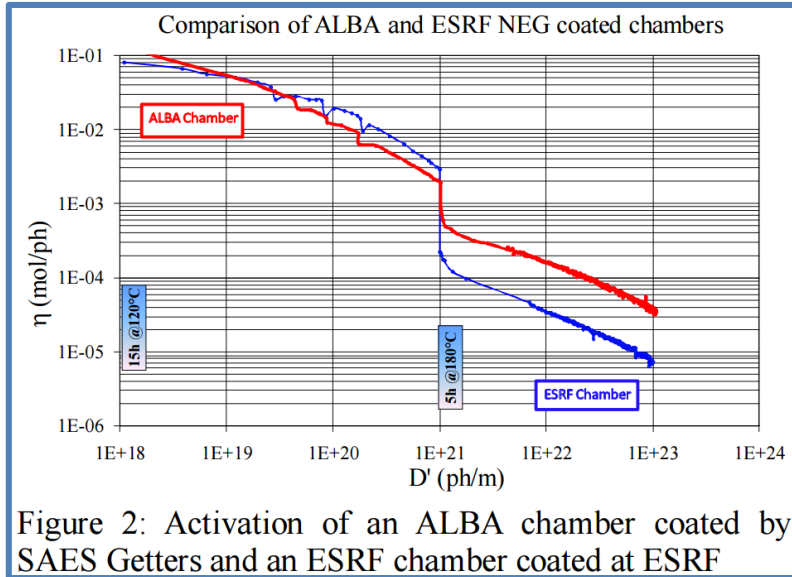


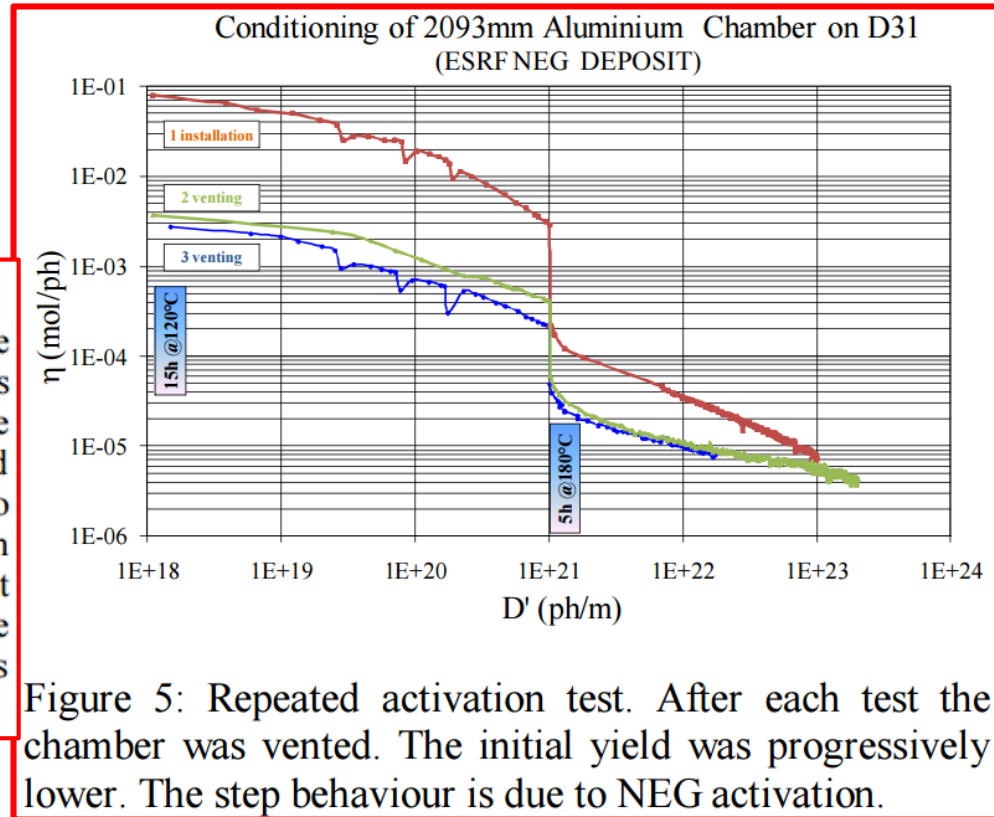
Figure 1: D31 schematics. PG – Pirani gauge; RV – Remote Valve ; SIP – Sputter Ion Pump; BAG – Bayard-Alpert Gauge ; P – Penning Gauge; TMP – Turbo Molecular Pump; PPG – Primary Pumping Group

Some examples of PID yield measurements: design of 6 GeV ESRF light source

(NEG-coating developments, 1999 onwards)

*Memory Effect*

When continually exposed to synchrotron radiation the yield of a surface decreases with accumulated dose. This decrease is in part due to the progressive cleaning of the adsorbed surface layers. In Figure 5 it can be observed that after exposure of a thoroughly irradiated chamber to air its yield, although increasing, remains at a lower than the initial value. Even at the second consecutive venting it can still be observed a small improvement. As such the chamber retains some “memory” of the previous condition.



Question: What happens if the PID yield is not sufficiently low and/or the corresponding pressure profile is too high-- for instance because of lack of pumping speed or conductance limitations?

→ **Beam-gas scattering** ←

Effect on the beam lifetime!

Proceedings of the 1999 Particle Accelerator Conference, New York, 1999

STUDY OF THE BESSY II BEAM LIFETIME *

S. Khan †, BESSY, Berlin, Germany

2 THEORY

In this section, the relations used in the analysis are reviewed. A list of symbols is given in table 1.

The beam lifetime τ is defined by the current decay rate $1/\tau = -\dot{I}/I$, which is the sum of the Touschek (T) rate and the gas scattering (G) rate

$$\frac{1}{\tau} = \frac{1}{\tau_T} + \frac{1}{\tau_G} = \frac{1}{\tau_T} + c n (\sigma_{\text{elast}}^N + \sigma_{\text{inel}}^N + \sigma_{\text{elast}}^e + \sigma_{\text{inel}}^e). \quad (1)$$

The Touschek decay rate can be written as (e.g. [4])

$$\frac{1}{\tau_T} = \frac{N r_e^2 c}{8\pi \sigma_x \sigma_y \sigma_z \gamma^2 (\Delta p/p)^3} \cdot D \left(\frac{(\Delta p/p)^2 \sigma_{x'}^2}{\gamma^2} \right), \quad (2)$$

where $D \approx 0.3$ is a slowly varying function that is evaluated numerically. Relativistic effects and beam polarization modify the Touschek rate on the level of 10-20% [5].

The total cross sections for elastic and inelastic scattering on residual gas nuclei (N) and electrons (e) are [4]

$$\sigma_{\text{elast}}^N = \frac{2\pi r_e^2 Z^2 \bar{\beta} \beta_a}{\gamma^2 a^2} \quad (3)$$

$$\sigma_{\text{inel}}^N = \frac{4r_e^2 Z^2}{137} \frac{4}{3} \left(\ln \frac{183}{Z^{1/3}} \right) \left(\ln \frac{1}{\Delta p/p} - \frac{5}{8} \right) \quad (4)$$

$$\sigma_{\text{elast}}^e = \frac{2\pi r_e^2 Z}{\gamma} \frac{1}{\Delta p/p}$$

$$\sigma_{\text{inel}}^e = \frac{4r_e^2 Z}{137} \frac{4}{3} \left(\ln \frac{2.5\gamma}{\Delta p/p} - 1.4 \right) \left(\ln \frac{1}{\Delta p/p} - \frac{5}{8} \right),$$

The distinctly different dependence of Touschek scattering and inelastic gas scattering on the momentum acceptance $\Delta p/p$ (equations 2 and 4) can be used to distinguish the two effects by changing the rf voltage (which also changes the bunch length). Coulomb scattering is identified by variation of the physical aperture using scrapers.

p here is momentum, not pressure!

Question: What happens if the PID yield is not sufficiently low and/or the corresponding pressure profile is too high-- for instance because of lack of pumping speed?

→ Beam-gas scattering → Generation of **bremsstrahlung (BS) radiation:**

Bremsstrahlung (BS) radiation:

It is a “braking” radiation generated by the e- in the beam interacting with the strong electric field of a proton in the field of a nucleus of a residual gas molecule/atom.

- Depends strongly on the atomic number Z of the gas species: generation of extremely high-energy gamma rays, with upper energy range close to the e- beam energy: $\sim Z(Z+1)$ see further below...
- Consequences: → the vacuum scientist must do his/her best to keep the residual gas composition as close as possible to “pure H_2 ” ($Z=1$), with as low as possible contributions from CH_4 , CO , CO_2 , Ar , etc... ←
- For light sources it is particularly important to keep BS low along the straight sections where experimental beamlines are installed: radiation protection dose limits are more and more stringent!... This has an impact on the availability of a given beamline.
- We’ll come back to this issue later...

3. SR-induced desorption

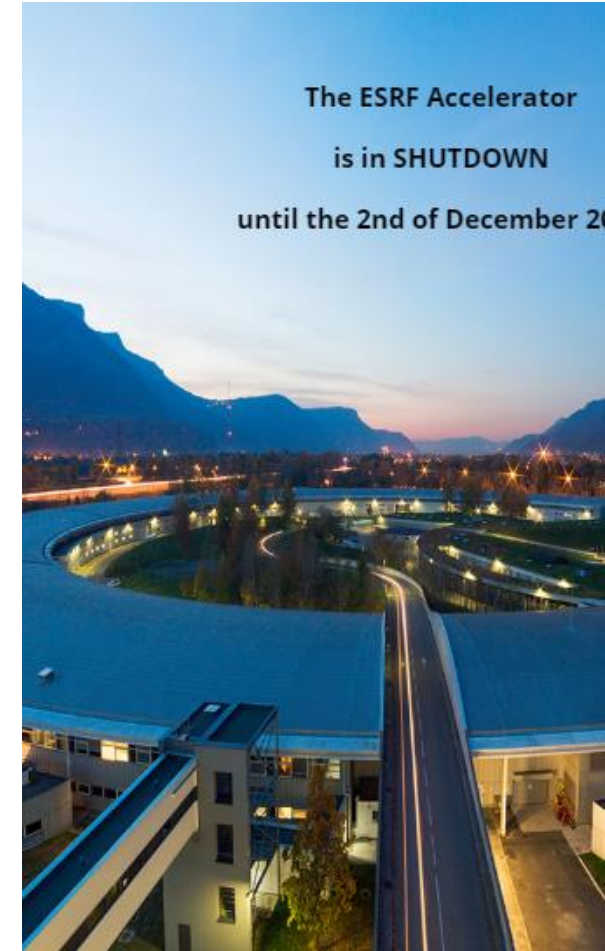
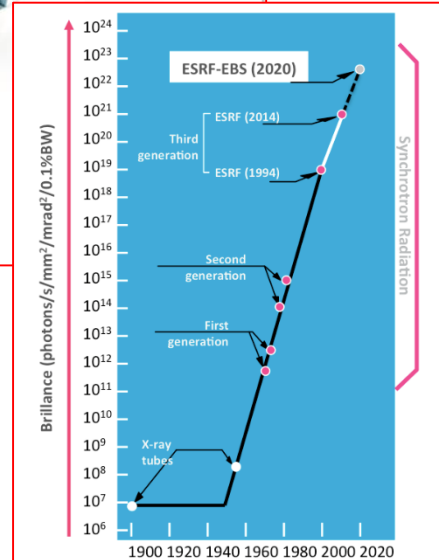
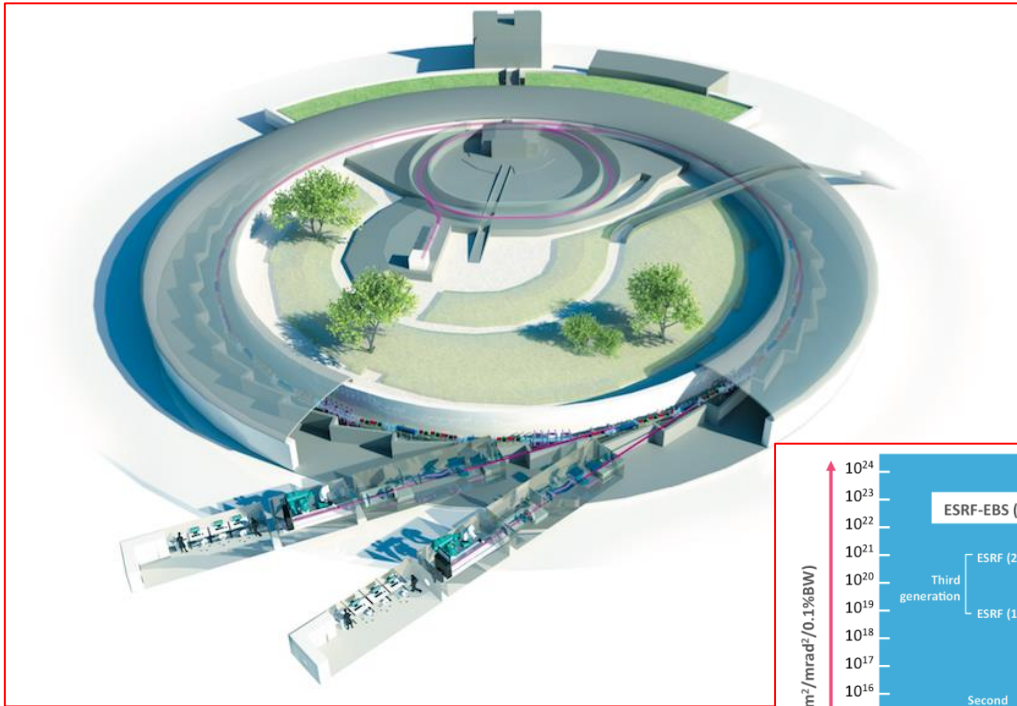
How to calculate the SR photon distribution and related gas loads?

(valid, of course, also for assuring proper cooling of surfaces)

Case study: 6 GeV European Synchrotron Radiation Facility (ESRF), Grenoble, FR

Circumference: 845 m; Energy: 6 GeV; Nominal current: 200 mA;

<https://www.esrf.eu/home/UsersAndScience/Accelerators.html>

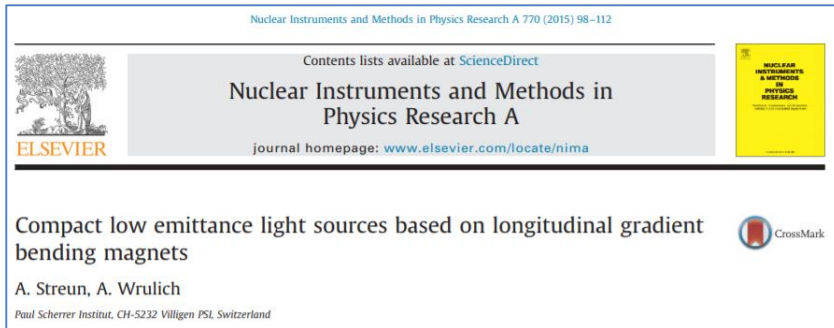


Conductance-limited systems: what are they?... What is the consequence?

Example:

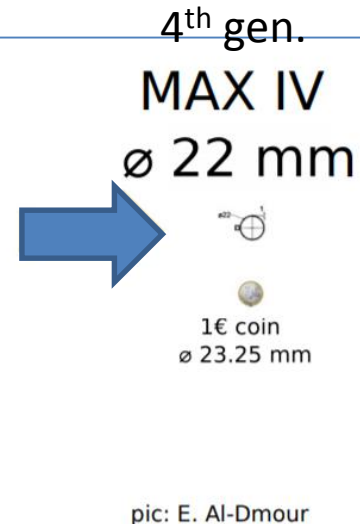
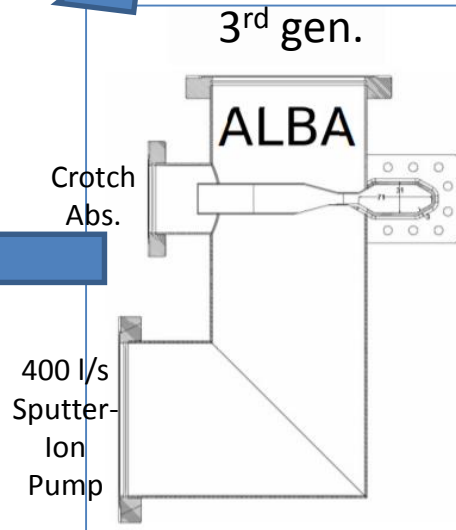
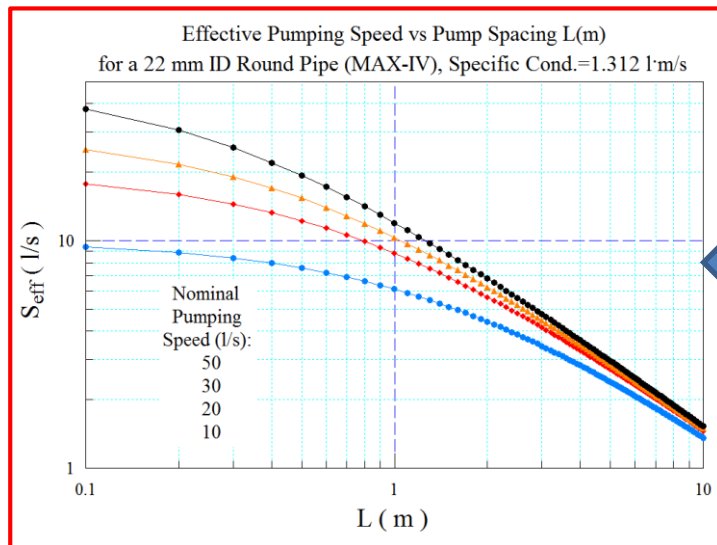
- The **specific conductance** of a 22 mm ID m circular cross-section is **1.312 l·m/s** (~MAX-IV and SIRIUS, mass 28 a.m.u., T=20 °C)
- In a uniform cross-section tube with uniform longitudinal outgassing, a **regular pump spacing** of L meters will decrease the installed pumping speed S_{inst} via the equation seen before:

$$1/S_{eff} = 1/S_{inst} + 1/C_{spec} \rightarrow S_{eff} = (1/S_{inst} + L/12/C_{spec})^{-1}$$



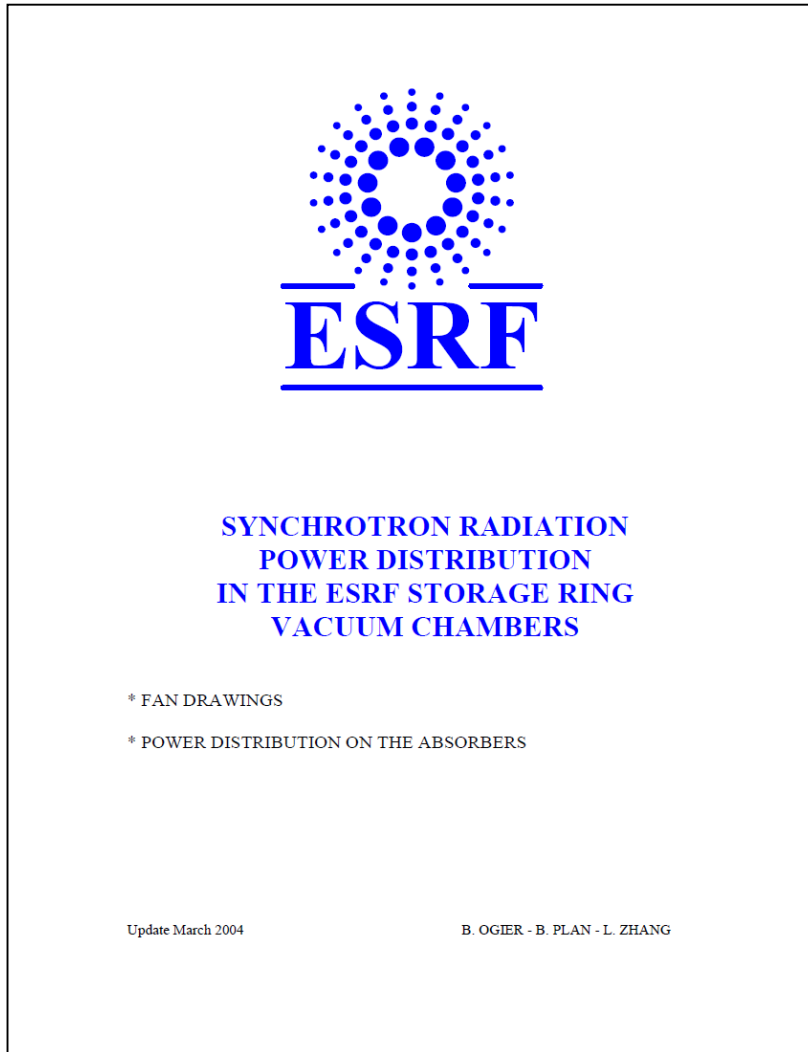
Accelerator Physics Challenges in the Design of Multi-Bend-Achromat-Based Storage Rings

M. Borland, ANL
R. Hettel, SLAC
S. C. Leemann, MAX IV Laboratory
D. S. Robin, LBNL



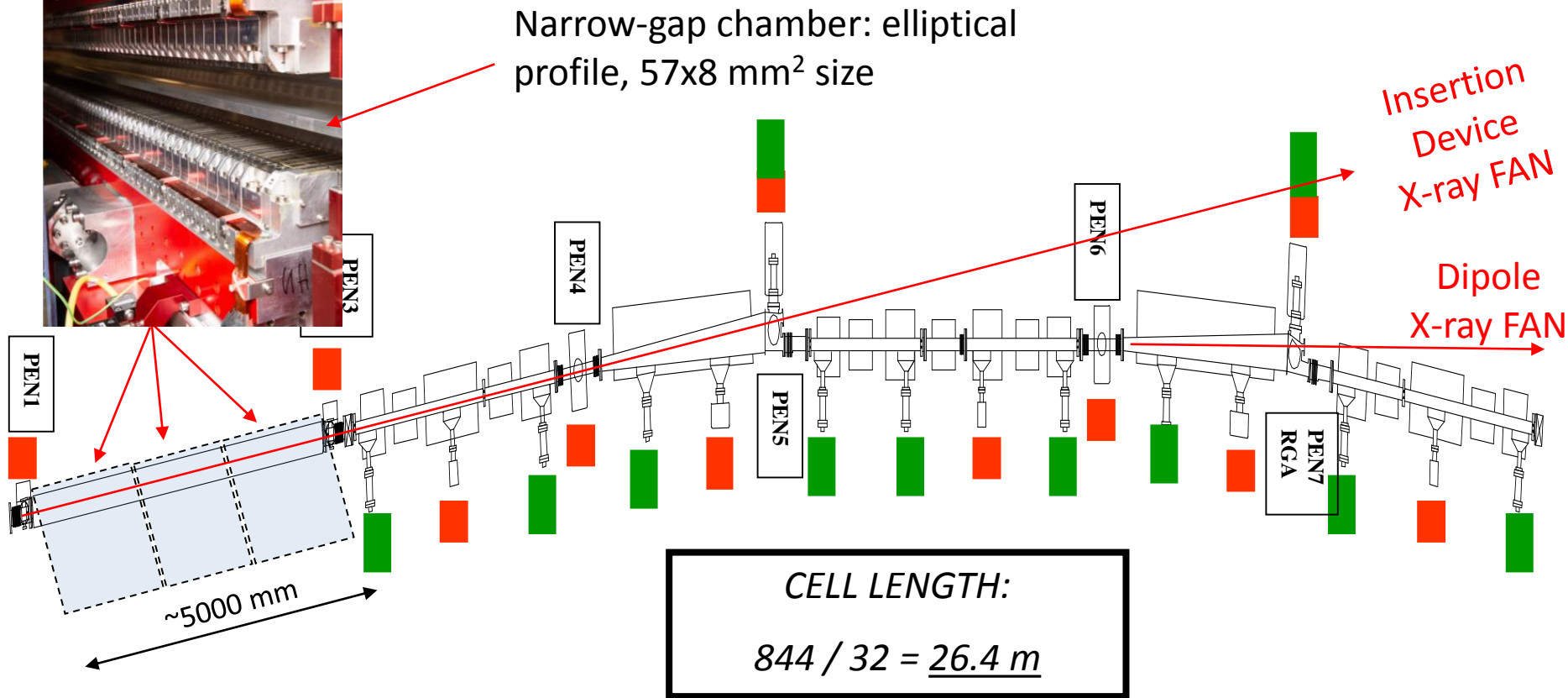
How to calculate the SR photon distribution and related gas loads? (valid, of course, also for assuring proper cooling of surfaces)

1) Do like the ESRF “Blue Book”, CAD ray-tracing (in the plane of the orbit only):



-CONTENTS-	
-INTRODUCTION	page: 03
-COMMON PART CELLS from CV03 to CV15 (except CELL 03,04,07 and 15)	page: 10
-STRAIGHT SECTION CV ID 5000x15mm , BEAM DECELERATOR KICKER K1 & K2 CELL 03	page: 31
-STRAIGHT SECTION INJECTION , SEPTUM S3 , BEAMKILLER KICKERS K3 & K4 CELL 04	page: 58
-STRAIGHT SECTION RF CELLS 05 & 25	page: 78
-STRAIGHT SECTION RF & GRAAL CELL 07	page: 87
-STRAIGHT SECTION MINIGAP & CV 3437x15mm CELL 10	page: 113
-STRAIGHT SECTION IN VACUUM UNDULATOR 1600 + 2000 CELL 11	page: 122
-STRAIGHT SECTION MACHINE DIAGNOSTICS 2 & WIGGLER 3 TESLA CELL 15	page: 132
-STRAIGHT SECTION CV 5000x19mm or 20mm CELL 17	page: 156
-STRAIGHT SECTION TWO IN VACUUM UNDULATOR 2000 CELL 27	page: 165
-STRAIGHT SECTION CV 5000x15mm CELLS 01-12-14-19-21-24-30	page: 175
-STRAIGHT SECTION CV 5000x15mm ALUMINIUM CELLS 02 & 08	page: 184
-STRAIGHT SECTION CV 5000x10mm ALUMINIUM CELLS 06-20-23-26-32	page: 193
-STRAIGHT SECTION IN VACUUM UNDULATOR 2000 CELLS 09-13-22-29	page: 203
-STRAIGHT SECTION CV 5175x10mm CELLS 16-18-28-31	page: 214
-TOTAL LINEAR POWER DENSITY CIRCULATION	page: 224

CELL IP/NEG DISTRIBUTION AND LOCATION OF VACUUM GAUGES:



■ Ion pumps (Varian): ID:120 l/s ; CV4/CV11: 120 l/s; CV3/CV10/CV15: 45 l/s;
dipoles: 60 l/s ; crotches: 400 l/s

■ NEG pumps (SAES): crotches: GP500 (500 l/s) ; elsewhere: GP200 (200 l/s)

3. SR-induced desorption

ESRF "Blue Book" CAD ray-tracing (in the plane of the orbit only):

Introduction

The basic synchrotron radiation sources are the bending magnets, which cover 2π radian angle. At the ESRF a major part of this synchrotron radiation is removed by water cooled heater absorbers installed inside the vacuum chambers of the Storage Ring. The power distribution on the absorbers is a basic data for the design of the vacuum chambers as well as the absorbers.

Additional sources of synchrotron radiation are Insertion Devices (ID's) placed in the straight section, between two successive bending magnets. At the ESRF the synchrotron radiation from the insertion devices has, in most cases, a very small horizontal opening angle so that it does not touch any components of the Storage Ring.

This document is intended to give out the power density and the spot size of the synchrotron radiation on all the absorbers of the ESRF Storage Ring vacuum chambers. Only the synchrotron radiation from bending magnets has been considered.

Basic Formula

The synchrotron radiation from a bending magnet in the ESRF has a much smaller vertical size and divergent angle than the horizontal ones. This synchrotron radiation can be considered as a horizontal divergent blade. The power distribution is then described by the angular power density which is defined by the power per unit angle in the horizontal plane, and a vertical Gaussian height.

The angular power density P_θ is given by

$$P_\theta = 4.224 B E^3 I \quad (1)$$

where E : electron beam energy, in GeV
 I : electron beam current intensity, in A
 B : magnet field intensity of the bending magnet, in T
 P_θ : angular power density in horizontal plane, in W/mrad

In the case of the ESRF, $E = 6 \text{ GeV}$, $I = 200 \text{ mA} = 0.2 \text{ A}$, (nominal values)

- for the standard bending magnet $B = 0.857 \text{ T}$,
 $P_\theta = 156.38 \text{ W/mrad}$
- for the soft end magnet $B = 0.40 \text{ T}$,
 $P_\theta = 72.99 \text{ W/mrad}$

The linear power density P_1 on the absorber is then

$$P_1 = P_\theta \sin(\beta)/d \quad (2)$$

where d is the distance between the source point and the absorber, in meter, β the incident angle of photon beam on the absorber (see Figure 1), P_1 in W/mm.

The photon beam size on an absorber is characterised by the vertical Gaussian height σ (mm) which is calculated by

$$\sigma = \sqrt{\sigma_0^2 + (\sigma' d)^2 + (d/\gamma)^2} = \sqrt{\sigma_0^2 + (\sigma'' d)^2} \quad (3)$$

where σ_0 : vertical standard deviation of the e-beam at source point (mm)
 σ' : vertical angular standard deviation of the e-beam at source point (mrad)
 σ'' : total effective vertical angular standard deviation at source point (mrad)
 d : distance between source point and the absorber (m)
 γ : $= 1957 E$ (GeV)

For a coupling factor of 1% and a vertical emittance $\epsilon_2 = 4 \cdot 10^{-11} \text{ m.rad}$ in the case of the ESRF,

$$\begin{aligned} \sigma_0 &= 37 \mu\text{m} \\ \sigma' &= 1.07 \mu\text{rad} \\ \gamma &= 1.174 \cdot 10^4 \\ \sigma'' &= \sqrt{\sigma'^2 + 1/\gamma^2} = 85.2 \mu\text{rad} \end{aligned}$$

3. SR-induced desorption

ESRF "Blue Book" CAD ray-tracing (in the plane of the orbit only):

The surface power density on the absorber P_a is given by

$$P_a(z) = P_a \exp\left(-\frac{z^2}{2\sigma^2}\right) \quad (4)$$

with peak power density per unit surface area :

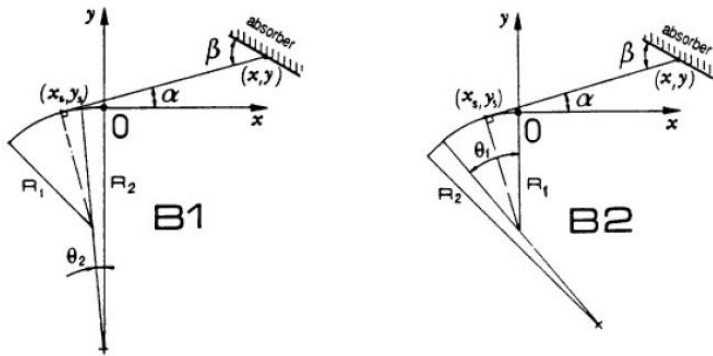
$$P_a = \frac{P_l}{\sqrt{2\pi}\sigma} \quad (5)$$

Once the distance d between the source point and the absorber is defined as well as the incidence angle β of the synchrotron radiation on the absorber, the power densities P_s , P_a and spot size on the absorber can be calculated by equations (2)-(5).

Geometrical calculation

There are two types of dipole bending magnets per cell in the ESRF storage ring :

- 1) with downstream soft end B1
- 2) with upstream soft end B2



case 1 : dipole magnet B1

case 2 : dipole magnet B2

Figure 1 : Co-ordinate systems

The co-ordinate systems concerning the two types of dipole magnets are shown in Figure 1. The origin of the co-ordinate system is always at the exit of the magnets, the axis-x is parallel to the electron beam in the straight section. The absorber is defined by a certain number of key points and inclined angles $\gamma = \alpha + \beta$ of surface to the axis-x (or to the electron beam trajectory in the straight section).

It is easy to give out the co-ordinates of a point on the absorber (x, y) and the angle γ . The associated source point (x_s, y_s) and the angle α between the photon beam and the electron beam (see Figure 1) can be calculated from the co-ordinates (x, y) and the geometrical parameters of the bending magnets.

Case 1 : dipole magnet B1 :

- 1) $\alpha > \theta_2$: source point on the main bending magnet (B1)

$$x_s = -R_1 \sin(\alpha) - (R_2 - R_1) \sin(\theta_2) \quad (6a)$$

$$y_s = -R_2 + R_1 \cos(\alpha) + (R_2 - R_1) \cos(\theta_2) \quad (6b)$$

- 2) $\alpha < \theta_2$: source point on the soft end magnet

$$x_s = -R_2 \sin(\alpha) \quad (7a)$$

$$y_s = -R_2 (1 - \cos(\alpha)) \quad (7b)$$

Case 2 : dipole magnet B2 :

- 3) $\alpha < \theta_1$: source point on the main bending magnet (B2)

$$x_s = -R_1 \sin(\alpha) \quad (8a)$$

$$y_s = -R_1 (1 - \cos(\alpha)) \quad (8b)$$

- 4) $\alpha > \theta_1$: source point on the soft end magnet

$$x_s = -R_2 \sin(\alpha) + (R_2 - R_1) \sin(\theta_1) \quad (9a)$$

$$y_s = -R_1 - (R_2 - R_1) \cos(\theta_1) + R_2 \cos(\alpha) \quad (9b)$$

where R and θ are respectively the radius and the curvature angle of the magnet, index 1 for standard magnet and 2 for soft end magnet. At the ESRF,

3. SR-induced desorption

ESRF "Blue Book" CAD ray-tracing (in the plane of the orbit only):

Notation

The power distribution on the absorbers installed inside the vacuum chambers of the Storage Ring is presented as following.

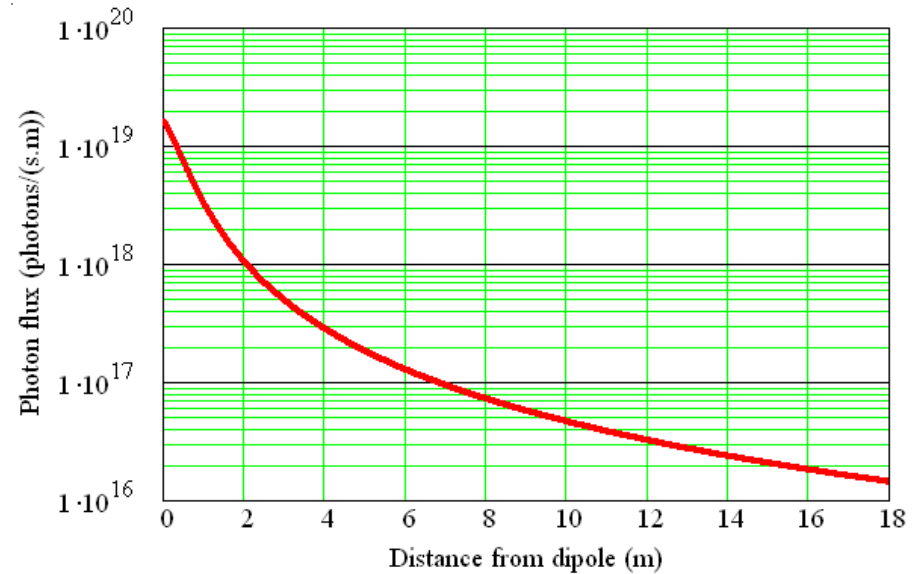
(sample)

Pt n°	Src	Src n°	X mm	Y mm	α °	β °	σ mm	Pl W/mm	Pa W/mm ²	Ptot W	CV n° / drawing n°
1		2	10 614	37.00	0.199	0.199	0.518	0.05	0.04		
2		2	12 728	37.00	0.166	0.166	0.620	0.04	0.02		
3	2H	2	12 846	37.34	0.166	9.628	0.625	2.03	1.29	130	CV 03 / 85.41.0073
4		2	12 848	37.00	0.165	9.627	0.626	2.02	1.29		
5		2	13 965	37.00	0.151	0.151	0.679	0.03	0.02		

Some symbols in the notation have been used in the previous sections. Here below is a summary of the notation.

Pt n°		number of points, marked in the drawings
Src		synchrotron radiation source type
Src n°		synchrotron radiation source number
	1H :	dipole type 1, n° =1
	2H :	dipole type 2, n° =2
	1S :	soft end dipole type 1, n° =0
	2S :	soft end dipole type 2, n° =3
X	(mm)	co-ordinate X, axis X parallel to the e-beam orbit
Y	(mm)	co-ordinate Y, axis Y parallel to radial direction of the ring <i>the origin of the co-ordinate system X-Y is at the intersection of e-beam orbit and the exit of upstream dipole magnet (B1)</i>
α	(degree °)	angle between X-ray and e-beam orbit
β	(degree °)	X-ray incidence angle on the absorbers
σ	(mm)	Gaussian vertical height of X-ray
Pl	(W/mm)	linear power density on the absorber in the horizontal plan
Pa	(W/mm ²)	surface power density on the absorber
Ptot	(W)	total power on the absorber
CV n° / drawing n°		name of vacuum chamber / number of corresponding drawing

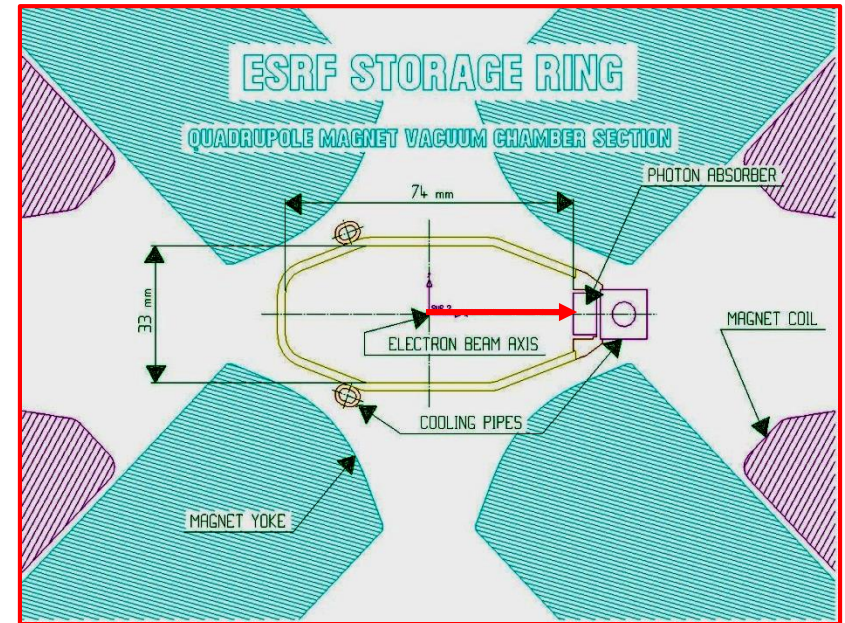
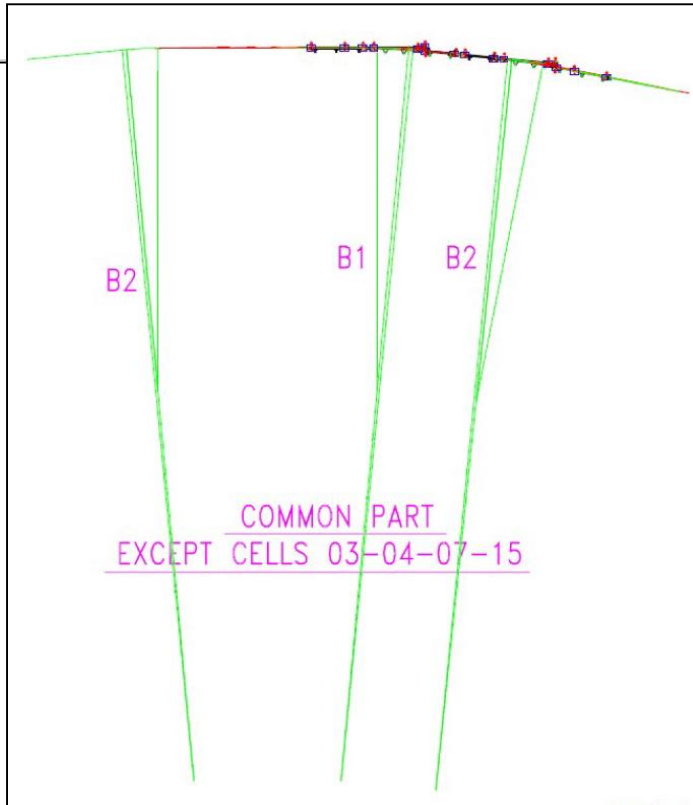
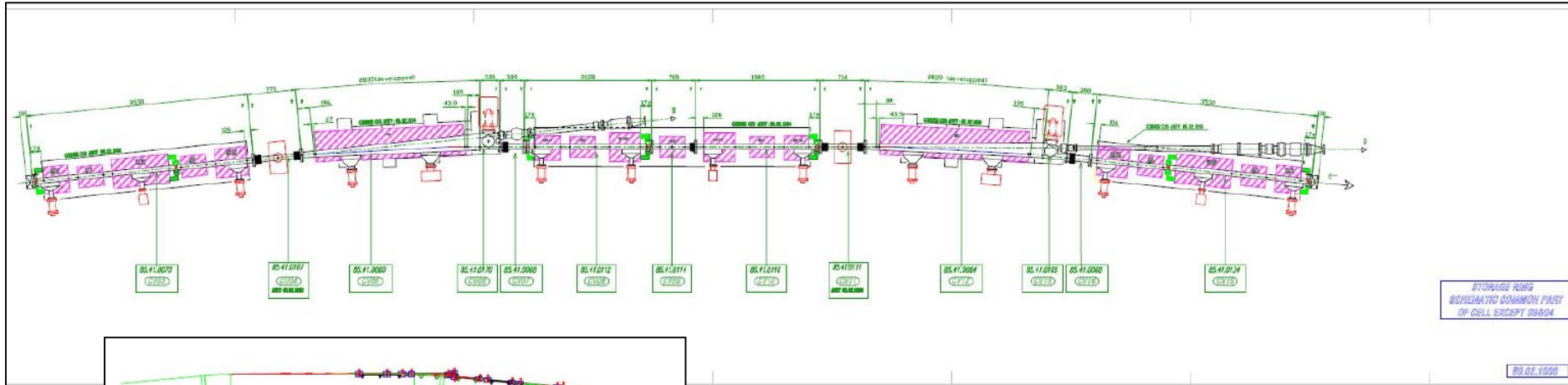
-COMMON PART CELLS- from CV03 to CV15 (except CELL 03-04-07-15)



Source: O.B. Malyshev, pers. comm., for the DIAMOND Light Source

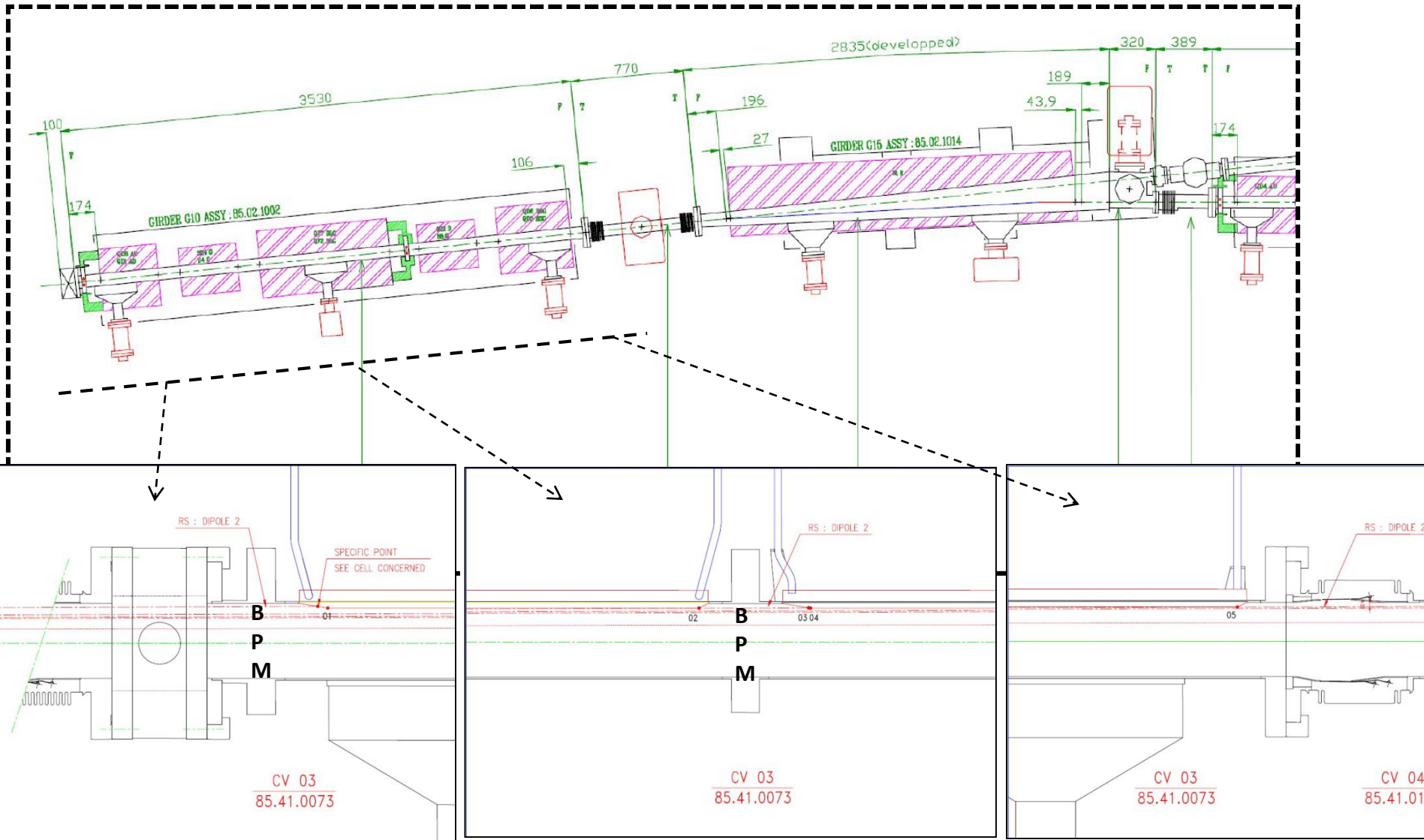
3. SR-induced desorption

ESRF "Blue Book" CAD ray-tracing (in the plane of the orbit only):



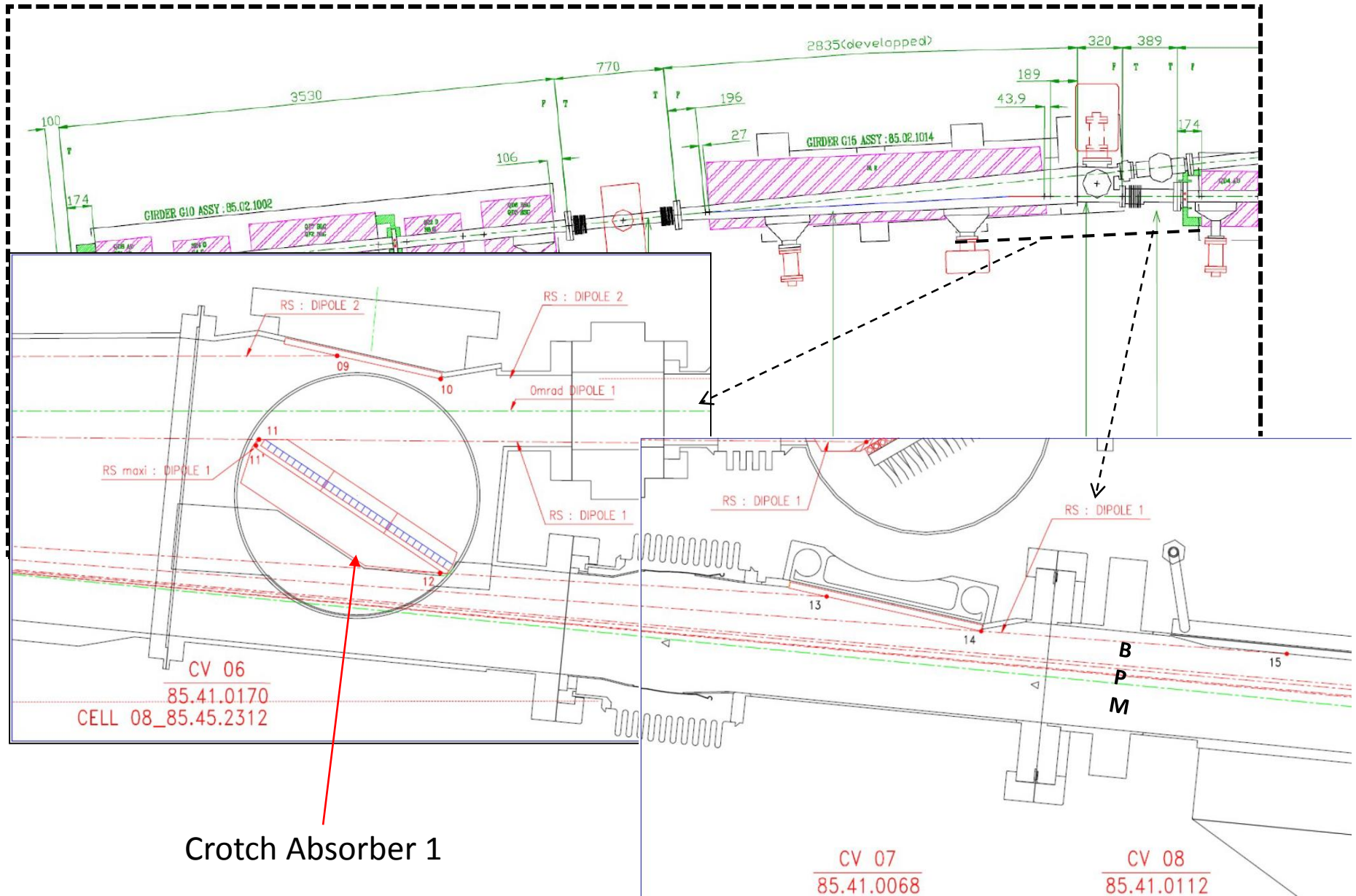
3. SR-induced desorption

ESRF "Blue Book" CAD ray-tracing (in the plane of the orbit only):



3. SR-induced desorption

ESRF "Blue Book" CAD ray-tracing (in the plane of the orbit only):



Crotch Absorber 1

3. SR-induced desorption

ESRF "Blue Book" CAD ray-tracing (in the plane of the orbit only):

Synchrotron Radiation Power Distribution on the Absorbers in the ESRF Storage Ring : *Standard part of a Cell*

common parts for all cells except cell 03-04-07-15

E=6 GeV, I=200 mA

64 bending magnets with soft end : B=0.857 T, B(softend)=0.40 T

Vertical emittance =4E-11 m.rad, Vertical dimension at source point 37 μm, Angular deviation =1.07 μrad

Pt n°	Src	Src n°	X mm	Y mm	α °	β °	σ mm	PI W/mm	Pa W/mm ²	Ptot W	CV n° / drawing n°
1		2	10 614	37.00	0.199	0.199	0.912	0.05	0.02	130	CV 03 / 85.41.0073
2		2	12 728	37.00	0.166	0.166	1.090	0.04	0.01		
3	2H	2	12 846	37.34	0.166	9.628	1.101	2.03	0.73		
4		2	12 848	37.00	0.165	9.627	1.101	2.02	0.73		
5		2	13 965	37.00	0.151	0.151	1.195	0.03	0.01		
6		2	14 200	37.62	0.151	9.614	1.215	1.83	0.60	18	CV 04 / 85.41.0107
7	2H	2	14 204	37.00	0.149	9.611	1.216	1.83	0.60		
8		2	14 620	37.00	0.145	0.145	1.251	0.03	0.01		
9	2H	2	17 750	44.90	0.145	12.770	1.517	1.94	0.51	167	CV 06 / fixed absorber 85.41.0170
10	2H	2	17 835	26.00	0.083	12.708	1.522	1.93	0.50		
11	1H	1	249	127.02	5.064	56.936	0.214	52.90	98.51	8 160	CV 06 / crotch absorber 85.41.0170
11'	1H	1	247	121.48	4.939	90.000	0.210	64.51	122.71		
12	1H	1	406	35.20	2.074	30.074	0.126	55.65	176.88		
6_a	2H	2	18 273	26.64	0.083	29.917	1.560	4.26	1.09	1 759	Beam Port
6_b	2H	2	18 227	0.00	0.000	30.000	1.553	4.29	1.10		
6_b'	1H	1	781	204.89	5.625	150.000	0.279	24.11	34.52		
6_c	1H	1	732	169.79	5.064	149.789	0.255	26.57	41.57		
13	1H	1	717	46.46	2.074	9.074	0.151	14.34	37.88	1 833	CV 07 / 85.41.0068
14		1	843	31.00	1.403	8.403	0.139	14.54	41.79		

3. SR-induced desorption

CROTCH-2 AND CV13 GEOMETRY:

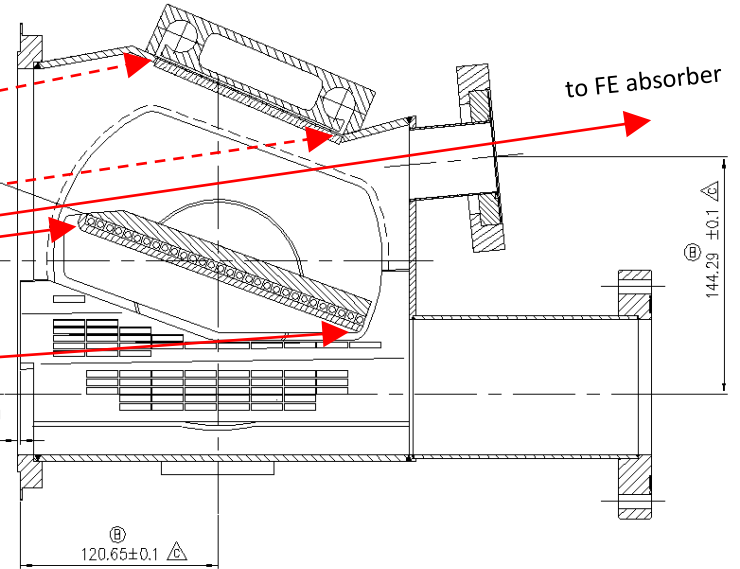
Total flux @200ma: $5.82E+18$ ph/s (46mrad)

Critical Energy Dipole SR: 19.5 keV

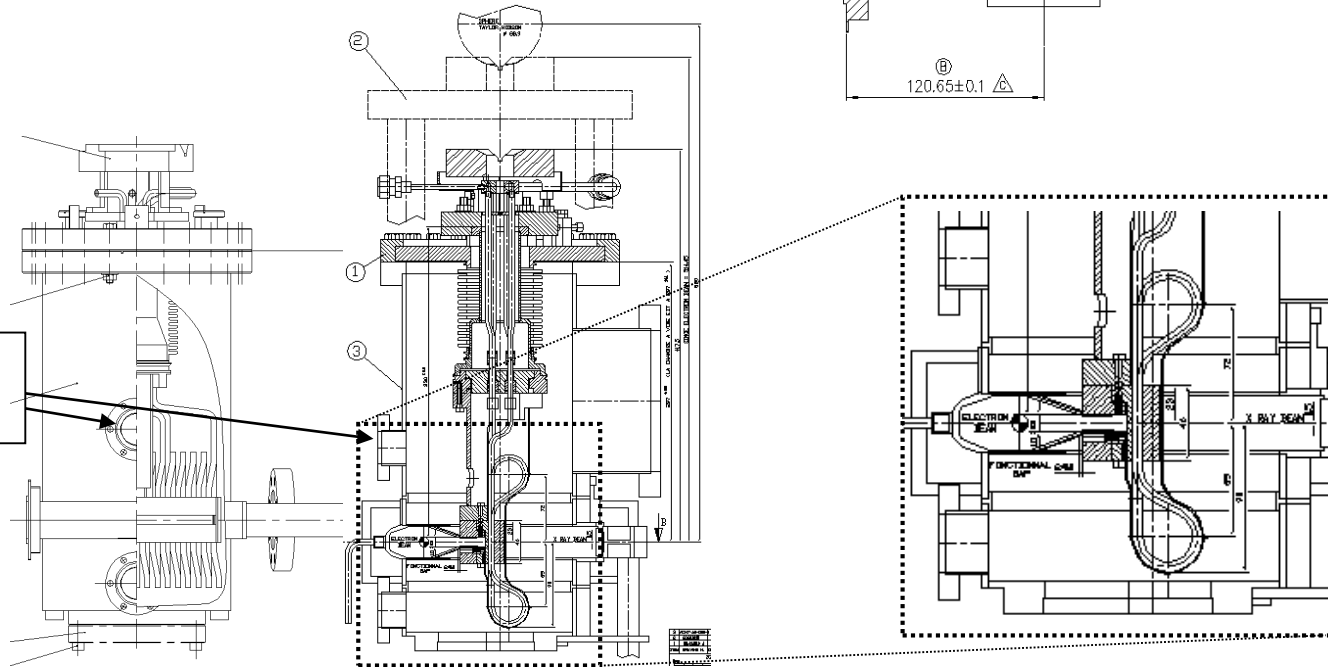
X-rays from preceding dipole (430W)

X-rays from this dipole (7200W)

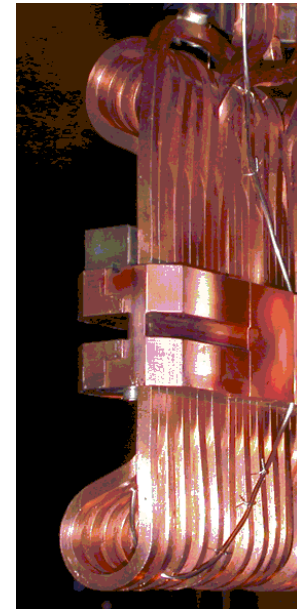
TOP-VIEW



PEN7 location

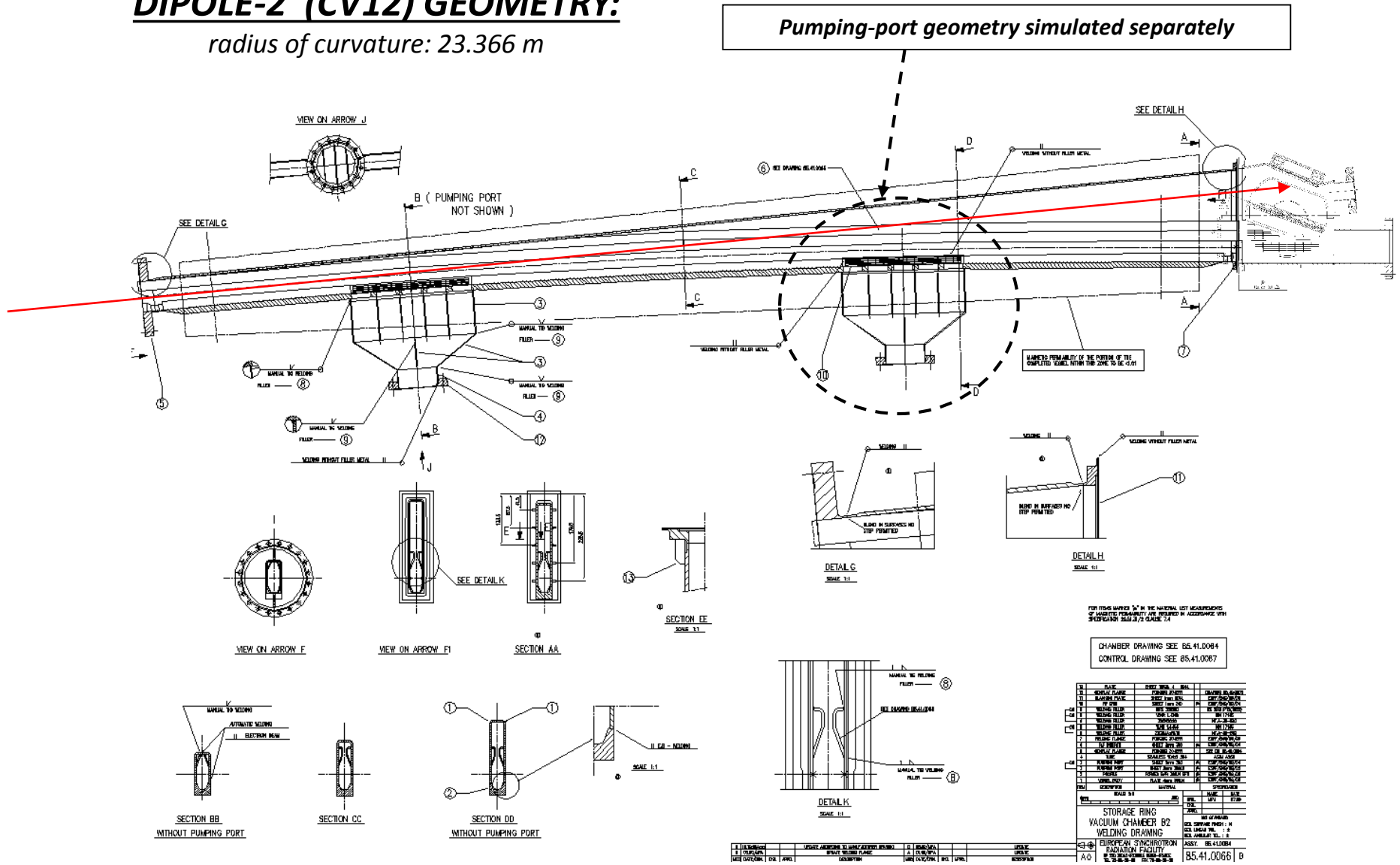


<----- SIDE-VIEW / CUT-OUTS ----->



DIPOLE-2 (CV12) GEOMETRY:

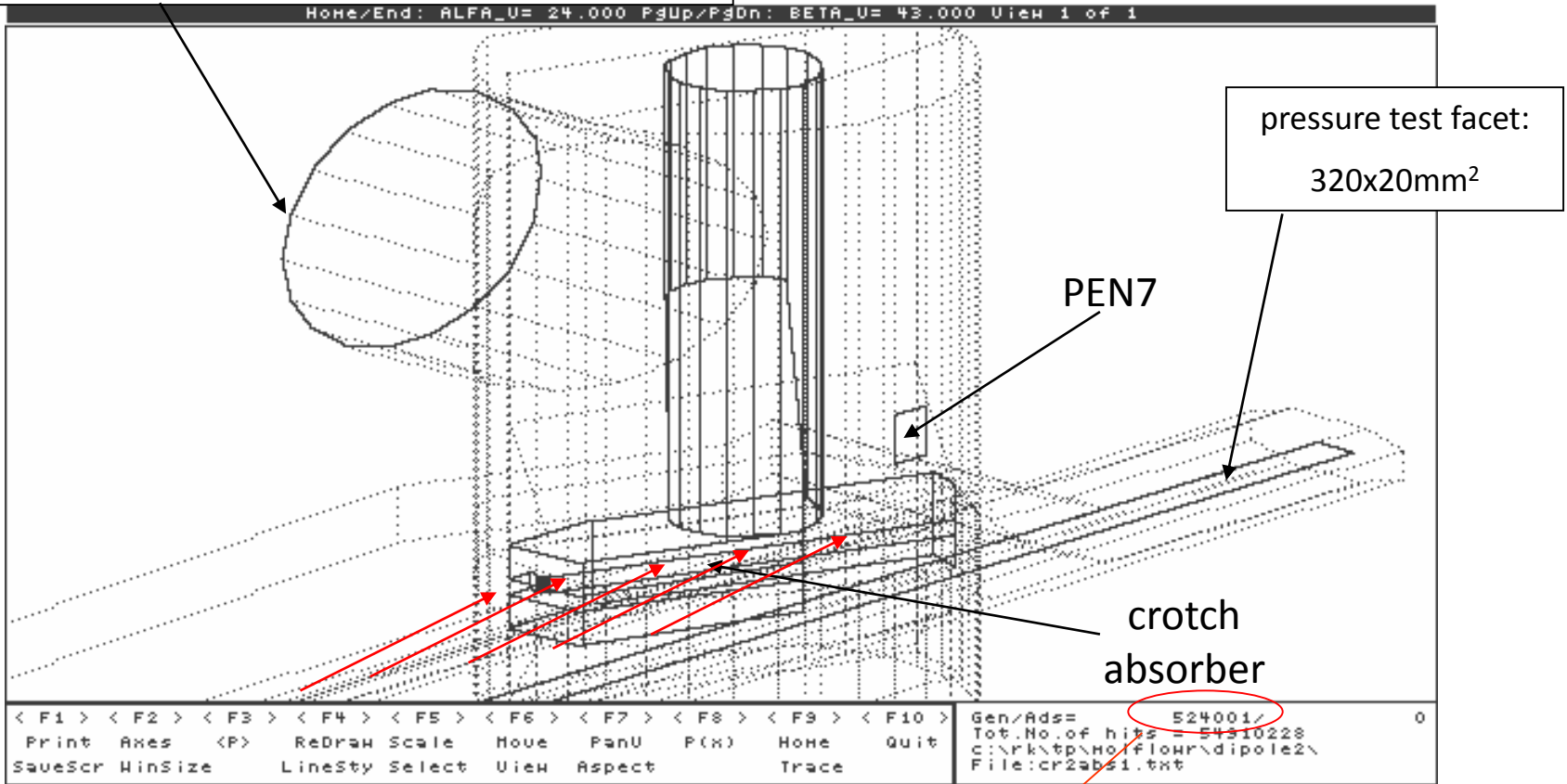
radius of curvature: 23.366 m



3. SR-induced desorption

400 I/s SIP + GP500 NEG:
**simulated total pumping speeds of 500, 750,
1000 I/s**

OLD DOS-based Molflow code (1989 → 2008)



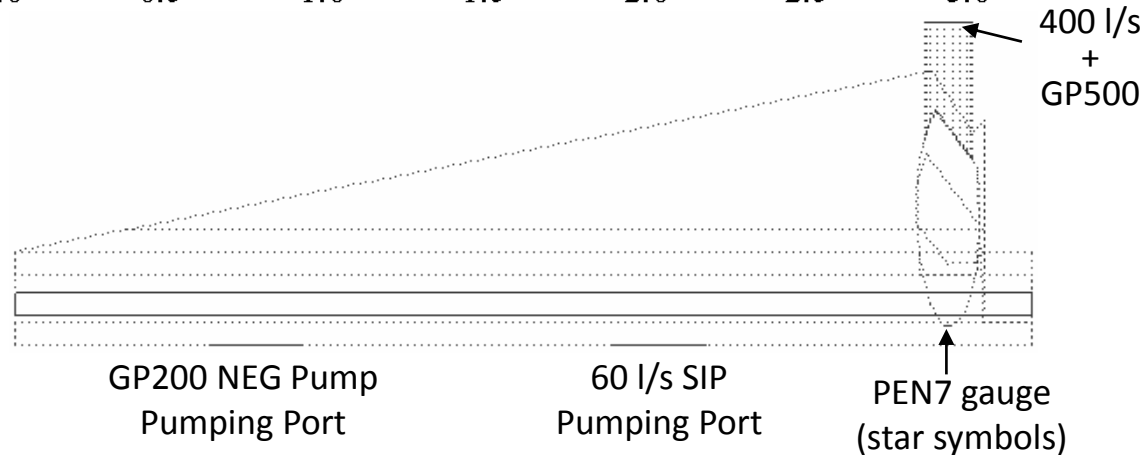
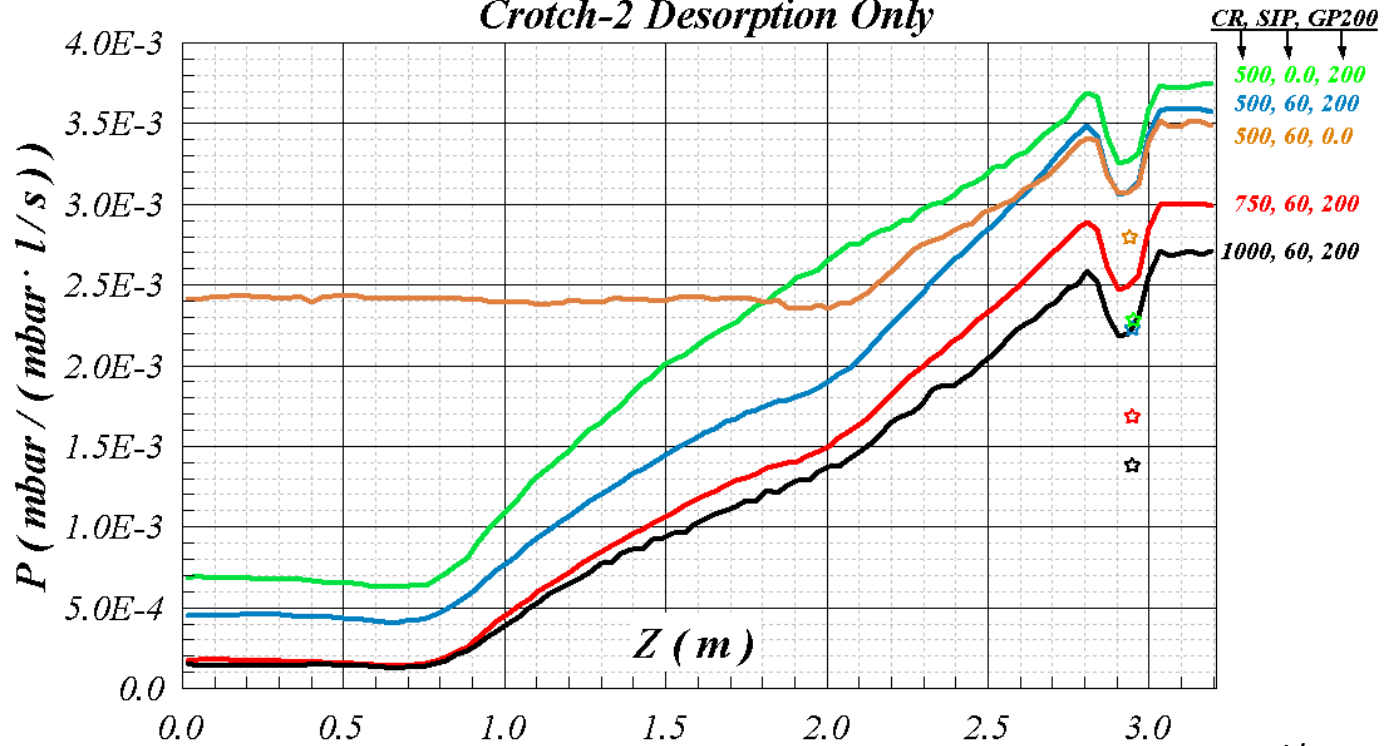
Closer view of the Molflow simulation model:

total number of points: 339; total number of facets: 131

computation time: ~15 hours

3. SR-induced desorption

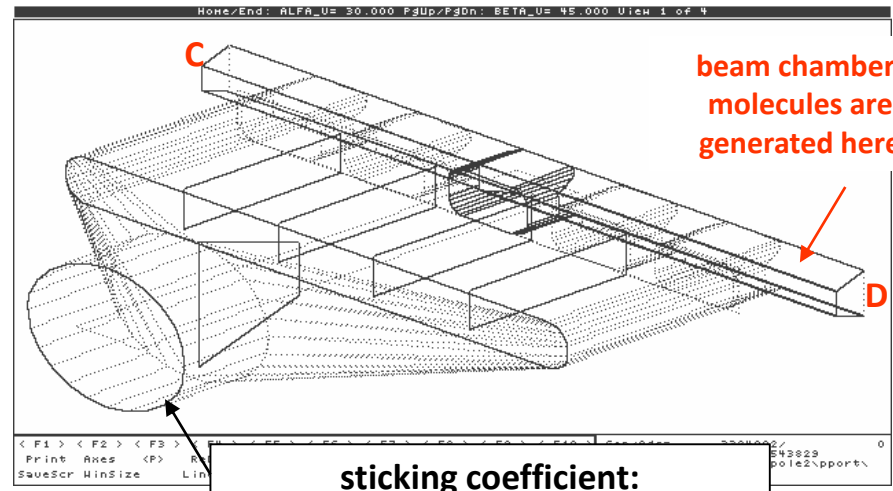
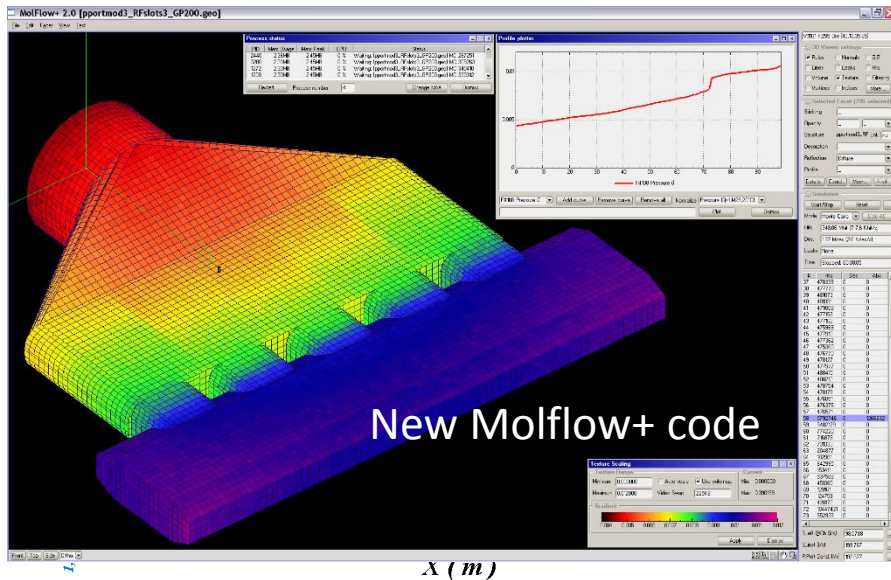
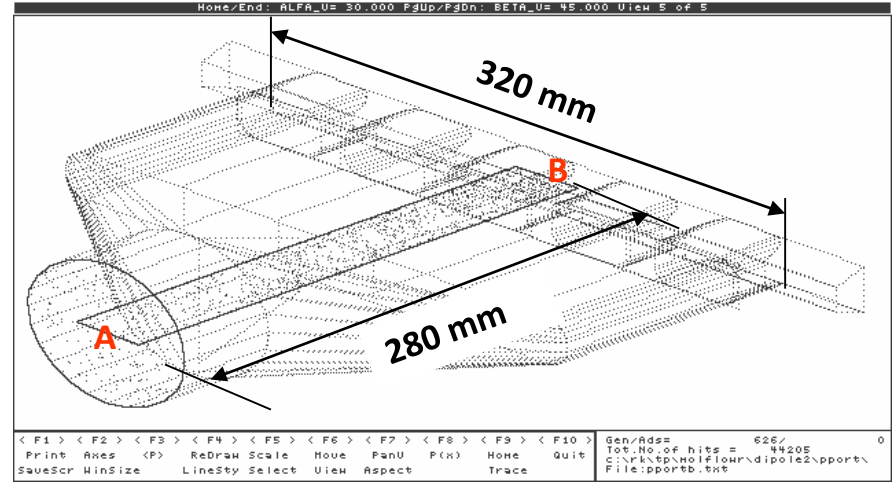
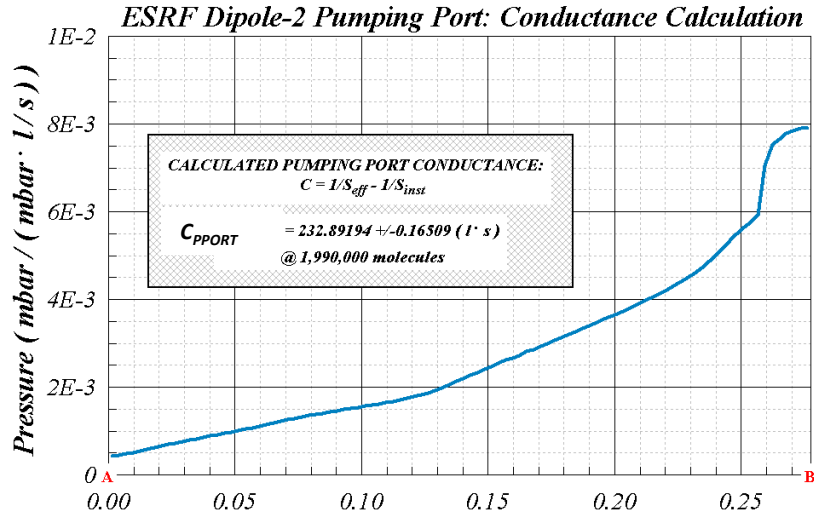
*MC Calculation of the Pressure Profile for a Dipole-2 Chamber:
Crotch-2 Desorption Only*



3. SR-induced desorption

ESRF DIPOLE PUMPING PORT GEOMETRY

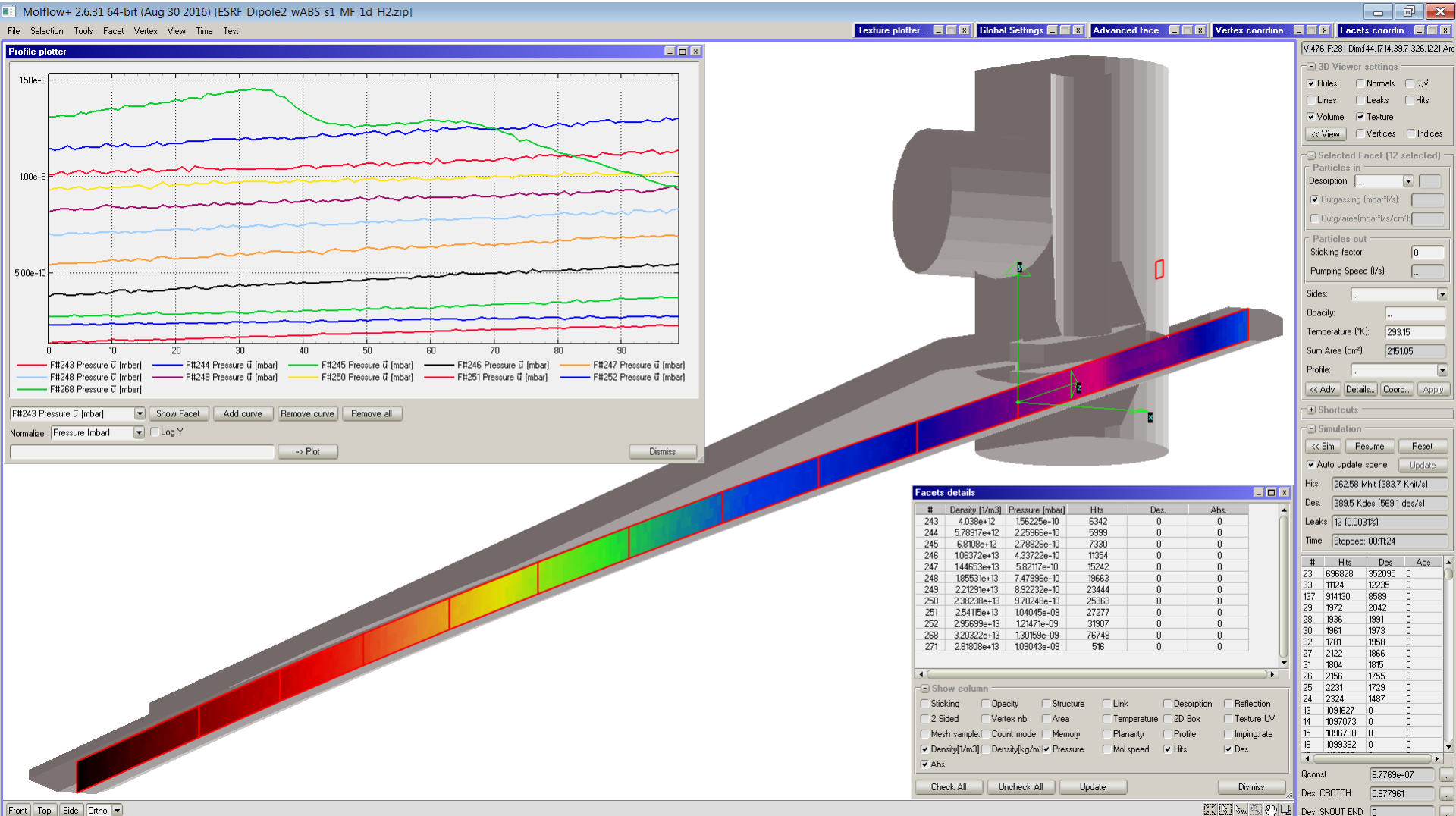
MODELED AND SIMULATED WITH MOLFLOW:



sticking coefficient:
 $s=1.0 \rightarrow 913 \text{ l/s}$
 $s=0.0656 \rightarrow 60 \text{ l/s}$

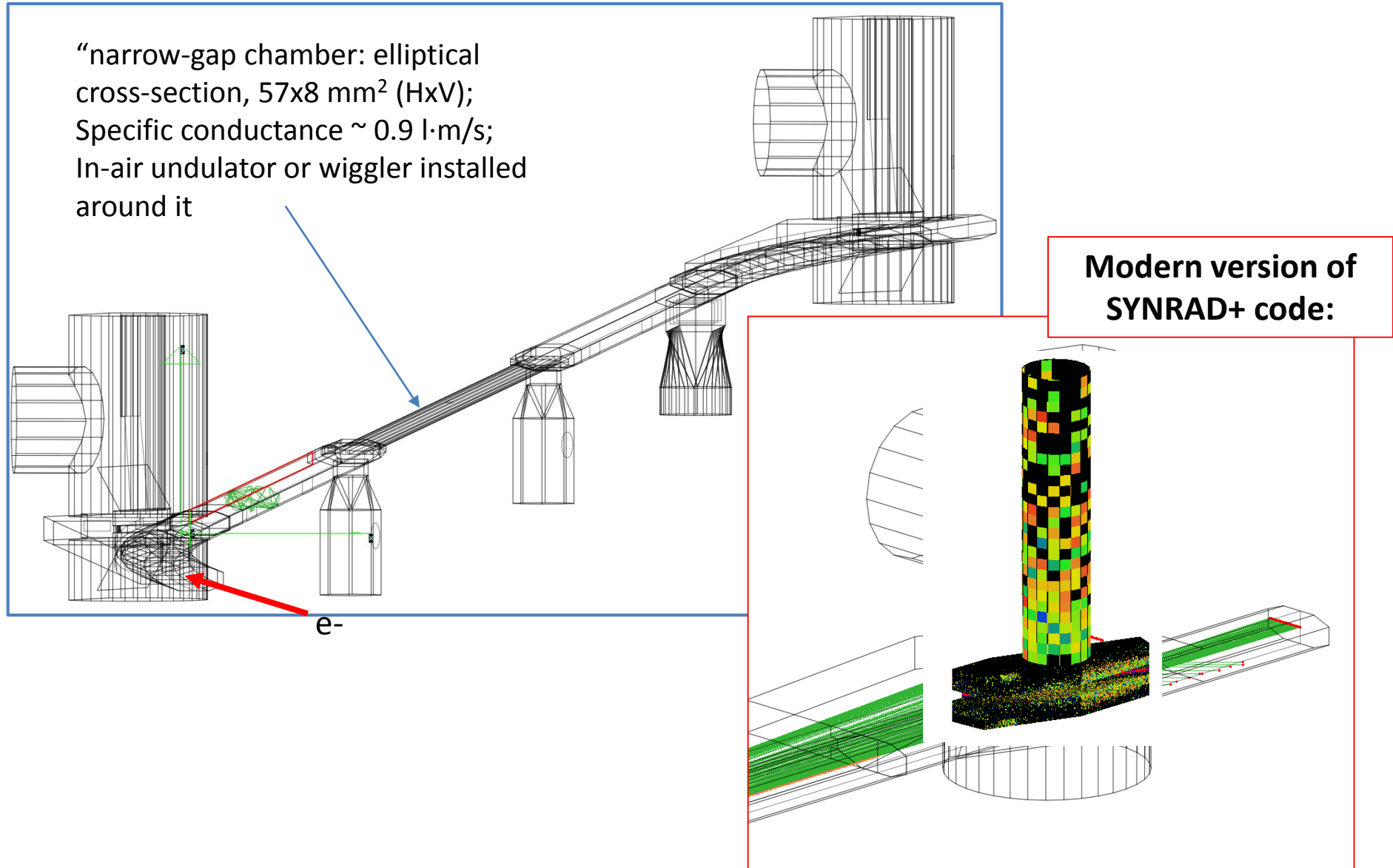
1. Basics of gas dynamics: outgassing, conductance, pumping speed

Molflow+ TPMC code: sample of modelling of one ESRF dipole/crotch 2 vacuum chamber and its pressure profile



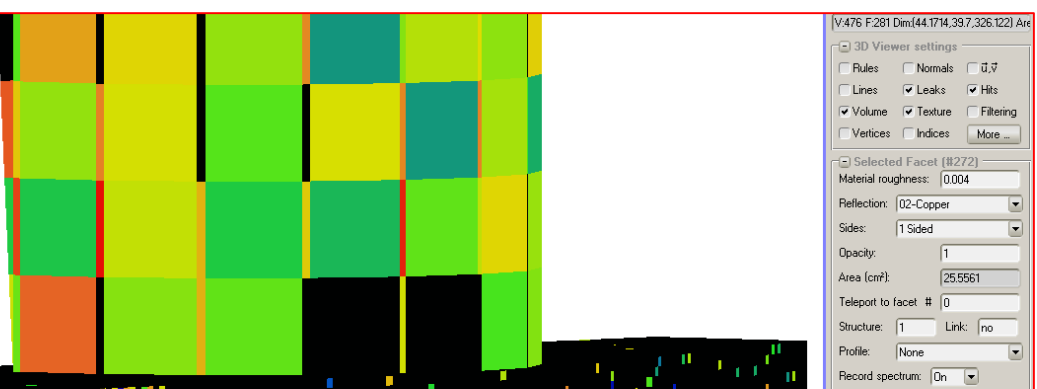
Modern version of Molflow code:

“narrow-gap chamber: elliptical cross-section, $57 \times 8 \text{ mm}^2$ (HxV);
Specific conductance $\sim 0.9 \text{ l}\cdot\text{m/s}$;
In-air undulator or wiggler installed around it

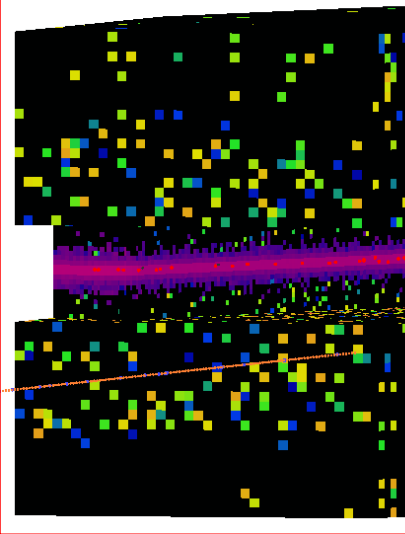
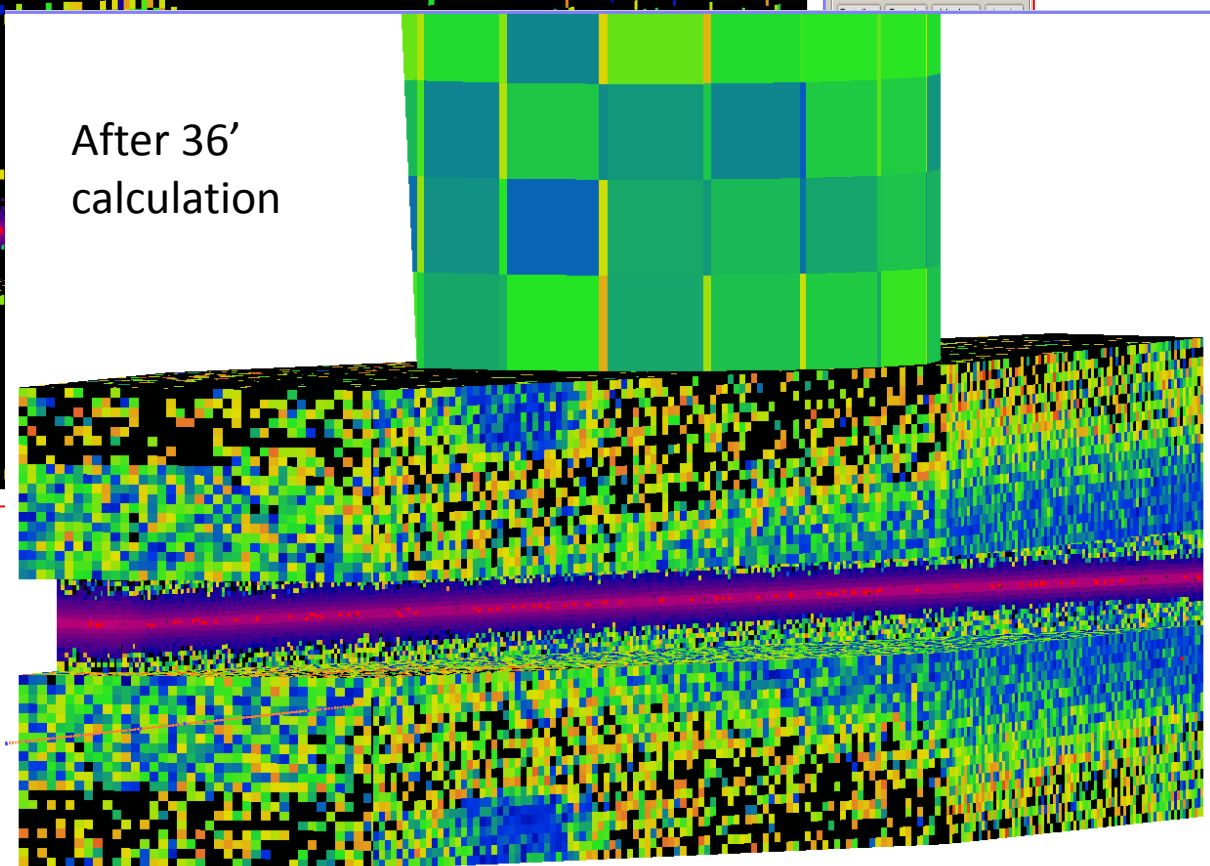


Details of a crotch absorber ray-tracing with SYNRAD+; Texture scale proportional to flux absorbed by corresponding facet

After 2' calculation



After 36' calculation



V:476 F:281 Dim(44.1714,39.7,326.122) Are

3D Viewer settings

- Rules
- Normals
- \vec{d}, \vec{v}
- Lines
- Leaks
- Hits
- Volume
- Texture
- Filtering
- Vertices
- Indices
- More...

Selected Facet #8272

Material roughness: 0.004

Reflection: 02-Copper

Sides: 1 Sided

Opacity: 1

Area (cm²): 25,5561

Teleport to facet #: 0

Structure: 1 Link: no

Profile: None

Record spectrum: On

V:476 F:281 Dim(44.1714,39.7,326.122) Are

3D Viewer settings

- Rules
- Normals
- \vec{d}, \vec{v}
- Lines
- Leaks
- Hits
- Volume
- Texture
- Filtering
- Vertices
- Indices
- More...

Selected Facet #874

Material roughness: 0.004

Reflection: 02-Copper

Sides: 1 Sided

Opacity: 1

Area (cm²): 14,6146

Teleport to facet #: 0

Structure: 1 Link: no

Profile: None

Record spectrum: On

Details... Coord... Mesh... Apply

Simulation

Resume Reset

Auto update scene Update

Mode: Powerwise

Hits: 595.40 Mhit (272.9 Khit/s)

Gen: 545.37 Mgen (249.9 Kgen/s)

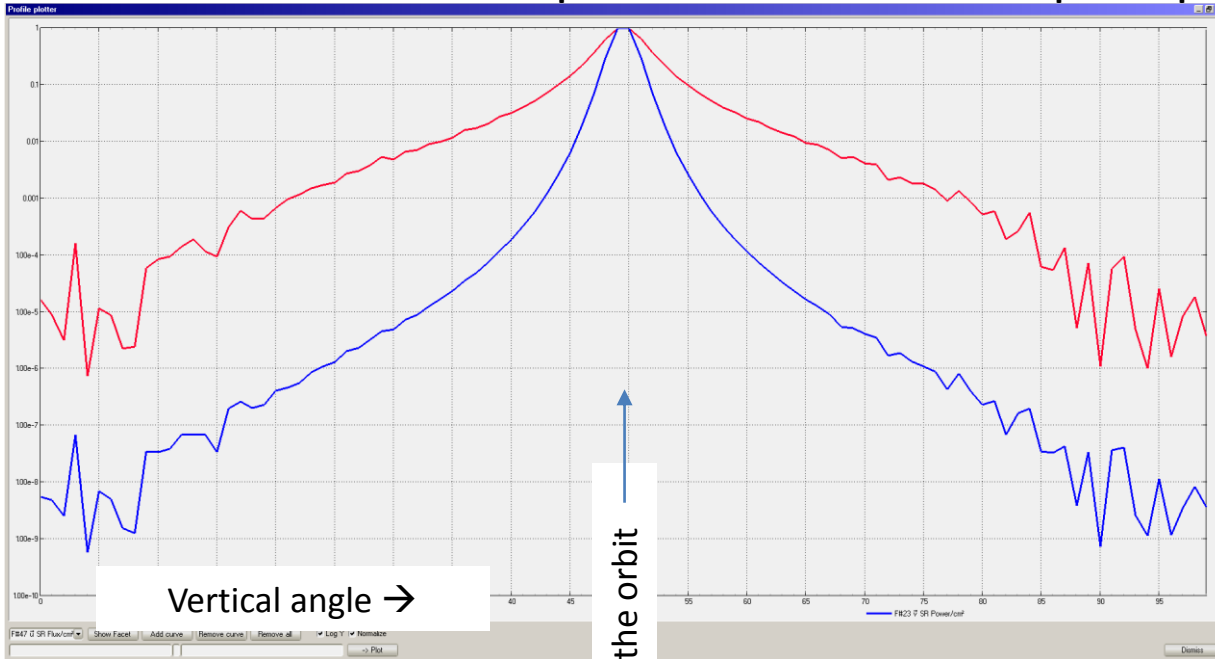
Leaks: None

Dose: Scn222590 F=1.42e+19 P=152

Time: Stopped: 00:36:22

#	Hits	Flux	Power
221	30610	103e+14	0.000171
219	30933	101e+14	0.000166
211	30257	109e+14	0.00017
179	30695	15e+14	0.000225
181	30562	14e+14	0.000216
213	29928	102e+14	0.000169
275	26552	1e+14	0.000162
273	26817	109e+14	0.000166
189	24312	119e+14	0.000173
187	25030	111e+14	0.000167
88	25487	243e+14	0.000481
229	26096	679e+13	0.000126
87	26226	296e+14	0.000552
227	25744	795e+13	0.000139
265	23598	183e+14	0.000286
266	23174	178e+14	0.000275

SR flux and power distribution and flux and power spectra with SYNRAD+

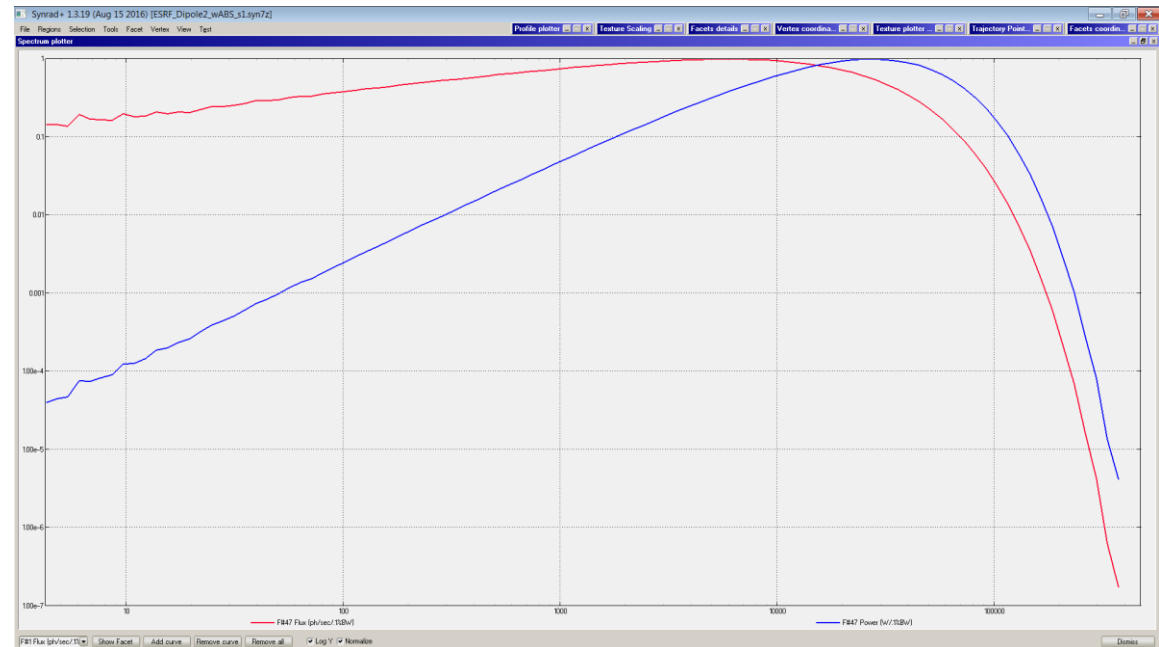


Left:

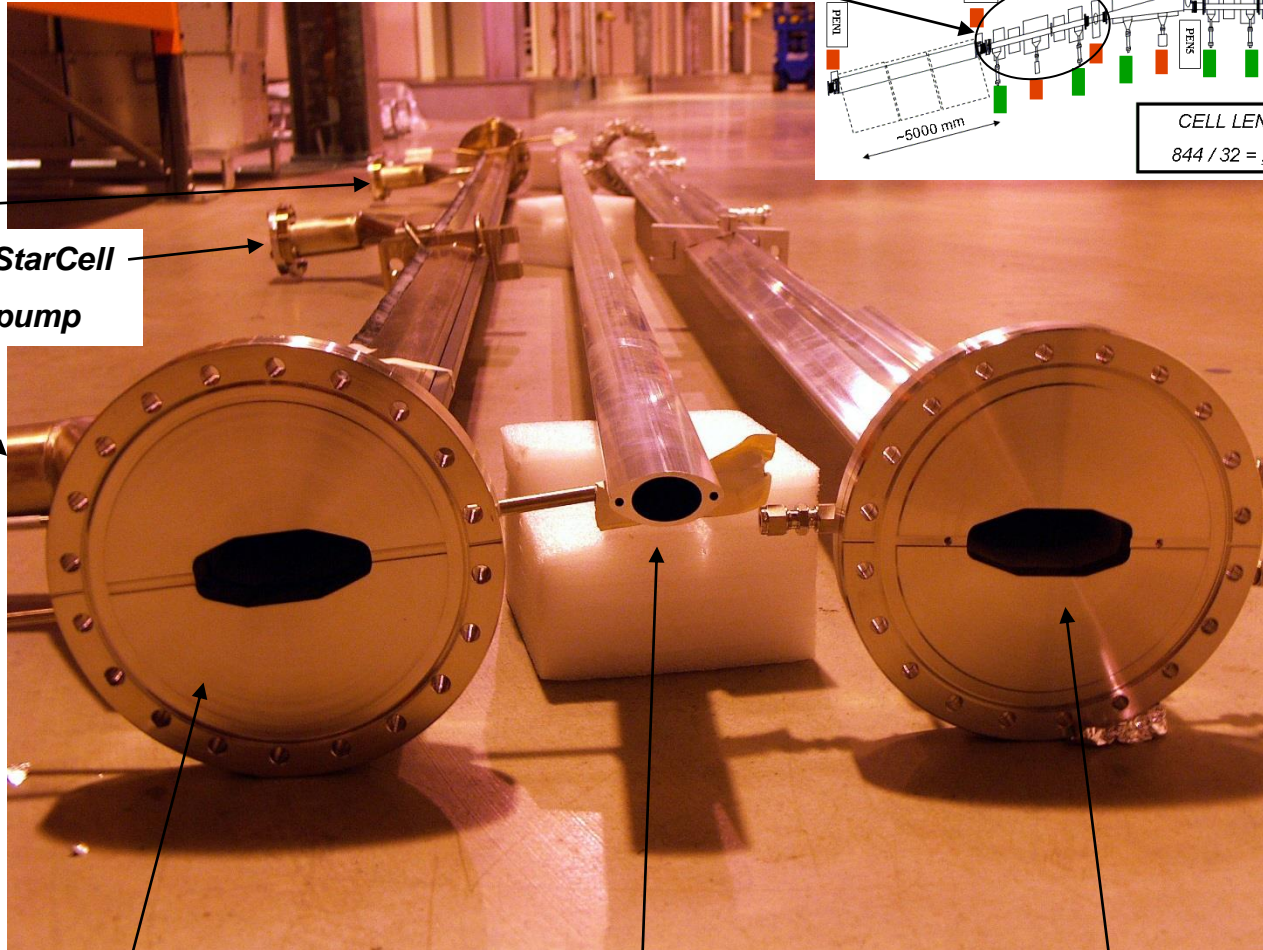
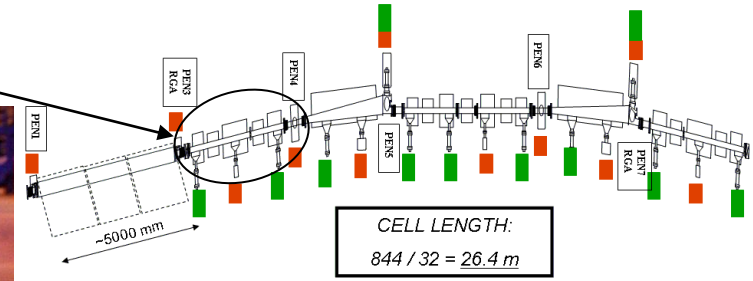
- SR flux and power distributions along the ~ 150 mm long flat absorber facet
- Note different width of “Gaussian” profile for F and P in the vertical direction (Red vs Blue curve)
- All curves normalized to 1

Right:

- SR flux and power spectra generated by SYNRAD+, normalized to 1;



CV3-Type Vacuum Chambers, 3530 mm long:



GP200
NEG

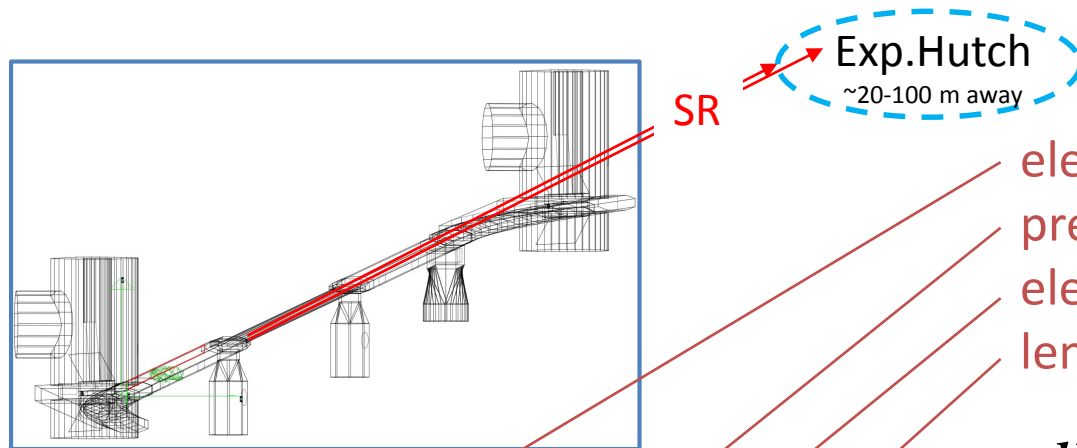
45 l/s StarCell
Ion-pump

Standard CV3 chamber: 2xNEG + 1 SIP
Hi-temp brazing of Cu absorber ; precision eb-welding of SS parts

ESRF-2 extrusion: 30x20mm² (HxV)
chamber NO pumps, only NEG-coating

Soleil-type CV3:
Al extrusion 70x35mm²;
NO pumps, only NEG-coating

Gas-bremsstrahlung power P_{BS} generated along straight section: (to be minimized at the beamline hutch!)



electron stopping power
pressure in straight section
electron beam intensity
length of straight section

$$P_{BS} = C \times \frac{dE}{dx}(E_e) \times p \times I \times L,$$

$$\frac{dE}{dx}(E_e) \propto E_e$$

$$p \propto E_e \times I$$

$$P_{BS} \propto E_e^2 \times I^2 \times L$$

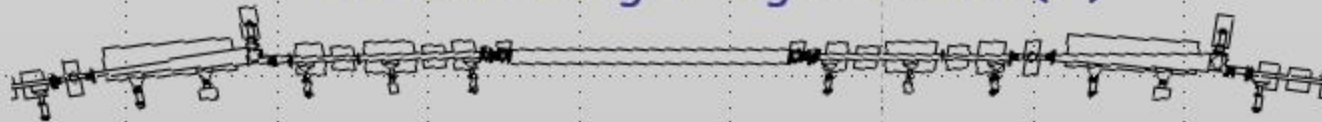
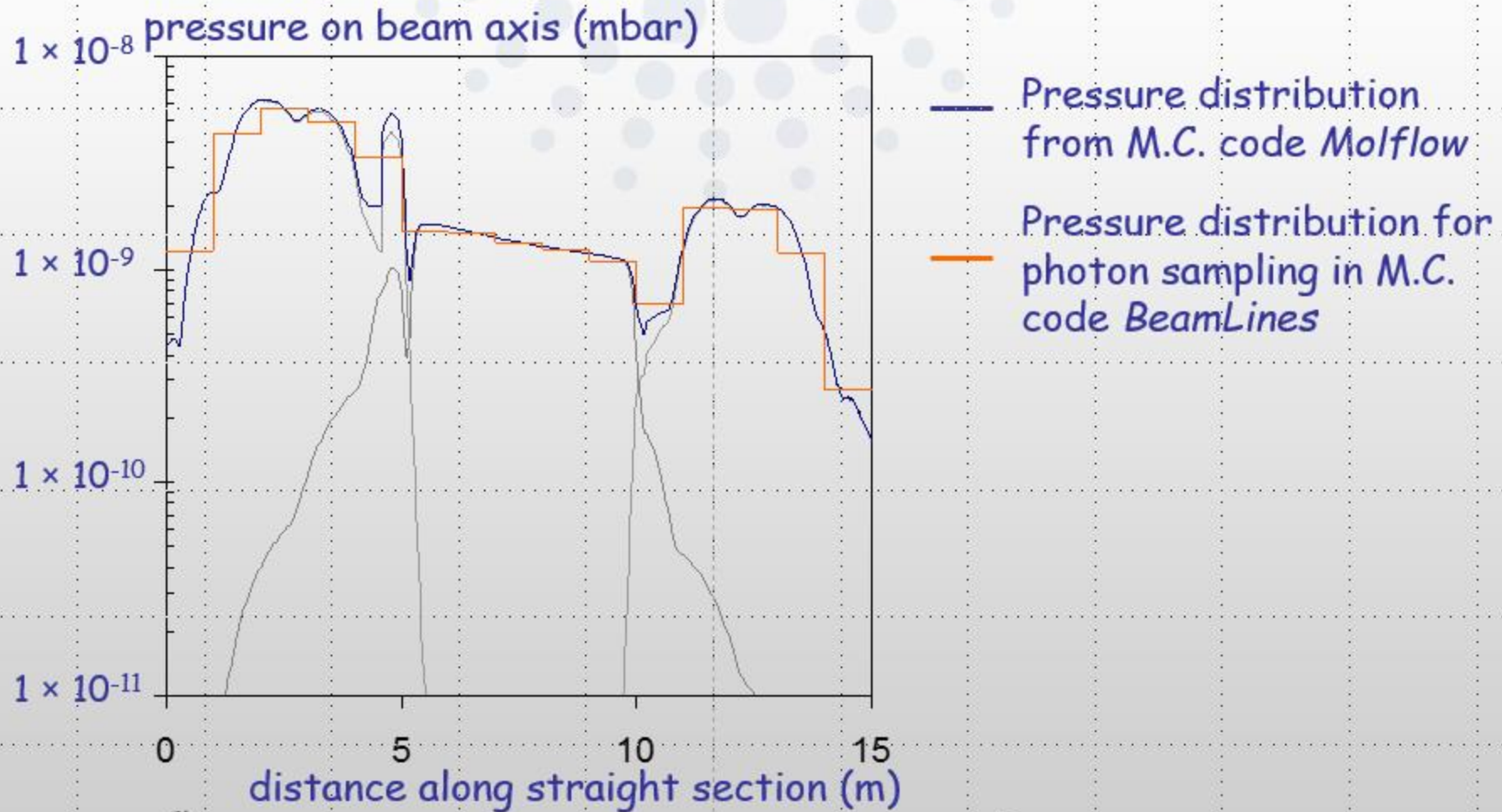
ESRF: going from 200 mA \rightarrow 300 mA: $P \times 2.25$

Ref.: P. Berkvens et al., "Assessment of beamline shielding at the ESRF", 7th RadSynch Workshop, Saskatoon, CA, 2007

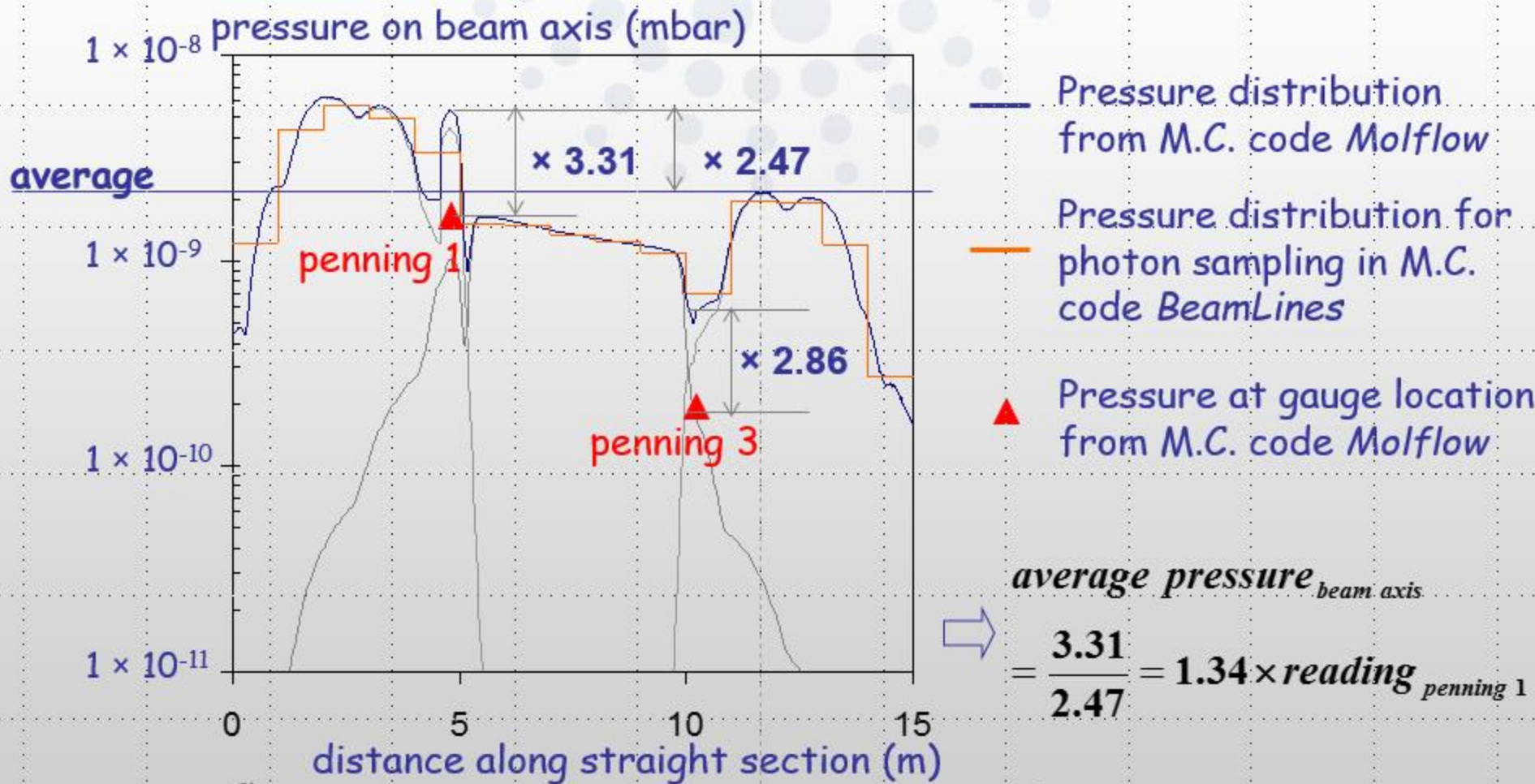
Assessment of beamline shielding at the ESRF

P. Berkvens, P. Colomp and R. Kersevan
European Synchrotron Radiation Facility

MOLFLOW: 3D Monte Carlo calculation of pressure distribution in storage ring vacuum chamber (developed by R. Kersevan)



MOLFLOW: 3D Monte Carlo calculation of pressure distribution in storage ring vacuum chamber (developed by R. Kersevan)

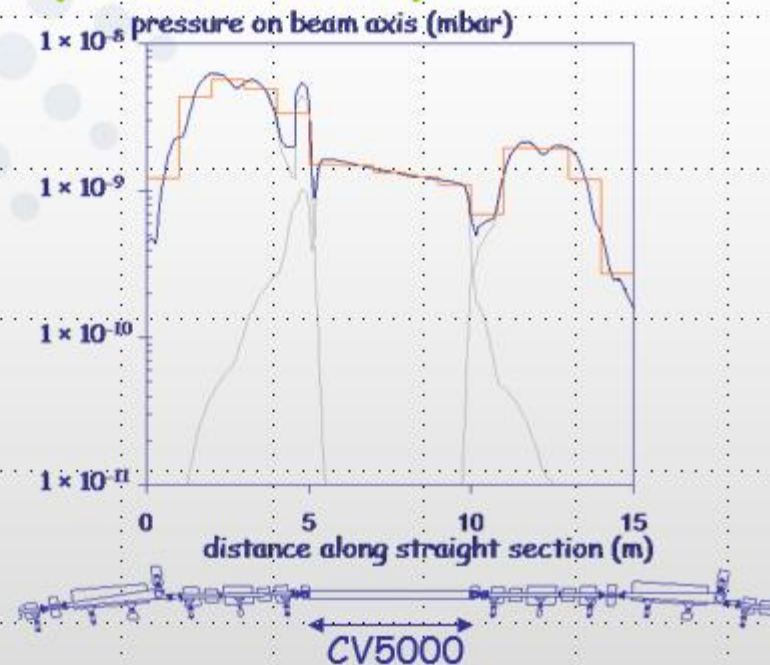


MOLFLOW: 3D Monte Carlo calculation of pressure distribution in storage ring vacuum chamber (developed by R. Kersevan)

$$\text{average pressure}_{\text{beam axis}} = 1.34 \times \text{reading}_{\text{gauge}}$$

for average pressure of 1×10^{-9} mbar in straight section :

- CV500: 6.37×10^{-10} mbar
- rest: 1.18×10^{-9} mbar



Residual gas composition in straight section (from RGA analysers)

molecule	relative pressure (%) inside CV5000	relative pressure (%) rest of straight section
H ₂	85	80
CO	15	10
CO ₂	-	5
CH ₄	-	3
H ₂ O	-	2

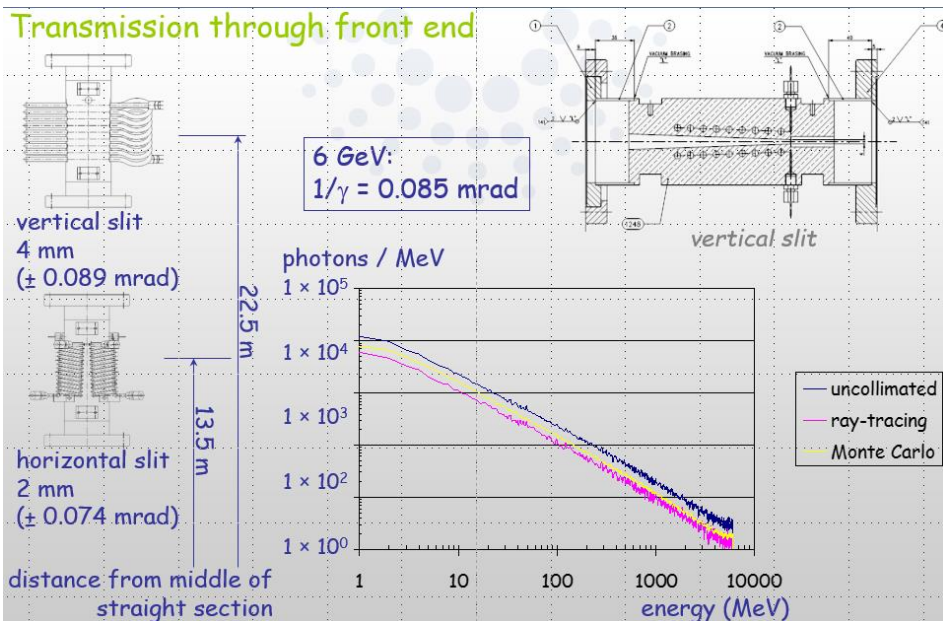
Shielding calculations are done with Monte Carlo code *BeamLines* developed by P. Berkvens:

- ✦ Electromagnetic shower description based on EGS4.
- ✦ Bremsstrahlung differential fluence calculated from theoretical cross sections, using realistic pressure distributions and residual gas compositions in the storage ring straight section.
- ✦ Direct sampling of photons (instead of electrons).
- ✦ 3D description of front end and optical components.
- ✦ Photo neutron dose distributions using differential photon track lengths and assuming an isotropic angular distribution.

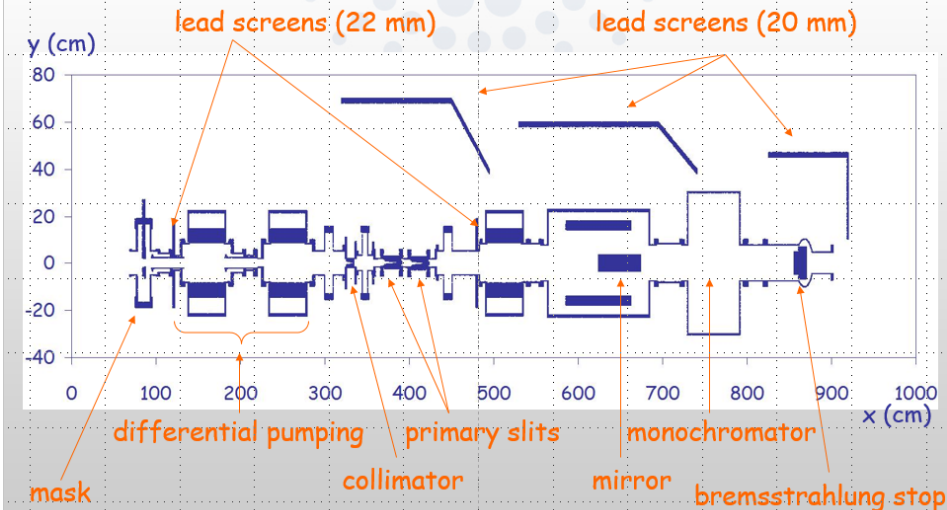
Examples:

- ✦ ID20 Magnetic scattering beamline;
- ✦ ID12 Circular polarisation beamline.

3. SR-induced desorption



ID20 - Magnetic scattering beamline



Summarizing: a double MC scheme is used;

- First a detailed 3D model of the storage ring's vacuum system is made:
 - SR ray tracing (SYNRAD+) generates the photon flux
 - TPMC simulation (Molflow+) converts the flux on all surfaces to local desorption, and then calculates the pressure profile along the e- beam path
- A second detailed model of the shielding of the Front-Ends (absorbers, collimators, etc...) and of the experimental beamline hutches is made:
 - Another independent MC simulation (based on EGS4-derived custom code) is run taking into account as source terms the beam-gas scattering in the storage ring and the subsequent scattering of the high-energy gamma rays along the FE and the BL components

Another example: Analysis and optimization of the crotch absorber of MAX-IV

Proceedings of EPAC08, Genoa, Italy

THPP141

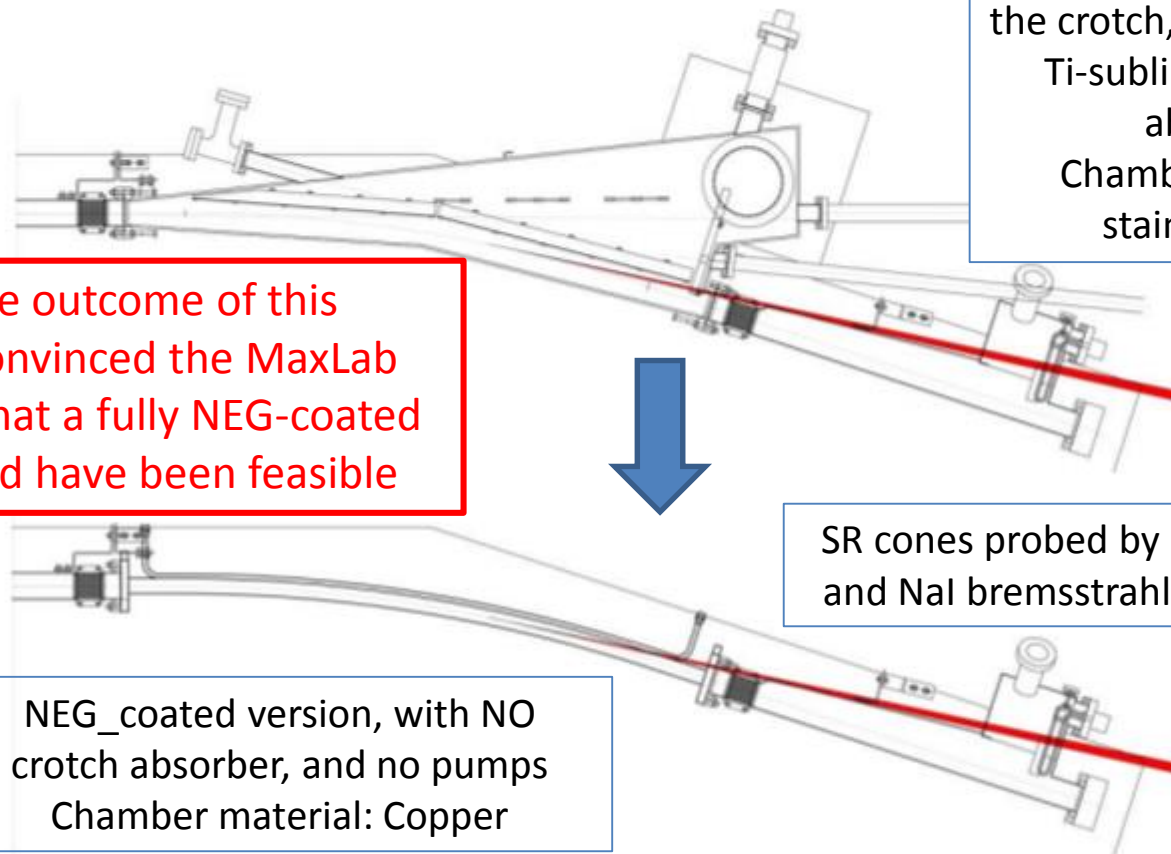
TEST OF A NEG-COATED COPPER DIPOLE VACUUM CHAMBER

Anders Hansson[#], Magnus Berglund, Erik Wallén, MAX-lab, Box 118, SE-221 00 Lund, Sweden
Roberto Kersevan, ESRF, BP 220, FR-38043 Grenoble Cedex, France

1.5 GeV MAX-II ring, Lund, Sweden

Normal configuration of the crotch, with Ion-pump, Ti-sublimator, crotch absorber
Chamber material: stainless steel

The positive outcome of this experiment convinced the MaxLab management that a fully NEG-coated machine would have been feasible



SR cones probed by Geiger-Muller and NaI bremsstrahlung detectors

NEG_coated version, with NO crotch absorber, and no pumps
Chamber material: Copper

Figure 1: Drawings of the second half of cell 3 (top) and cell 2 (bottom) in the MAX II storage ring. The added red beam paths show the cone of bremsstrahlung radiation detected by the NaI detectors.

Another example: Analysis and optimization of the crotch absorber of MAX-IV

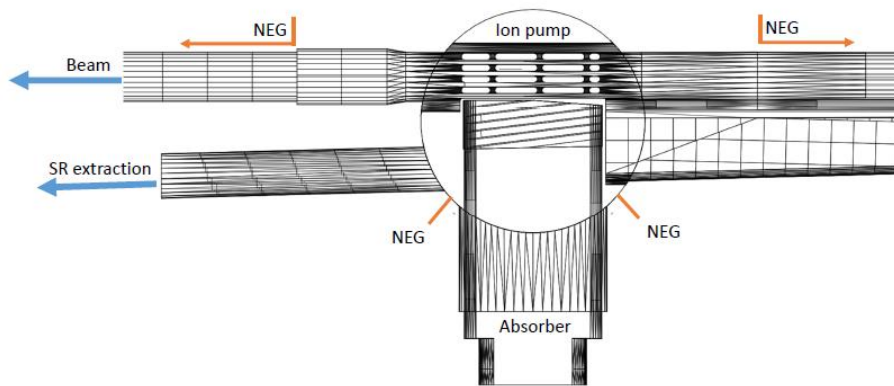


Figure 4.7: Top view of the vacuum chamber with the MAX IV crotch absorber

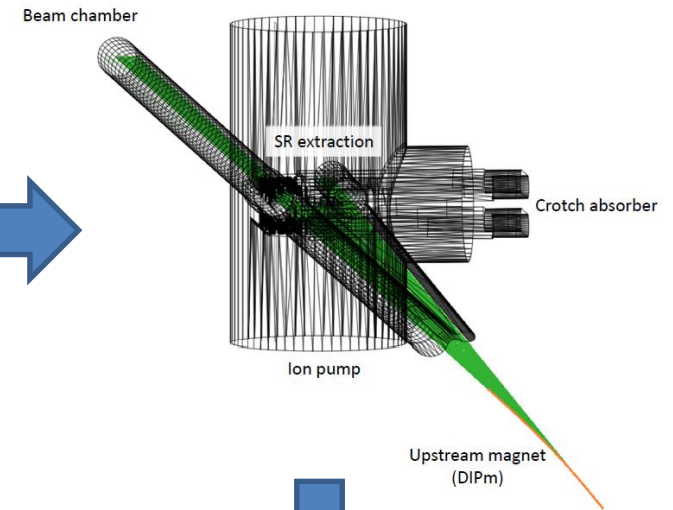
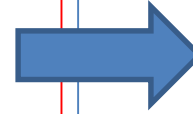


Figure 4.9: The dipole magnet SR radiation schematics in Synrad+



From CAD model to SYNRAD+ simulation

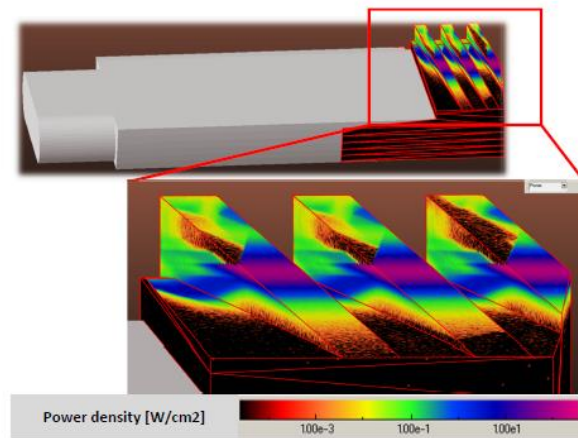


Figure 4.11: Power density on the lower jaw of the absorber

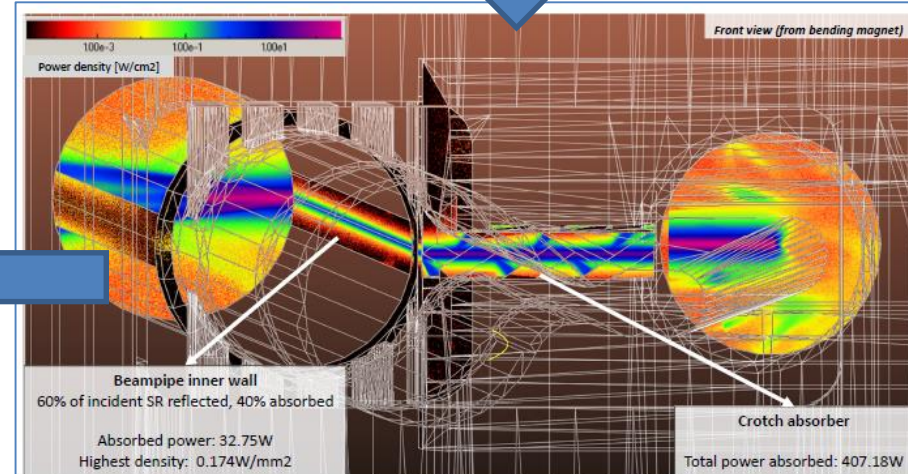
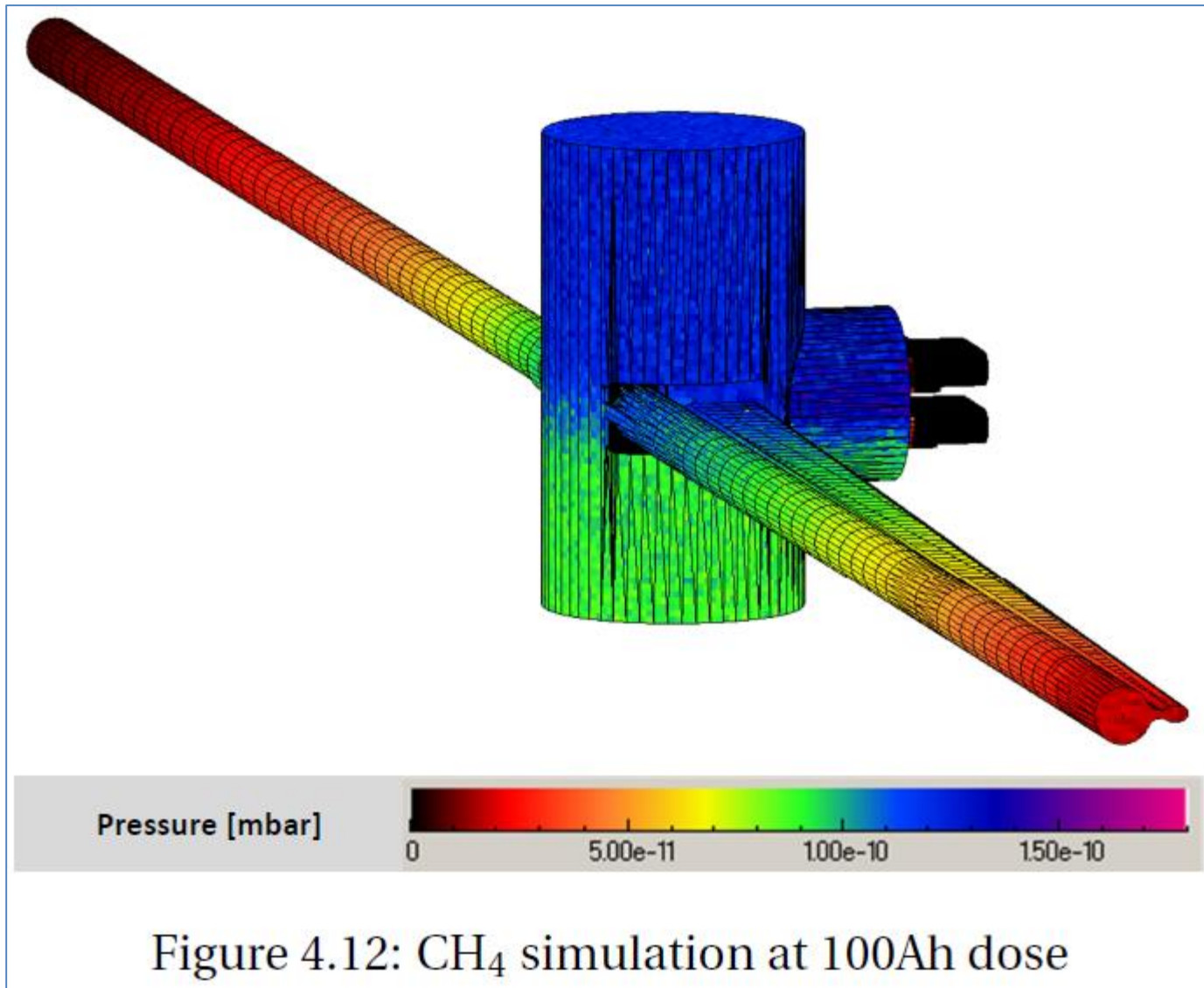


Figure 4.10: Power distribution on the walls

Ref.: "Monte Carlo simulations of Ultra High Vacuum and Synchrotron Radiation for particle accelerators", M. Ady, CERN, doctoral dissertation at EPFL, Lausanne, CH, May 2016; also as an IPAC-15 paper;

From SYNRAD+ simulation to Molflow+: → Pressure profile for CH₄



Molflow+ : simulation of NEG-coating saturation

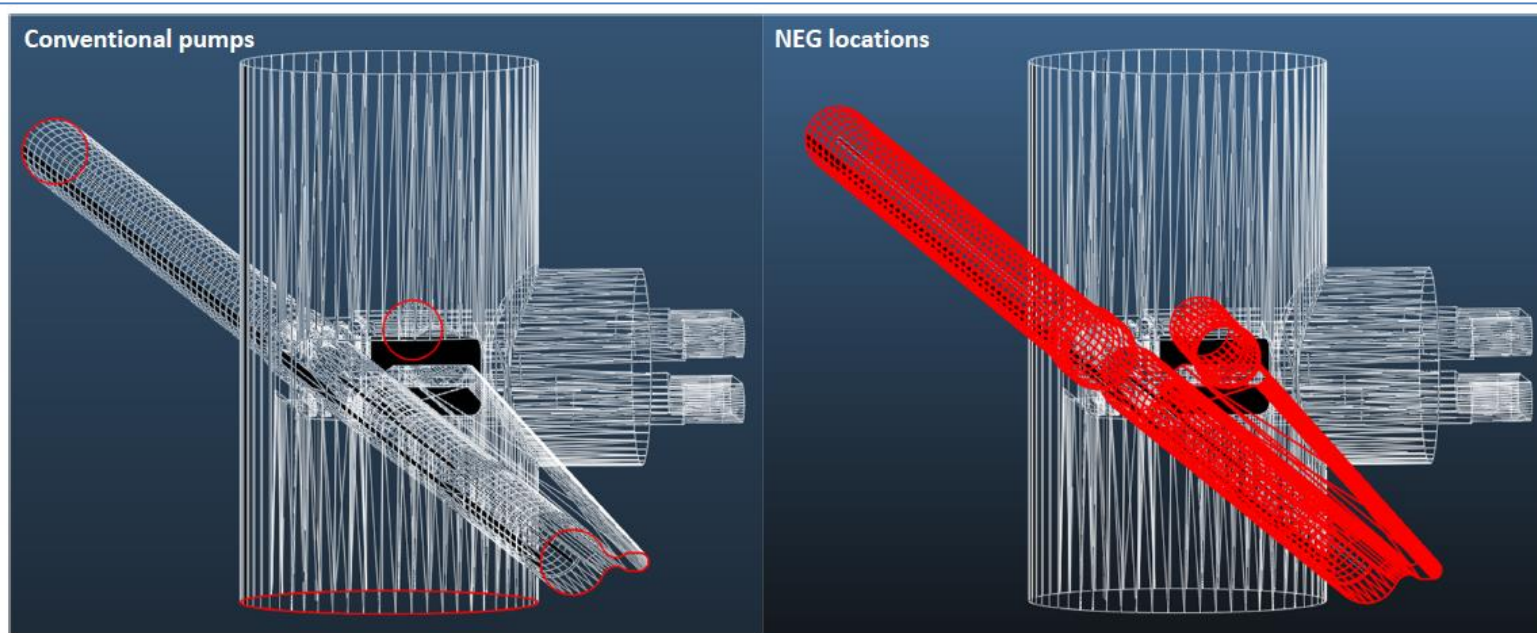


Figure 4.14: Pump locations defined for CO and CO₂ for the Molflow simulations.
 Left: End of modeled regions (sticking 0.1) and ion pump
 Right: NEG locations (The central vertical cylinder is also NEG-coated, not shown for visibility)

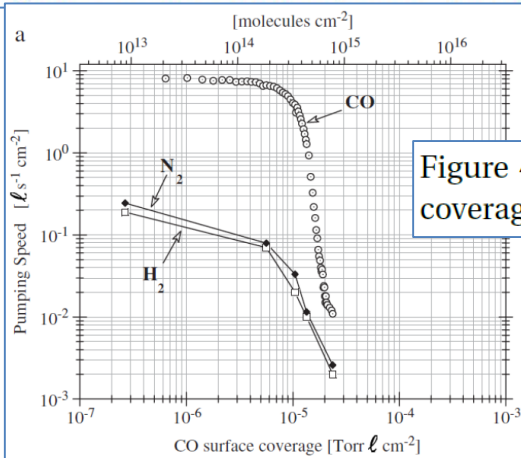


Figure 4.13: Figure 1.a from [79]: NEG pumping speed of CO as a function of its surface coverage

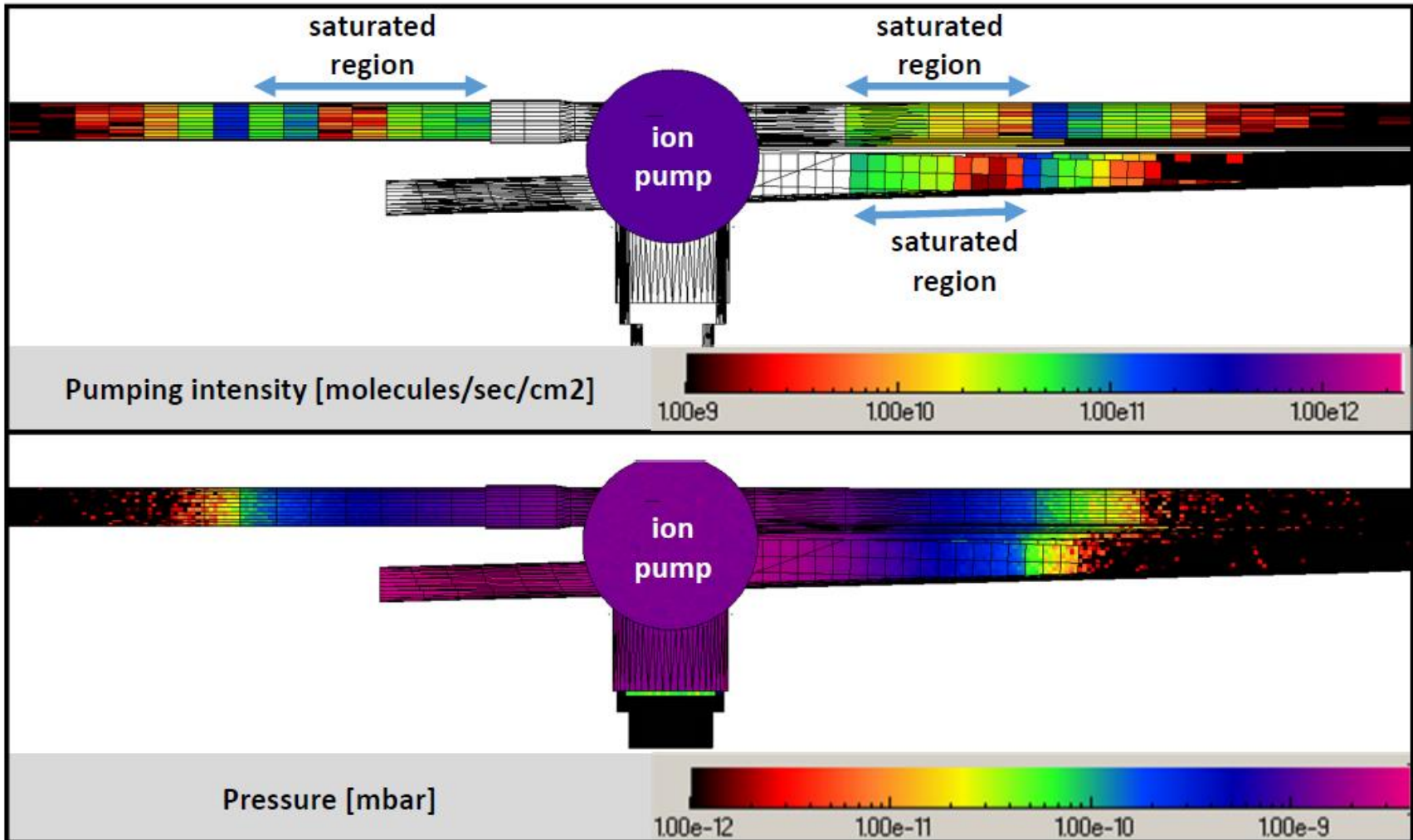
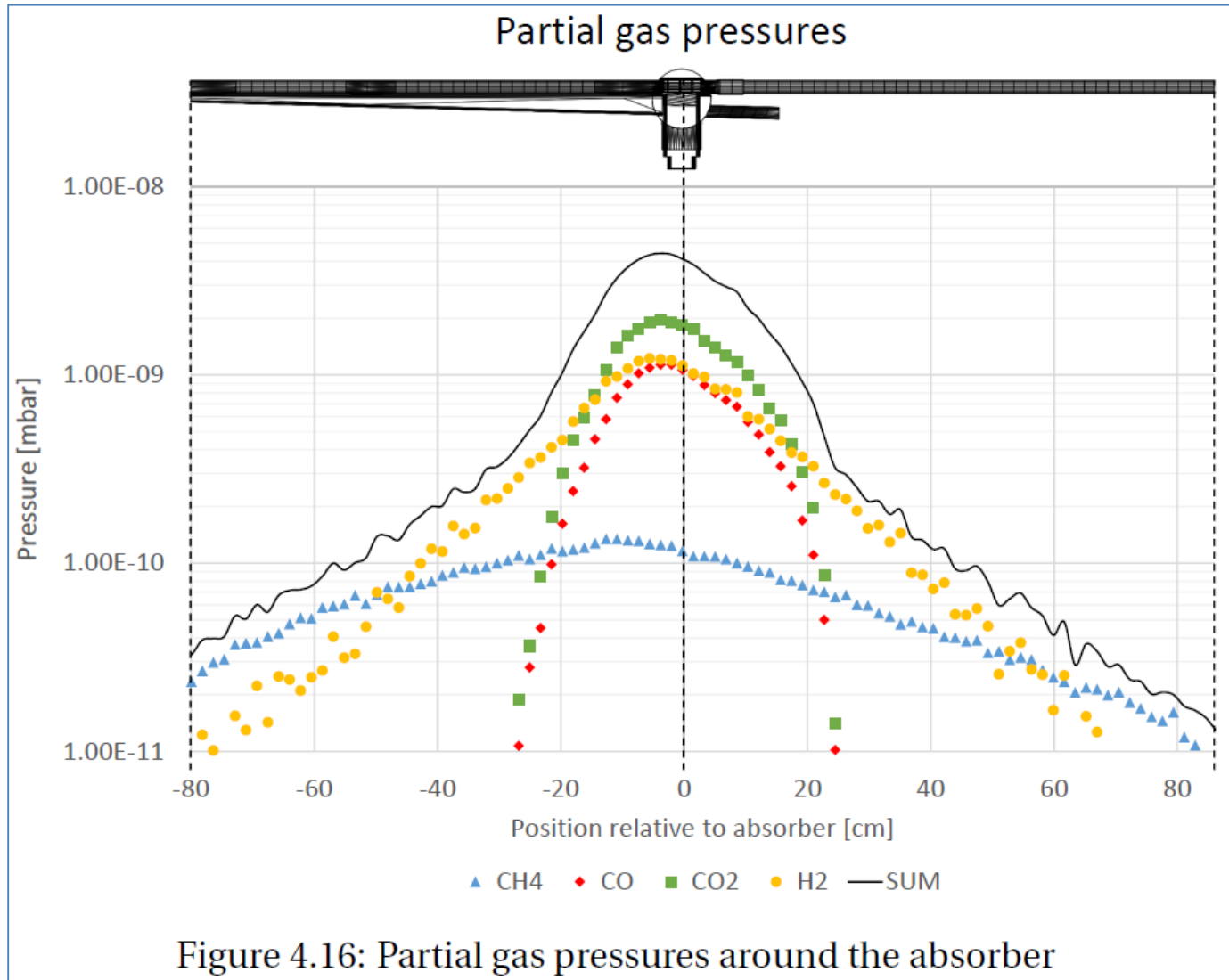
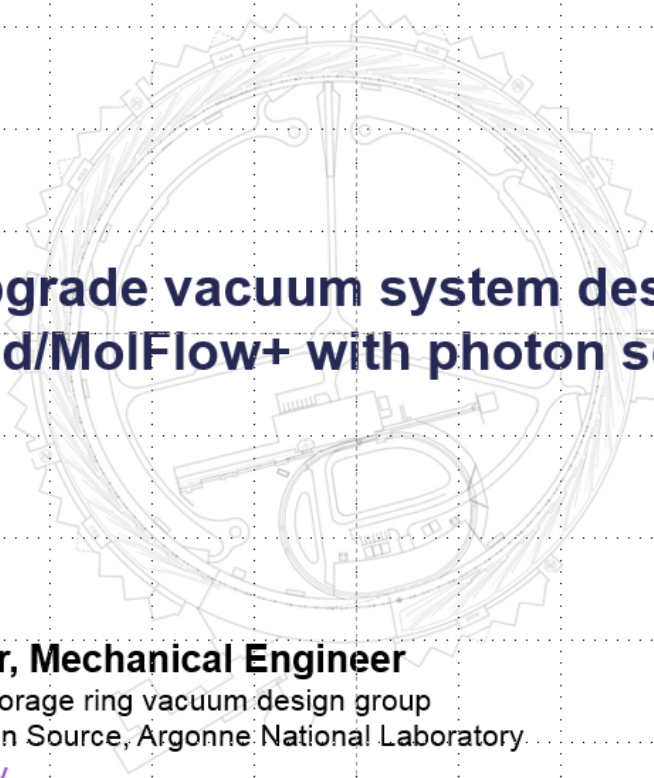

Molflow+ : simulation of NEG-coating saturation

Figure 4.15: NEG saturation and its effect on pumping speed and pressure profile

Molflow+ : simulation of NEG-coating saturation, pressure profile for several gas species




SYNRAD+ : simulation of SR power and flux on crotch absorbers of the APS ring



APS-Upgrade vacuum system design using SynRad/MolFlow+ with photon scattering

Jason Carter, Mechanical Engineer
APS-Upgrade storage ring vacuum design group
Advanced Photon Source, Argonne National Laboratory
jacarter@anl.gov
AVS Symposium, October 2015



APS: Advanced Photon Source;
7 GeV 3rd generation light source → 6 GeV 4th generation with multi-bend and long. gradient dipoles

Source: J. Carter, APS Upgrade team, ANL, Argonne, AVS Conference, 2015

SR-induced desorption and its consequences

MOPMA008

Proceedings of IPAC2015, Richmond, VA, USA

SIMULATION OF GAS SCATTERING LIFETIME USING POSITION- AND SPECIES-DEPENDENT PRESSURE AND APERTURE PROFILES *

M. Borland, J. Carter, H. Cease, and B. Stillwell, ANL, Argonne, IL 60439, USA

BREMSSTRAHLUNG SCATTERING LIFETIME

The differential bremsstrahlung cross-section for atomic number Z is [8, 9]

$$\frac{d\sigma}{dk} = 4\alpha r_e^2 \left\{ \left(\frac{4}{3k} - \frac{4}{3} + k \right) T_1(Z) + \frac{T_2(Z)}{9} \left(\frac{1}{k} - 1 \right) \right\}, \quad (9)$$

where k is the energy of the emitted photon as a fraction of the electron energy,

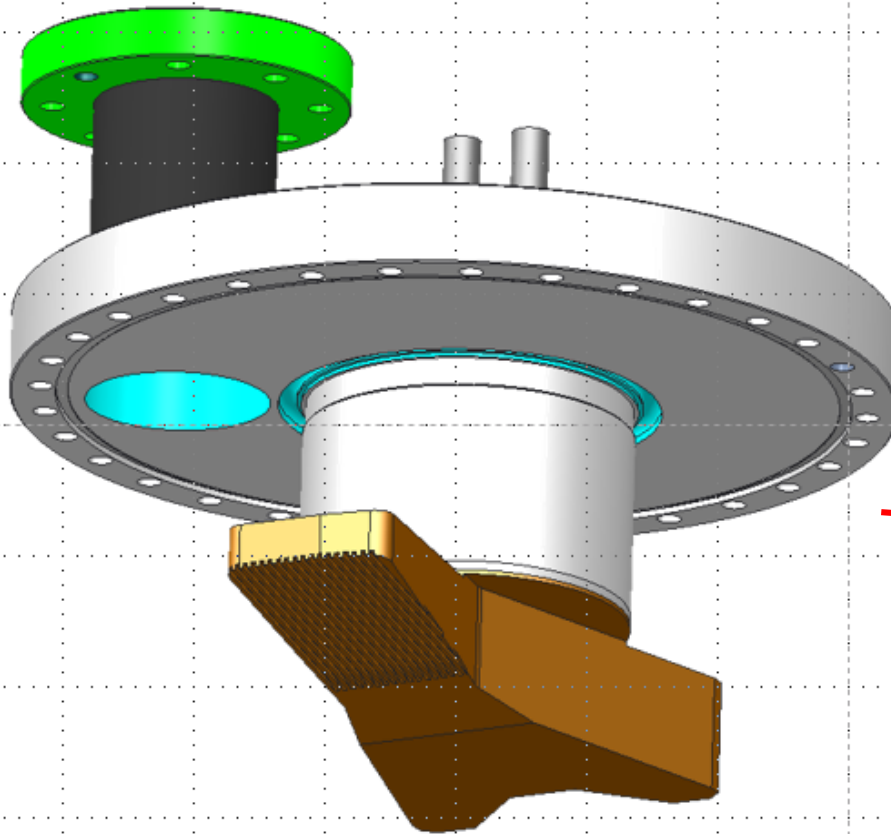
$$T_1(Z) = Z^2(L_{rad}(Z) - f(Z)) + ZL'_{rad}(Z), \quad (10)$$

and $T_2(Z) = (Z^2 + Z)$. The functions $L_{rad}(Z)$, $f(Z)$, and $L'_{rad}(Z)$ are described in [9]. The fractional change in energy of the electron is $u = -k$.

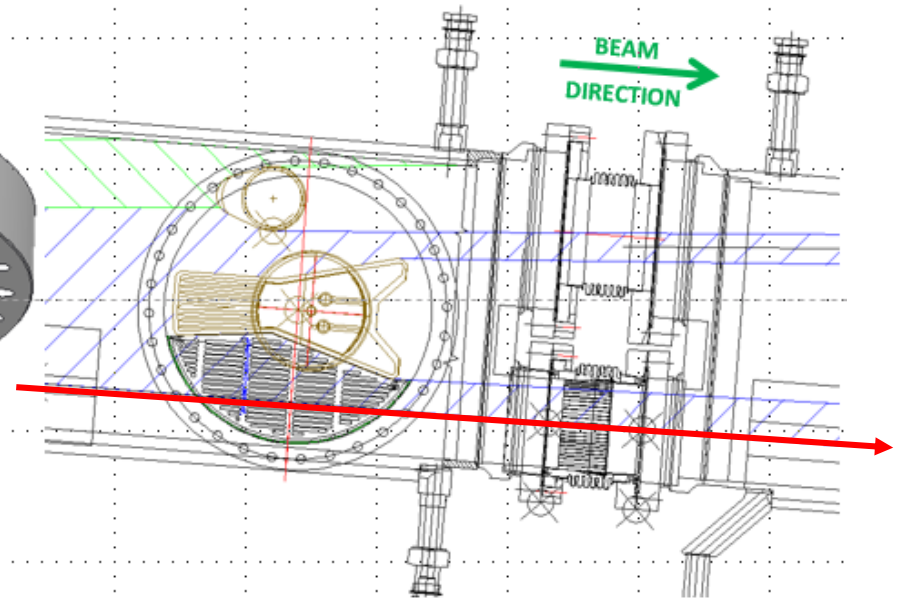
SYNRAD+ : simulation of SR power and flux on crotch absorbers of the APS ring

How SynRad works

- Demonstrate SynRad applications with APS photon absorber example



3D CAD model of absorber assembly

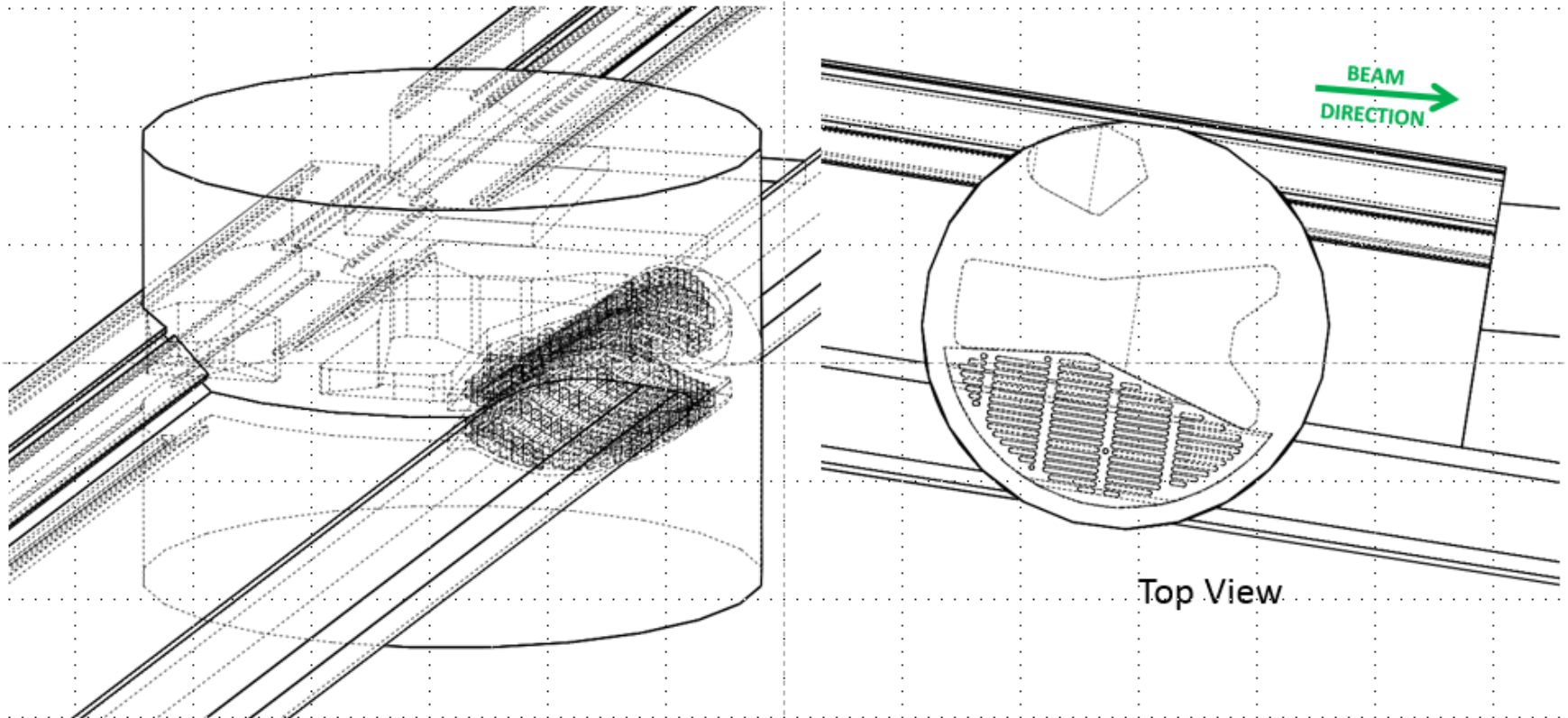


Top view of 2D CAD synchrotron ray trace

SYNRAD+ : simulation of SR power and flux on crotch absorbers of the APS ring

How SynRad works

- 3D CAD model built representing interior volume of vacuum system and all surfaces under vacuum

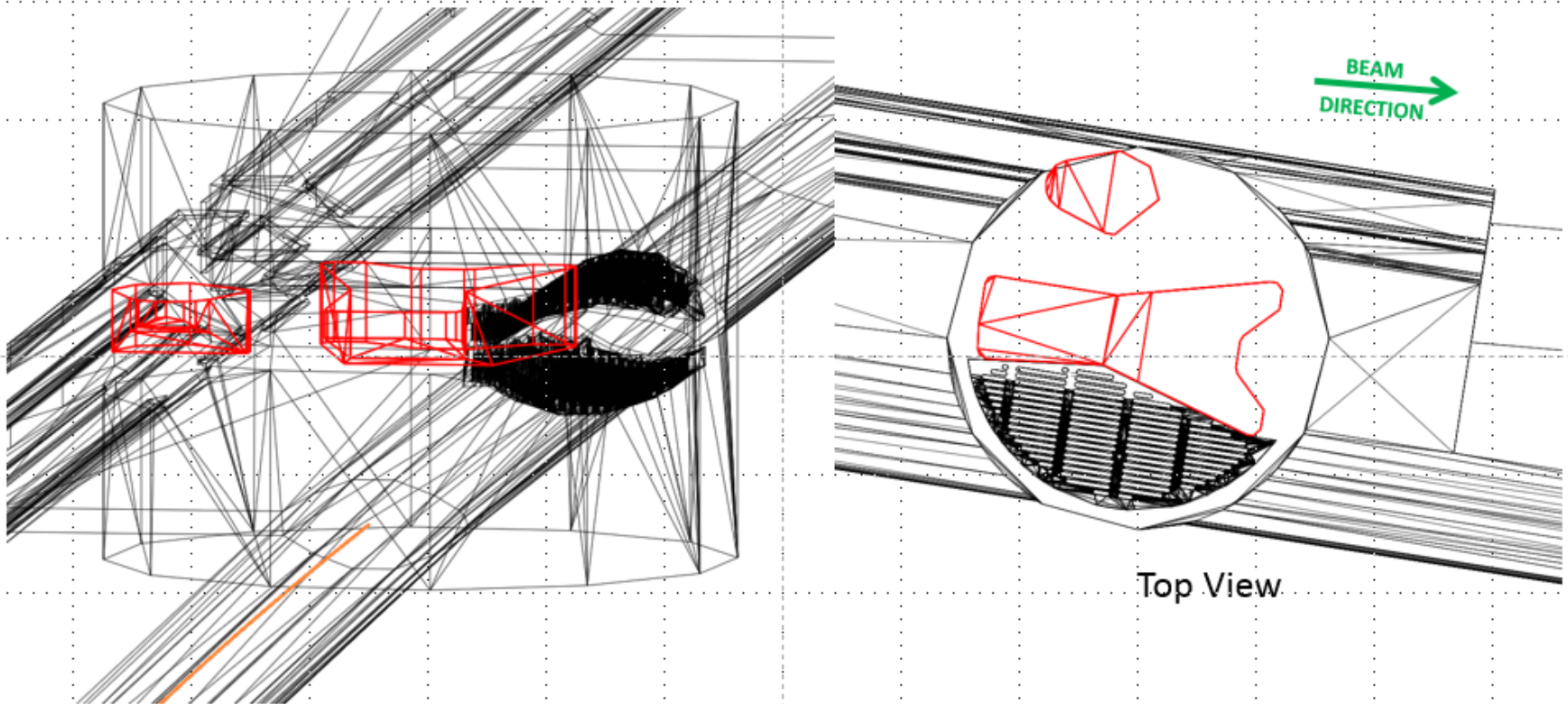


3D CAD with hidden lines shows two absorbers and an RF screen within a pumping port

SYNRAD+ : simulation of SR power and flux on crotch absorbers of the APS ring

How SynRad works

- Model exported as STL file type, imported into SynRad as planar surface 'facets'
 - Material definitions applied to surfaces to induce photon scattering

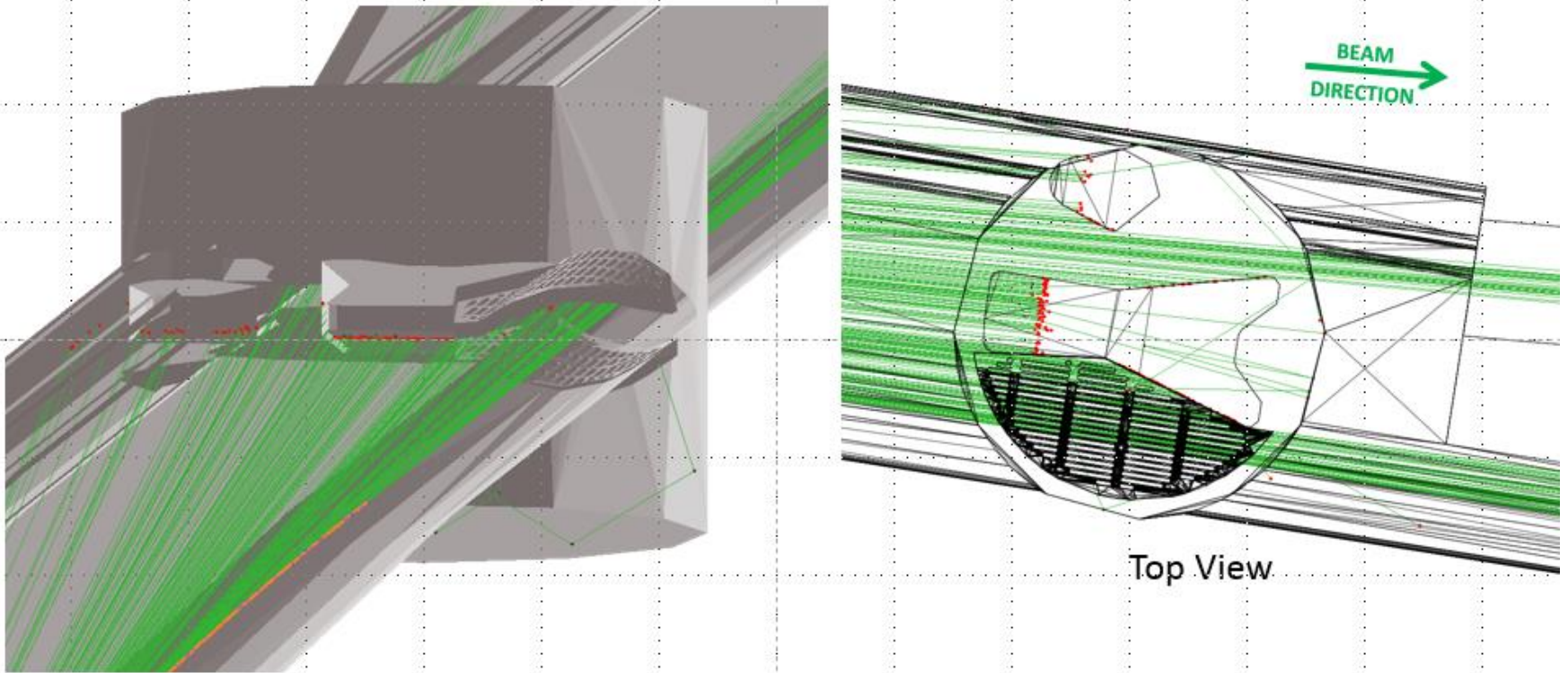


Absorber bodies highlighted in **red**

SYNRAD+ : simulation of SR power and flux on crotch absorbers of the APS ring

How SynRad works

- Magnetic elements generate synchrotron rays within 3D space

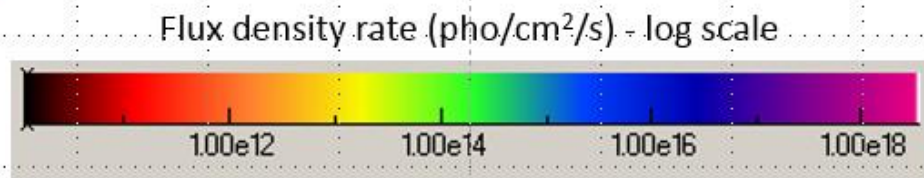
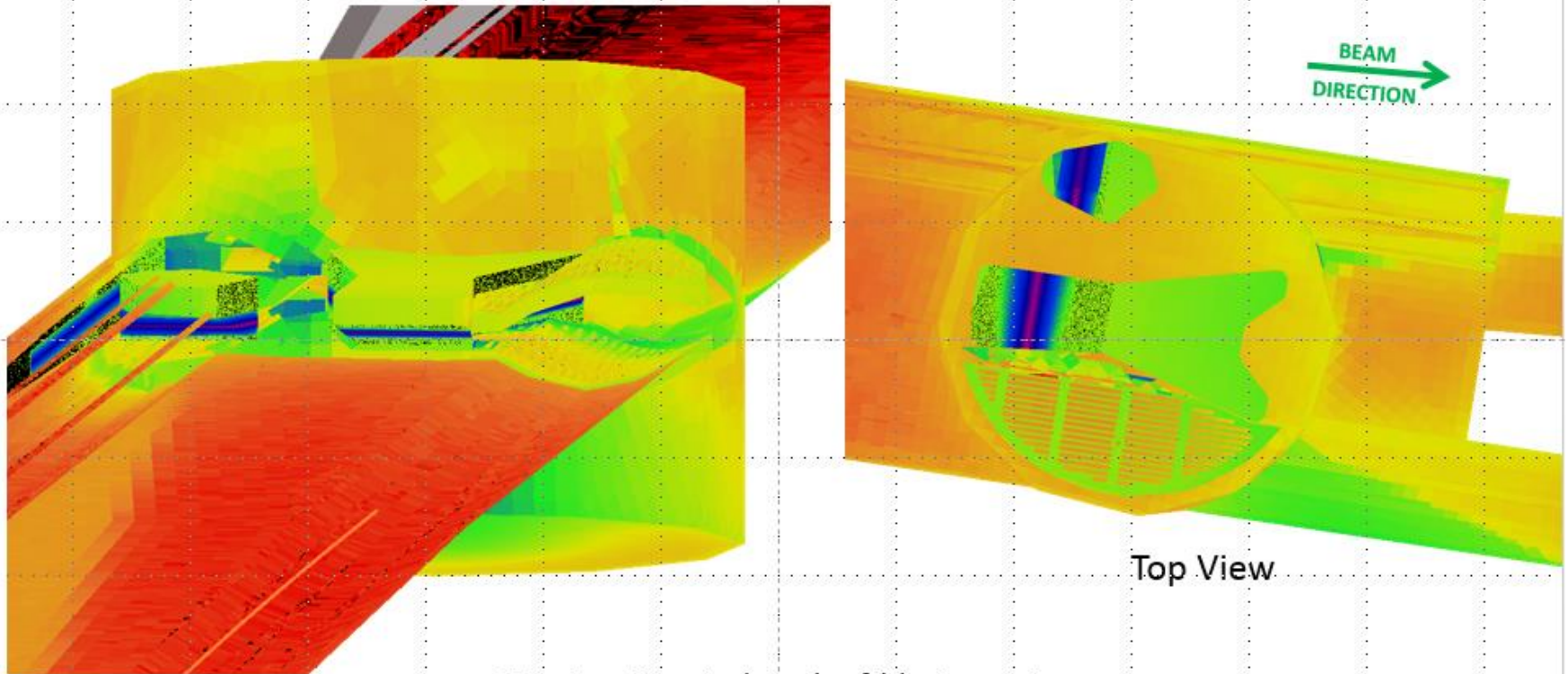


Magnetic elements in **orange**, program generated synchrotron fan in **green**,
surface hit points in **red**

SYNRAD+ : simulation of SR power and flux on crotch absorbers of the APS ring

How SynRad works

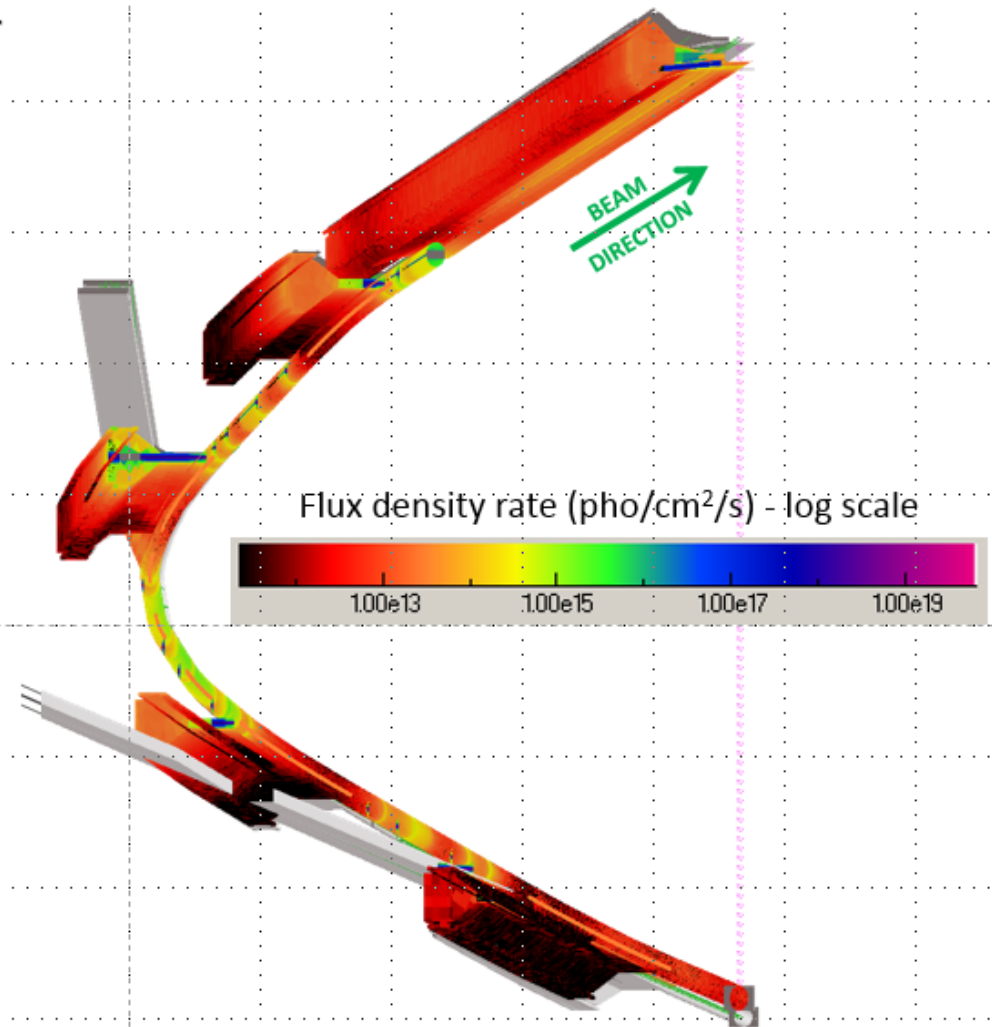
- Flux gradient collected on meshed surfaces
 - Finer mesh for direct incidence surfaces, coarser mesh on surfaces receiving scattered photons



SYNRAD+ : simulation of SR power and flux on crotch absorbers of the APS ring

SynRad model of APS-U sector

- Bending magnet elements generate photon flux in model
- Symmetric boundary condition passes downstream photons back to upstream
- Heat load ray trace verified to high accuracy
- Mesh applied to all vacuum surfaces
- Material reflection tables referenced to determine surface scattering

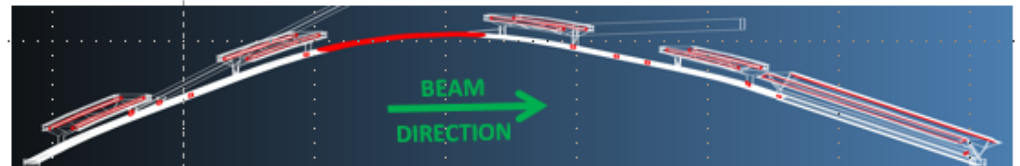
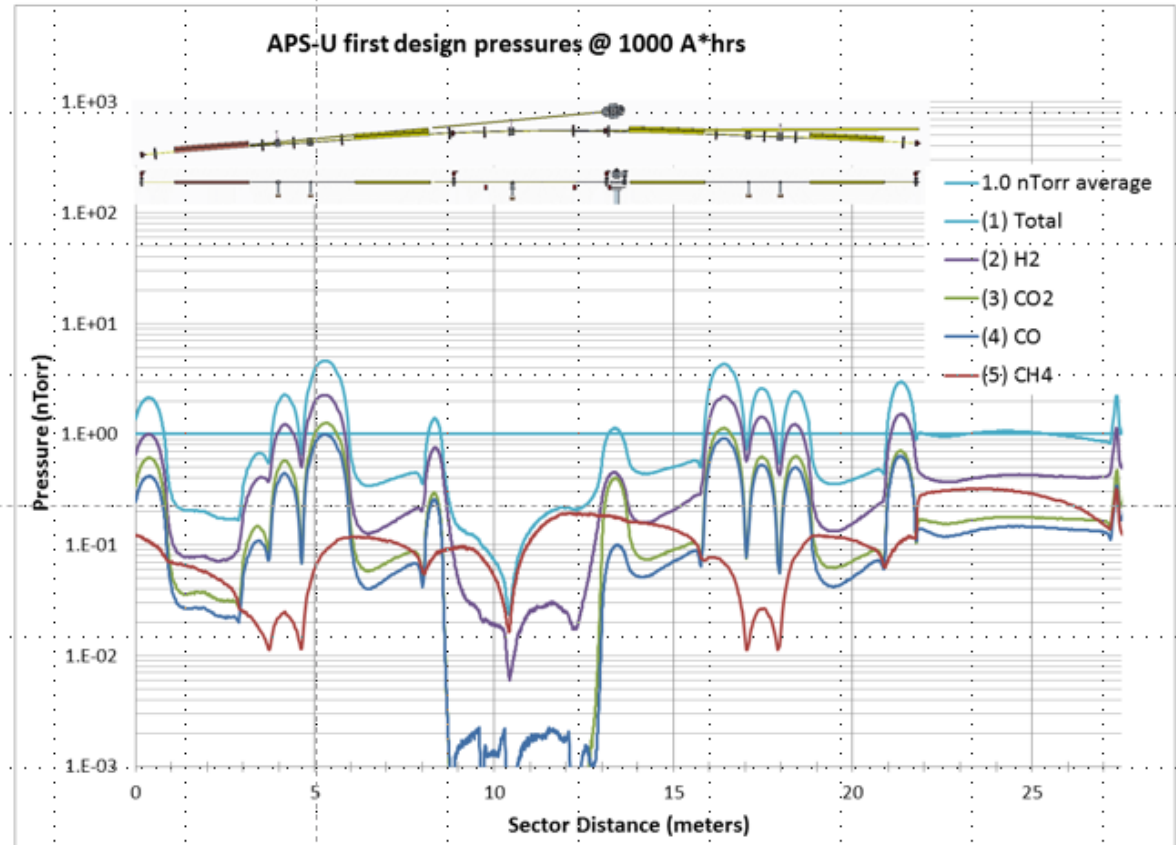


SynRad simulation of synchrotron radiation flux distributions with photon scattering

SYNRAD+ : simulation of SR power and flux on crotch absorbers of the APS ring

Pressures for each UHV gases

- Total pressure equals the sum of individual gases
- No distributed pumping assumed for CH₄ leading to unique profile
- Individual gas pressures used to estimate beam lifetime



Summary and conclusions

- Some basic concepts of vacuum technology and accelerators have been recalled
- We have then briefly seen how important it is to be able to calculate the pressure/gas density along the path of the e- beam stored in a **synchrotron radiation light source**
- The advantages of modern, fast computers and their application to **Montecarlo simulation codes** have been also highlighted with examples
- The importance of a **two-stage approach** to the calculation of pressure profiles has been also discussed at length, with examples for 1. ESRF: beamline shielding; 2. MAX-IV: crotch area saturation of the NEG-coating; 3. APS-U upgrade: pressure profiles
- The relevance of this two-stage approach with respect to accelerator issues other than vacuum has been demonstrated with the example of the **reduction of bremsstrahlung radiation fluence on the experimental beamline hutches**. This is extremely important as light sources have 100s of experiments per year, and need as close as possible 100% beam availability. **The experimental hutches must be accessible at all times**
- For light sources, the design of the vacuum system must put particular attention to protecting all vacuum surfaces from unwanted photon irradiation; Properly water-cooled absorbers must be foreseen, with appropriate geometry so as to trap as much as possible the scattered photons, and minimize irradiation of, and gas desorption from surfaces nearby

Many thanks for your attention 😊



BONUS SLIDES

TPMC method

TPMC method and algorithm:

- Let's assume, without loss of generality, that a vacuum system be modeled using polygonal planar facets;
- Let XYZ be an arbitrary cartesian frame of reference;
- Let X''Y''Z'' be the frame of reference whose origin corresponds to the location of a molecule located on the facet, with Z'' perpendicular to the facet;
- Let X'Y'Z' a frame of reference parallel to X''Y''Z'', whose origin is the same as XYZ;
- Let α and β be defined as such: β is the rotation about the Y axis which takes X onto X'; α is the rotation about X (X') which makes Y become Y';
- With such definitions, the following transformations can be written:

$$\begin{pmatrix} X'' \\ Y'' \\ Z'' \end{pmatrix} = \begin{pmatrix} 1 & 0 & 0 \\ 0 & \cos \alpha & \sin \alpha \\ 0 & -\sin \alpha & \cos \alpha \end{pmatrix} \begin{pmatrix} X' \\ Y' \\ Z' \end{pmatrix}$$

$$\begin{pmatrix} X \\ Y \\ Z \end{pmatrix} = \begin{pmatrix} \cos \beta & 0 & \sin \beta \\ 0 & 1 & 0 \\ -\sin \beta & 0 & \cos \beta \end{pmatrix} \begin{pmatrix} X'' \\ Y'' \\ Z'' \end{pmatrix}$$

- Upon desorption of the molecule from the source facet s , let L be the generic length of the trajectory to the next target facet t ;

$$X'' = L \sin \theta \cos \varphi$$

$$Y'' = L \sin \theta \sin \varphi$$

$$Z'' = L \cos \theta$$

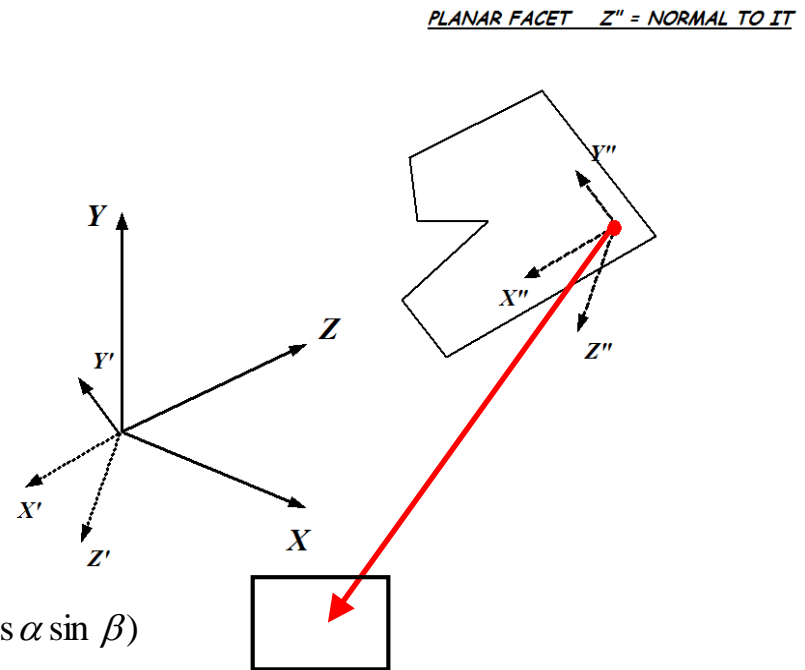
- Combining the two relations, one gets

$$X_t = X_s + L_t (\sin \theta \cos \varphi \cos \beta - \sin \theta \sin \varphi \sin \alpha \sin \beta - \cos \theta \cos \alpha \sin \beta)$$

$$Y_t = Y_s + L_t (\sin \theta \sin \varphi \cos \alpha - \cos \theta \sin \alpha)$$

$$Z_t = Z_s + L_t (\sin \theta \cos \varphi \sin \beta + \sin \theta \sin \varphi \sin \alpha \cos \beta + \cos \theta \cos \alpha \cos \beta)$$

where the value for L , L_t , i.e. the length of the trajectory to the next facet encountered, is a function of the geometric description of facet t , and it is not given here (see (*) and references therein)



TPMC method #2:

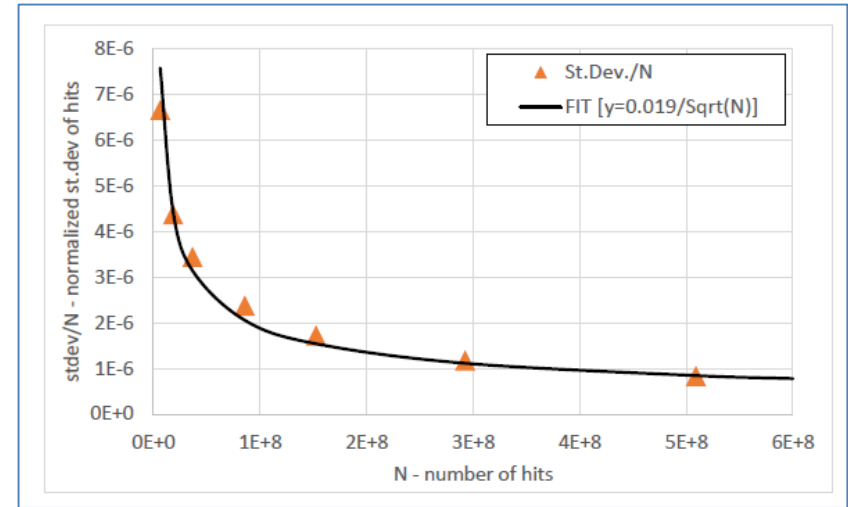
• Averaging over a large number of molecular traces yields estimates of the pressure, impingement rate, conductance, pumping speed, etc...:

- Let N be the number of molecules entering, for instance, a tube from one end;
- Let m be the number of molecules leaving the tube at the other end:

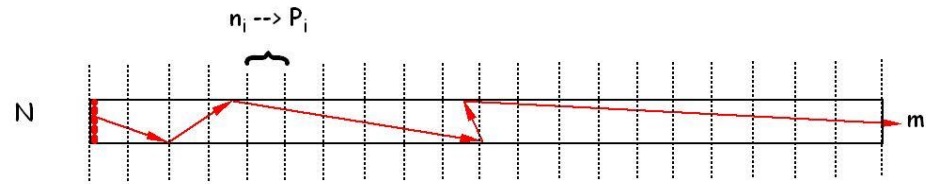
$w = m/N$ is the **transmission probability**;

- The values for w follow a **binomial distribution**, which has a standard deviation
- If n_i is the number of molecular hits in the i -th segment of the tube, and P_i the associated pressure, then the normalized standard deviation for the pressure P_i is:

$$\sigma_{n_i} (\%) = \sqrt{\frac{1}{n_i} \left(1 - \frac{n_i}{N}\right)} \cdot 100$$



$$\sigma = \sqrt{\frac{w \cdot (1 - w)}{N}}$$



TPMC method #3: how to convert from molecular hits to pressures:

- If n_i is the number of collisions on one segment of the vacuum chamber (A cm²), and Q is the outgassing (in mbar·l/s), then Q/kT is the number of molecules/s. If N is the number of molecules traced, then, the mean number of collisions/cm² in that segment is

$$Z_i = n_i / AN$$

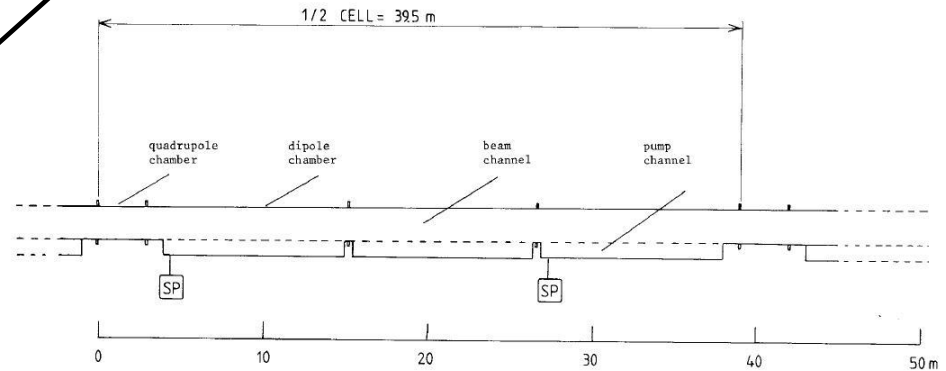
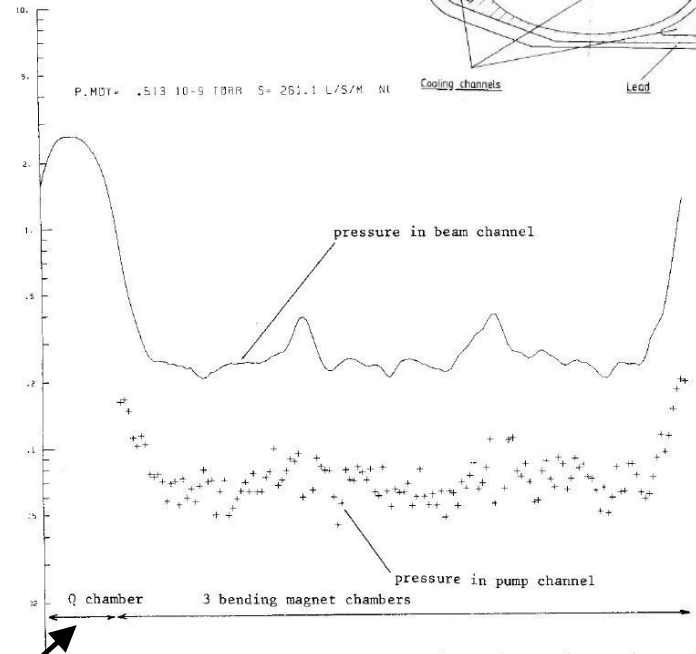
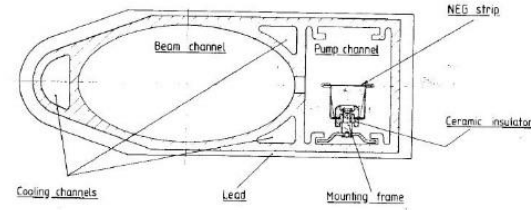
- The estimate of the impingement rate is

$$Z_i = \frac{n_i Q}{ANkT}$$

- At equilibrium, the relation between the pressure P_i (on segment i) and the corresponding impingement rate Z_i is

$$P_i = \frac{4kTZ_i}{v_a} = \frac{4Qn_i}{v_a AN}$$

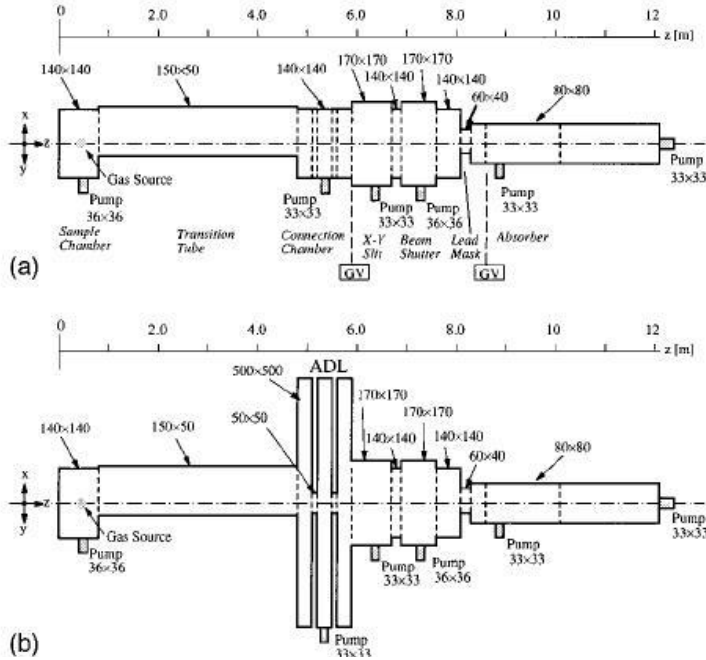
$$P_{avg} = \frac{4Q}{v_a AN} \sum n_i$$



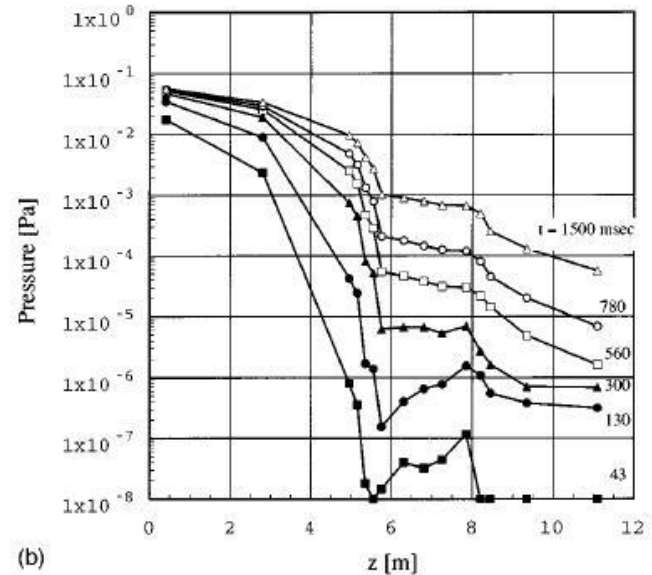
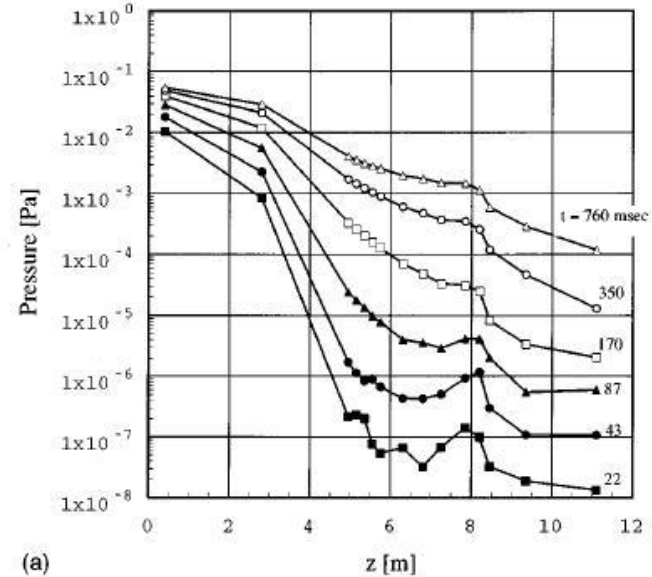
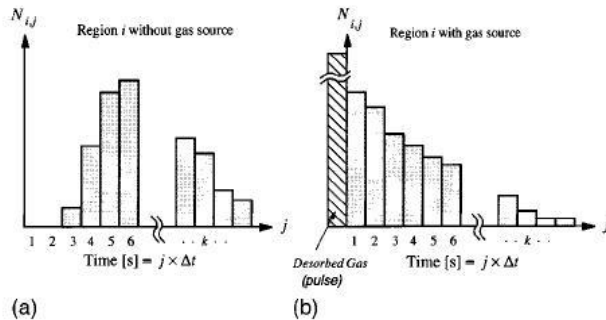
From T.Xu, JM. Laurent, O. Groebner CERN-LPVA/86-02

TPMC method #4: non-stationary, time-dependent case

- **Time-dependent case: acoustic delay line at Tristan synchrotron**



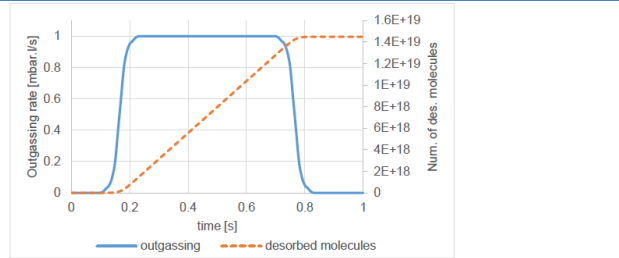
- **The length of all trajectories is translated into time intervals by means of the average molecular speed**



TPMC method

TPMC method #5: non-stationary, time-dependent case via Molflow+

When there is a need to simulate transient vacuum effect one can instruct Molflow+ to use “**moments**”, i.e. short intervals in time during which the collisions with the surfaces of the model are taken into consideration, and then translated into pressures or densities as in the steady-state, stationary case:



Desorption rate and number of desorbed molecules during injection

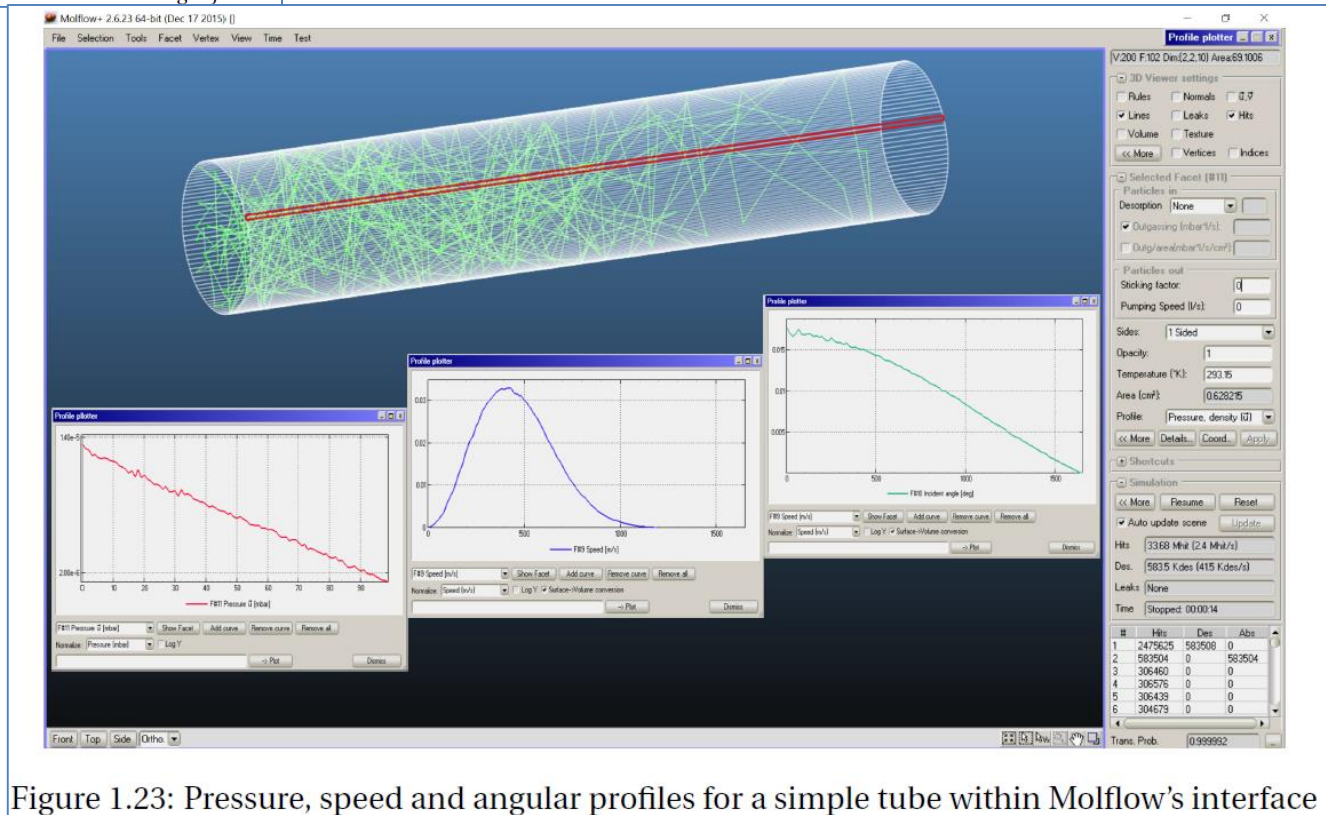


Figure 1.23: Pressure, speed and angular profiles for a simple tube within Molflow’s interface

TPMC method #6: convergence of the calculation

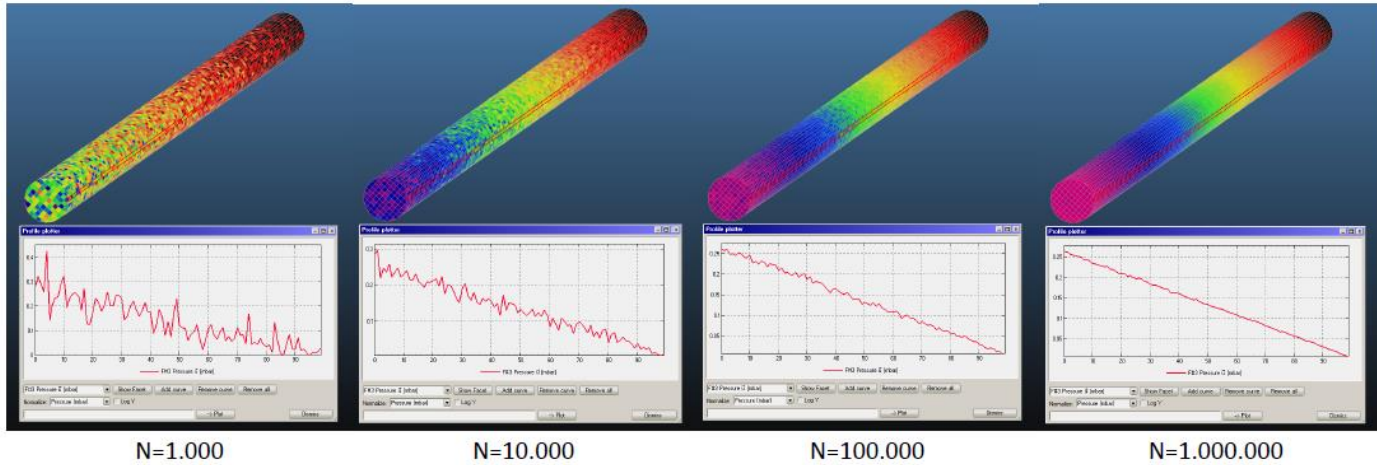


Figure 1.18: Texture and profile results for a vacuum tube with desorption at the left and pumping at both sides, as a function of the number of traced particles.

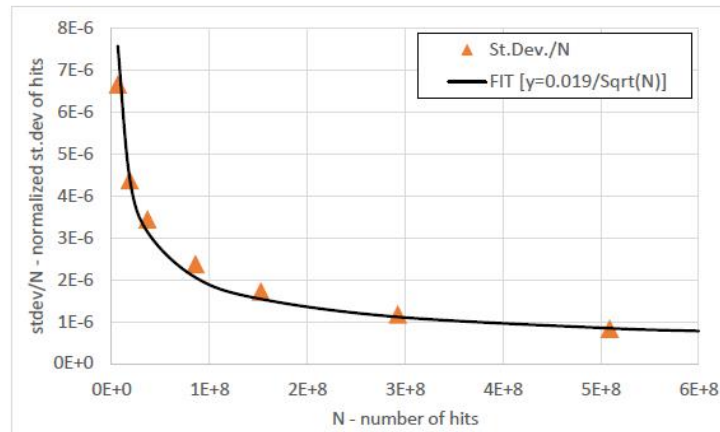


Figure 1.19: Normalized standard deviation of Molflow+ results as a function of the simulated